TECHNISCHE UNIVERSITÄT WIEN

DIPLOMARBEIT

Jet momentum broadening in a gluonic plasma from effective kinetic theory

zur Erlangung des akademischen Grades

Diplom-Ingenieur

im Rahmen des Studiums

066 461 Masterstudium Technische Physik

eingereicht von

Florian Lindenbauer
Matrikelnummer 01608107

ausgeführt am Institut für Theoretische Physik
der Fakultät für Physik der Technischen Universität Wien

Betreuung
Betreuer: Univ.Prof. Dipl.-Ing. Dr.techn. Anton Rebhan
Verantwortlicher Mitbetreuer: Univ.Ass. Dr.rer.nat. Kirill Boguslavski

Wien, 02.02.2022

(Unterschrift Verfasser)

(Unterschrift Betreuer)

(Unterschrift verantwortlicher Mitbetreuer)

Eidesstattliche Erklärung

Ich erkläre an Eides statt, dass die vorliegende Arbeit nach den anerkannten Grundsätzen für wissenschaftliche Abhandlungen von mir selbstständig erstellt wurde. Alle verwendeten Hilfsmittel, insbesondere die zugrunde gelegte Literatur, sind in dieser Arbeit genannt und aufgelistet. Die aus den Quellen wörtlich entnommenen Stellen, sind als solche kenntlich gemacht.

Das Thema dieser Arbeit wurde von mir bisher weder im In- noch Ausland einer Beurteilerin/einem Beurteiler zur Begutachtung in irgendeiner Form als Prüfungsarbeit vorgelegt. Diese Arbeit stimmt mit der von den Begutachterinnen/Begutachtern beurteilten Arbeit überein.

Wien, 02.02.2022 _____

(Unterschrift Verfasser)

Zusammenfassung

In relativistischen Schwerionenkollisionen entsteht ein neuer Materiezustand, das Quark-Gluon-Plasma. Eine Möglichkeit, dessen Eigenschaften zu untersuchen, sind Jets, in der Kollision entstandene hochenergetische Teilchen, die mit den Quarks und Gluonen wechselwirken und dann in einem Detektor gemessen werden können. Die transversale Impulsänderung eines solchen Teilchens kann mit dem *jet quenching* Parameter $\hat{q}$ quantifiziert werden, für den ich in dieser Arbeit eine Formel aus der effektiven kinetischen Beschreibung des Plasmas herleite. In unserer Beschreibung kann der Jet hierbei beliebigen Impuls und Richtung relativ zur Strahlachse haben. Wenn man den Grenzwert des Impulses gegen unendlich betrachtet, muss man einen maximalen Impulsübetrag definieren, damit $\hat{q}$ endlich bleibt. Dann beschreibe ich die Implementierung dieser Formeln in einem C++ Code, der die Zeitentwicklung eines gluonischen Plasmas simuliert. Die numerischen Resultate, die für isotrope Teilchenverteilungen erhalten werden, werden mit bekannten analytischen Berechnungen im thermischen Gleichgewicht und mit experimentellen Grenzwerten verglichen. Außerdem berechne ich $\hat{q}$ für verschiedene skalierte thermische Verteilungen.

Abstract

In relativistic heavy-ion collisions a new state of matter is created that is referred to as the Quark-Gluon Plasma (QGP). To probe its properties one can use jets, which are highly energetic particles that are formed in the collision and traverse the plasma, while interacting with quarks and gluons, and can then be measured in a detector. The rate of change of their transverse momentum squared is quantified by the *jet quenching parameter* $\hat{q}$, for which, in this thesis, I derive a formula for the effective kinetic theory description of the plasma. In our framework the jet can have an arbitrary momentum and direction with respect to the beam axis. When considering the limit of the jet momentum going to infinity, we need to introduce a momentum cutoff in order to render $\hat{q}$ finite. I then describe the implementation of the corresponding formulae in a C++ code that simulates the time-evolution of a gluonic plasma. The numerical results obtained for isotropic particle distributions are finally compared with previous analytic calculations in thermal equilibrium and with bounds from experimental observations. Moreover, I also compute $\hat{q}$ for different scaled thermal distributions.

Acknowledgements

Taking this journey of studying physics was certainly not always an easy task. There were hills to climb and valleys to cross, but I was very fortunate to be accompanied and guided by many wonderful people, far too many than I could possibly mention here.

First of all, I would like to thank my supervisors Kirill Boguslavski for guiding me through the highlands of thermal and non thermal field theory and kinetic theory and for keeping me on the right track, and Anton Rebhan for showing me the way towards the land of studying matter under extreme conditions during my Bachelor thesis. I am grateful for the discussions with Aleksi Kurkela, Tuomas Lappi and Jarkko Peuron, who helped me in implementing the code and understanding what was going on.

I am indebted to all the lecturers at TU Wien who taught me which paths to wander on, and also to my teachers at high school who somehow managed to ignite the spark of science and physics which started this wondrous journey. A journey, which is difficult to take alone, especially at the beginning when everything might seem overwhelming, so many tracks to choose, so many steps to take, so many things to learn. Fortunately, I was not alone and there were other people with whom I could walk part of the way together. Many of our paths have parted, in part during the seemingly endless thicket due to some novel corona virus, but some of us found our way out of this maze together. Out of all of them, I want to especially thank Benedikt Holter, Florian Steininger and Markus Leuthner, who I could always ask physics-related questions and who could show me bridges over canyons that seemed uncrossable to me.

Furthermore, I would like to thank my parents for supporting me during all this time and who provided me with the chance to embark on this adventure of studying physics.

Contents

1. Introduction

A path to understanding the fundamental building blocks of nature is to study matter under extreme conditions. This can be done, for example, in heavy-ion collision, where highly energetic nuclei (e.g. Au + Au or Pb + Pb) are accelerated in particle colliders and then brought to collision. This has been done at high energies at the BNL Relativistic Heavy Ion Collider (RHIC) and the CERN Large Hadron Collider (LHC). In these collisions a new state of matter is created, called the Quark-Gluon Plasma (QGP) [1, 2].

The Quark-Gluon Plasma can be described as a system of many interacting particles, called quarks and gluons, which are the constituents of atomic nuclei. If energy becomes high enough, the total particle number is no longer conserved, and real particles can be created due to Albert Einstein's famous formula $E = mc^2$, which describes how much energy E is needed for the creation of a particle with rest mass m, and c is the speed of light in vacuum. A description of this interacting system is usually done using quantum field theory, where also short-lived particles, called *virtual particles*, appear in our formalism and need to be considered. In quantum field theory particles are described as the excitations of underlying fields.

Another way to describe such an interacting system is kinetic theory, which is a probabilistic approach, in which the fundamental object is the particle distribution function that describes the particle density for a specific point in space-time and for a specific range of momenta. This effective description is, of course, heavily related to the more fundamental underlying quantum field theory.

This underlying theory needed to describe the Quark-Gluon Plasma is called Quantum Chromodynamics (QCD), which is, in more technical terms, a non abelian gauge theory with gauge group $SU(3)$, in which the interaction between quarks is mediated by the exchange of gauge bosons, the gluons. It is a generalization of the quantum theory of electromagnetism, called Quantum Electrodynamics (QED), which is an abelian gauge theory with gauge group $U(1)$. In QCD, however, certain features that are not present in QED exist, for example *asymptotic freedom* and *self-interacting gluons*.

Asymptotic freedom means that for high energy scales the interactions between the particles become weaker and we can describe the theory in a perturbative way. This will be the basis of the effective kinetic theory [3] description that is used in this Master thesis.

Because of *self-interacting gluons* the gluonic sector of QCD is itself an interesting theory and in this thesis mostly this gluonic sector of QCD is considered, but I will give an overview of the quark sector as well.

At very early times after a heavy-ion collision, the system can be described using a classical-statistical approximation, because of the the very large number of gluons. When the system expands and cools, this approximation breaks down and the system can then be described by kinetic theory and relativistic hydrodynamics [4, 5].

Highly energetic quarks or gluons that propagate through the Quark-Gluon Plasma,

called *jets*, experience energy loss due to interactions with the QGP and can thus serve as probes of its properties [6, 7]. This is known as *jet quenching*. In this Master thesis, I will consider the momentum broadening of a jet due to its interaction with the QGP. The rate of transverse momentum broadening is quantified by the jet quenching parameter $\hat{q}$, for which we give a formal definition in Section 3.1. This parameter is also closely related to radiative energy loss and to the shear viscosity η [7].

$\hat{q}$ has been calculated for a QGP in thermal equilibrium analytically at leading [8] and next-to-leading order [9]. We know, however, that an isotropic particle distribution like in thermal equilibrium does not capture the anisotropy coming from longitudinal expansion along the beam axis [4]. Anisotropic simulations for $\hat{q}$ have been done using classical statistical simulations [10]. An effective kinetic theory description of anisotropic systems becomes more complicated due to plasma instabilities [5, 11]. A way to proceed is to use isotropic screening [12, 13], which we will also use in this thesis and explain further below. However, it should be noted that anisotropic particle distributions are shown to yield different results for the jet quenching parameter $\hat{q}$ in special cases [14].

At leading order, the processes of jet-medium interaction can be categorized as elastic scattering and inelastic radiation. These processes can be restructured to allow for a next-to-leading order treatment [15], but we will restrict ourselves to leading order here, but not to thermal equilibrium.

In this thesis we will derive a formula for $\hat{q}$ for an arbitrary jet direction from effective kinetic theory in and out of equilibrium that is then implemented and its value is extracted for different non-evolving plasmas. We compare its value in thermal equilibrium with [8] and with experimental bounds [7] using a momentum cutoff from the CUJET model [16, 17, 18] and then calculate numerically $\hat{q}$ for different isotropic particle distributions.

1.1. Outline

This thesis is organized in the following way: In Chapter 2 we provide a summary of the theoretical background, upon which this thesis is based. We give a short introduction to Quantum Chromodynamics in Section 2.1, including a short overview of non equilibrium field theory and in-medium cutting rules. We then present the effective kinetic theory description of the QGP in Section 2.2, which will provide the basis for this thesis. Although we do not consider the time-evolution of particle distribution functions, which is described by EKT, we nevertheless provide an overview of the EKT, because we do use parts of it, namely the elastic collision term, to derive $\hat{q}$. This is followed by a short introduction to the method of Monte Carlo integration in Section 2.3. We then derive a formula for $\hat{q}$ in Chapter 3, where we also discuss its behavior for large jet momenta p and how a cutoff can be implemented. After specializing our formula for $\hat{q}$ for the case of infinite jet momentum in Section 3.10 we discuss its relation to known analytical results in the soft limit in Section 3.11. We discuss the implementation in Chapter 4, where we first introduce momentum bounds to our integrals and then describe the way we implement the Monte Carlo integration. In Chapter 5 we provide numerical results and compare them to known expressions in thermal equilibrium and bounds obtained from experiments.

1.2. Conventions

We use units in which $c = \hbar = 1$ for notational convenience. By setting $c = 1$ we effectively use the same units for length and time, by additionally setting $\hbar = 1$ we can now express length and time in inverse energy. The factors c and $\hbar$ can always be restored by dimensional analysis.

We use the mostly-plus or East coast metric convention, i.e. the Minkowski metric $\eta_{\mu\nu}$ has the form

$$\eta_{\mu\nu} = \begin{pmatrix} -1 & 0 & 0 & 0 \\ 0 & 1 & 0 & 0 \\ 0 & 0 & 1 & 0 \\ 0 & 0 & 0 & 1 \end{pmatrix}, \tag{1.1}$$

to be consistent with [3, 15].

Boldface lower-case quantities denote 3-vectors, capital letters denote 4-vectors, while non bold-face lower-case quantities give the modulus of the corresponding 3-vector, e.g.

$$P^\mu = (P^0, \mathbf{p}), \qquad P^2 = -\left(P^0\right)^2 + \mathbf{p}\cdot\mathbf{p} = -\left(P^0\right)^2 + p^2. \tag{1.2}$$

A hat over a bold quantity denotes a unit vector, e.g. $\hat{\mathbf{p}}$ points in the direction of $\mathbf{p}$ and has unit length, $|\hat{\mathbf{p}}| = 1$.

Greek indices denote Lorentz indices and for them the position is important, an index can be "pulled down" with the Minkowski metric (1.1),

$$P_\mu = g_{\mu\nu}P^\nu. \tag{1.3}$$

Latin indices denote indices in the color group, their position is not important and will be at our convenience,

$$\psi_a = \psi^a. \tag{1.4}$$

2. Theoretical background

In this chapter I will summarize the theoretical background underlying the effective kinetic theory description. We will start with a short overview of the QCD Lagrangian. As it will turn out, the scattering rate is given by in medium self-energies [19], $\Pi^{>}$, $\Pi^{<}$, which can be most easily calculated by a cutting rule. For this, we need to introduce a few concepts of the real-time formalism [20], especially the r/a basis, in which the cutting rule has a very simple form [21]. We will then proceed to present the effective kinetic theory developed in [3] and make it plausible by our previous formalism.

2.1. Introduction to QCD

No text concerning the quark-gluon plasma can, of course, omit a short introduction to its underlying fundamental theory, Quantum Chromodynamics (QCD), the quantum field theory of the strong interaction. Although in this thesis we need very little QCD explicitly, some terms often pop up, so it is good to summarize them here.

A textbook treatment of QCD in vacuum is given in [22, 23, 24] and in thermal media in [25, 19].

2.1.1. The QCD Lagrangian

A usual starting point for a relativistic quantum field theory is a Lagrangian density $\mathcal{L}$, for QCD it has the form [23]

$$\mathcal{L} = \bar{\psi}\left(i\not{D}\right)\psi - \frac{1}{4}\left(F^i_{\mu\nu}\right)^2 - m\bar{\psi}\psi. \tag{2.1}$$

This compact form hides some important structure and the rest of this section is devoted to its explanation.

First, $\left(F^i_{\mu\nu}\right)^2$ is a short notation for $F^i_{\mu\nu}F^{\mu\nu}_i$.

ψ is a spinor field, an element of an N_C dimensional vector space and can be equipped with an additional label f labelling different quark flavors. All together, this complex object can be represented by its components using index notation,

$$\psi(X)_{\alpha,a,f}, \tag{2.2}$$

where the three indices are its spinor, color and flavor index, respectively.

Let us begin with the first index, the spinor index. Because we want our theory to be Lorentz invariant we need a way to apply a Lorentz transformation to our object. There are different representations of the Lorentz group and as it turns out for fermions we need an object ψ_α that lives in a vector space on which the Lorentz group acts in its

spinor representation, which can be represented by 4×4 dimensional matrices satisfying a Clifford algebra relation,

$$\{\gamma^\mu, \gamma^\nu\} := \gamma^\mu\gamma^\nu + \gamma^\nu\gamma^\mu = -2\eta^{\mu\nu}. \tag{2.3}$$

Note that many of the signs are due to convention. The negative sign in this relation agrees with [22], but not with [23], and is due to our choice of the Minkowski metric, (1.1). Note that $(\gamma^\mu)_{\alpha\beta}$ are matrices with the indices α, β, which are not Lorentz indices but we call them *spinor* indices. $\bar{\psi}$ in the Lagrangian (2.1) is numerically defined to be

$$\bar{\psi} := \psi^\dagger\gamma^0, \tag{2.4}$$

where $\psi^\dagger$ means complex conjugation and transposition. $\not{D}$ is defined as

$$\not{D} = \gamma^\mu D_\mu. \tag{2.5}$$

The Lagrangian density (2.1) was constructed in such a way that it is symmetric under specific symmetry transformations, called gauge transformations under the gauge group $SU(N_C)$,

$$\psi(x) \to U(x)\psi(x), \qquad A_\mu(x) \to U(x)A_\mu(x)U^\dagger(x) + \frac{i}{g}U(x)\partial_\mu U^\dagger(x), \tag{2.6}$$

where $U(x)$ is an element of the Lie group $SU(N_C)$, the group of all $N_C \times N_C$ unitary matrices with unit determinant. For QCD, $N_C = 3$, but we will leave it arbitrary, since it provides no additional complications. The gauge field A_μ, which is a generalization of the vector potential in electrodynamics [26], is an element of the Lie algebra[1] $\mathfrak{su}(N_C)$ corresponding to the gauge Lie group. As such, it can be represented by $N_C \times N_C$ matrices, which allows us to write (2.6). To distinguish physical degrees of freedom, we can expand the gauge field in terms of the Lie algebra basis vectors t_a,

$$A_\mu = A_\mu^a t^a. \tag{2.7}$$

The basis vectors, also called *generators*, can be represented by $N_C \times N_C$ matrices and satisfy the commutation relation

$$[t^a, t^b] := t^a t^b - t^b t^a = i f^{abc} t^c, \tag{2.8}$$

where f^{abc} are called *structure coefficients*. Note that we do not write the matrix indices explicitly, $(t^a)_{bc} \to t^a$.

The gauge field A_μ has thus $N_C^2 - 1$ independent components A_μ^a, which can be assembled in an $N_C^2 - 1$ dimensional vector.

The quantity D_μ is called *covariant derivative* and is defined as

$$D_\mu := \partial_\mu - igA_\mu(X). \tag{2.9}$$

In principle, the Lie algebra commutation relations (2.8) *define* the abstract objects t^a. For practical purposes it is convenient to choose a matrix *representation* of the abstract

[1] An algebra is a vector space endowed with a product structure, in this case (2.8). A condensed introduction to Lie groups and Lie algebras can be found in every QFT book, e.g. [22, 23, 24], for a more precise mathematical treatment, see e.g. [27].

elements t^a. Previously, we have referred to all objects as $N_C \times N_C$ matrices, this representation is called the *fundamental* representation. (2.8) can also be represented by a different set of matrices, consisting of the structure constants themselves,

$$(t^a)^{bc} \to (T^a)^{bc} = (-if^a)^{bc}, \tag{2.10}$$

which is called the *adjoint* representation. It consists of $N_C^2 - 1$ $(N_C^2 - 1) \times (N_C^2 - 1)$ matrices that we denote as T^a, whereas the fundamental representation consists of $N_C^2 - 1$ $N_C \times N_C$ matrices that we denote as t^a.

The covariant derivative (2.9) can also be represented in the fundamental or in the adjoint representation, depending on how the gauge field is represented, $A_\mu = A_\mu^a t^a$ or $A_\mu = A_\mu^a T^a = -iA_\mu^a f^{abc}$.

Then the covariant derivative acts on the components ψ_a as

$$(D_\mu)_{ab} \psi_b = \left(\delta_{ab}\partial_\mu - igA_\mu^c (t^c)_{ab}\right) \psi_b \tag{2.11}$$

and on the gauge field components A_μ^a as

$$(D_\mu)_{ab} A_\nu^b = \left(\delta_{ac}\partial_\mu + gf^{abc}A_\mu^b\right) A_\nu^c. \tag{2.12}$$

Thus, on the N_C-dimensional color vector ψ_a the covariant derivative acts in its fundamental representation, and on the $N_C^2 - 1$-dimensional color vector A_μ^a the covariant derivative acts in its adjoint representation. Therefore, we often refer to ψ as a field *in the* fundamental representation and A_μ as a field *in the* adjoint representation. We call the dimension of the vector space on which a representation acts its dimension d, d_A and d_F denote the dimension of the adjoint and fundamental representation. There is another number that can be assigned to every representation, the *quadratic casimir* C_R, defined to be $t_a t_a = C_F \mathbb{I}$, $T_a T_a = C_A \mathbb{I}$, where $\mathbb{I}$ is the unit matrix. Furthermore, the generators obey the relation $\mathrm{Tr}\,(t_a t_b) = t_F \delta_{ab}$, $\mathrm{Tr}\,(T_a T_b) = t_A \delta_{ab}$, and t_F, t_A is called the *index*. For the fundamental and adjoint representation, those quantities take the values

$$\begin{aligned} d_F &= C_A = t_A = N_C, \\ C_F &= \frac{N_C^2 - 1}{2N_C}, \\ d_A &= N_C^2 - 1, \\ t_F &= \frac{1}{2}. \end{aligned} \tag{2.13}$$

In the Lagrangian (2.1) there appears also a generalization of the field-strength tensor $F_{\mu\nu}$ of electrodynamics,

$$F_{\mu\nu} = \partial_\mu A_\nu - \partial_\nu A_\mu - ig\left[A_\mu, A_\nu\right], \tag{2.14}$$

or, its components $F_{\mu\nu} = F_{\mu\nu}^a t^a$,

$$F_{\mu\nu}^c = \partial_\mu A_\nu^c - \partial_\nu A_\mu^c + gf^{abc}A_\mu^a A_\nu^b. \tag{2.15}$$

We also define, for later convenience,

$$\alpha := \frac{g^2}{4\pi}, \tag{2.16}$$

$$\lambda := g^2 N_C. \tag{2.17}$$

The third index in $\psi(X)_{\alpha,a,f}$ denotes the flavor of the corresponding quark, i.e. we consider a plasma consisting of different quarks (with in principle different masses). The flavor index is just a label that labels these different quark fields. We will denote the total number of quark flavors by N_f.

2.1.2. Quantization

One way of quantizing a classical theory is to take a Hamiltonian description, promote (generalized) position q and momentum variables p to operators, and then impose canonical commutation relations,

$$[\hat{q}, \hat{p}] = i. \tag{2.18}$$

The same can be done for fields, though we usually do not write the hat explicitly,

$$\psi \to \hat{\psi}, \qquad\qquad A \to \hat{A}. \tag{2.19}$$

Then the thermal expectation value of some operator $\hat{A}$ is given by

$$\langle \hat{A} \rangle_\beta = \frac{1}{Z(\beta)} \operatorname{Tr}\left(\hat{A} e^{-\beta \hat{H}}\right). \tag{2.20}$$

The trace can be represented as a path integral,

$$\langle \hat{A} \rangle = \frac{1}{Z} \int_{\mathfrak{C}} \mathcal{D}\phi \, e^{iS} A, \tag{2.21}$$

$$Z = \int_{\mathfrak{C}} \mathcal{D}\phi \, e^{iS}, \tag{2.22}$$

where we denote by ϕ a collection of fields and $\mathfrak{C}$ denotes a path in the (complex) time plane and suitable boundary conditions have to be imposed, for thermal equilibrium and time-independent $\hat{A}$, we can think of $e^{-\beta H}$ as a time evolution operator in negative imaginary time, from t_0 to $t_0 - i\beta$. For the trace, we then need to have the boundary conditions $\phi(X^0; \mathbf{x}) = \phi(X^0 - i\beta; \mathbf{x})$ for bosonic fields and $\phi(X^0; \mathbf{x}) = -\phi(X^0 - i\beta; \mathbf{x})$ for fermionic fields.

S denotes the action, obtained from the Lagrangian density via

$$S = \int \mathrm{d}^4 X \, \mathcal{L}(X). \tag{2.23}$$

For gauge theories, we factor out physically equivalent field configurations (related by gauge transformations) by the Faddeev-Popov procedure, which results in two additional "ghost" fields η, $\bar{\eta}$ and an additional term in the Lagrangian that depends on the chosen gauge. For covariant gauges, we make the replacement in (2.1)

$$\begin{aligned} \frac{1}{4}\left(F^a_{\mu\nu}\right)^2 \to \frac{1}{4}\left(F^a_{\mu\nu}\right)^2 + \frac{1}{2\xi}\left(\partial^\mu A^a_\mu\right)^2 \\ + \bar{\eta}_a(X)\left[\partial^2 \delta_{ab} + g f_{abc} A^c_\mu(X) \partial_\mu\right] \eta_b(X). \end{aligned} \tag{2.24}$$

After the quantization procedure, we have the operators $A_\mu(x)$, $\bar{\psi}_f(x)$, $\psi_f(x)$, with which we then proceed to define different *propagators*[2] [20, 28] or *correlation functions*,

$$D^{>ab}_{\mu\nu}(X,Y) = \langle A^a_\mu(X) A^b_\nu(Y)\rangle, \tag{2.25}$$
$$D^{<ab}_{\mu\nu}(X,Y) = \langle A^b_\nu(Y) A^a_\mu(X)\rangle, \tag{2.26}$$
$$D^{Rab}_{\mu\nu}(X,Y) = \Theta(X^0-Y^0)\langle [A^a_\mu(X) A^b_\nu(Y)]\rangle, \tag{2.27}$$
$$D^{Aab}_{\mu\nu}(X,Y) = -\Theta(Y^0-X^0)\langle [A^a_\mu(X) A^b_\nu(Y)]\rangle, \tag{2.28}$$
$$\begin{aligned} D^{ab}_{\mu\nu}(X,Y) &= \langle \hat{\mathcal{T}} A^a_\mu(X) A^b_\nu(Y)\rangle \\ &= \Theta(X^0-Y^0) D^{>ab}_{\mu\nu}(X,Y) + \Theta(Y^0-X^0) D^{<ab}_{\mu\nu}(X,Y). \end{aligned} \tag{2.29}$$

We will not need most of them here, they are just written down for completeness. Note that in these expressions, the As are operators and thus cannot be simply exchanged. D^R is called *retarded propagator*, and D^A is called *advanced propagator*. $\hat{\mathcal{T}}$ is called the time-ordering symbol, which orders the field operators according to their time arguments. $\Theta(x)$ is the step function, defined to be

$$\Theta(x) = \begin{cases} 1, & x \geq 0 \\ 0, & x < 0 \end{cases}. \tag{2.30}$$

For completeness, we also give the corresponding propagators for fermionic fields, but for notational convenience we suppress their spinor and color indices,

$$S^>(X,Y) = \langle \psi(X)\bar{\psi}(Y)\rangle, \tag{2.31}$$
$$S^<(X,Y) = -\langle \bar{\psi}(Y)\psi(X)\rangle, \tag{2.32}$$
$$S^R(X,Y) = \Theta(X^0-Y^0)\langle \{\psi(X),\bar{\psi}(Y)\}\rangle, \tag{2.33}$$
$$S^A(X,Y) = -\Theta(Y^0-X^0)\langle \{\psi(X),\bar{\psi}(Y)\}\rangle, \tag{2.34}$$
$$\begin{aligned} S(X,Y) &= \langle \hat{\mathcal{T}} \psi(X)\bar{\psi}(Y)\rangle \\ &= \Theta(X^0-Y^0) S^>(X,Y) + \Theta(Y^0-X^0) S^<(X,Y). \end{aligned} \tag{2.35}$$

For the path integral it is convenient to define two different sets of fields, A_1 and A_2:

Let us start by looking more closely at the definition for $D^> = \mathrm{Tr}\,(\mathcal{D}\phi(X)\phi(Y))$, which we have written in terms of arbitrary fields ϕ with arbitrary additional indices and $\mathcal{D} = e^{-\beta H}$ is the density operator[3]. The field operators $\phi(X)$ and $\phi(Y)$ are in the Heisenberg picture and might have different time arguments $X^0 \neq Y^0$. We can relate them to the operators in the Schrödinger picture via $\phi(X) = e^{i(X^0-t_0)H}\phi(t_0,\mathbf{x})e^{-i(X^0-t_0)H} = U(t_0-X^0)\phi(t_0,\mathbf{x})U(X^0-t_0)$, where

$$U(t) = e^{-iHt} \tag{2.36}$$

[2] Instead of the Feynman propagator at zero temperature, we also need to define additional propagators. Note that there are different (metric) conventions in [20] and [28], and we will stick to those in [20].

[3] Following [28] we use the symbol $\mathcal{D}$ for the density operator. It should not be confused with the symbol $\mathcal{D}$ in the integration measure of path integrals.

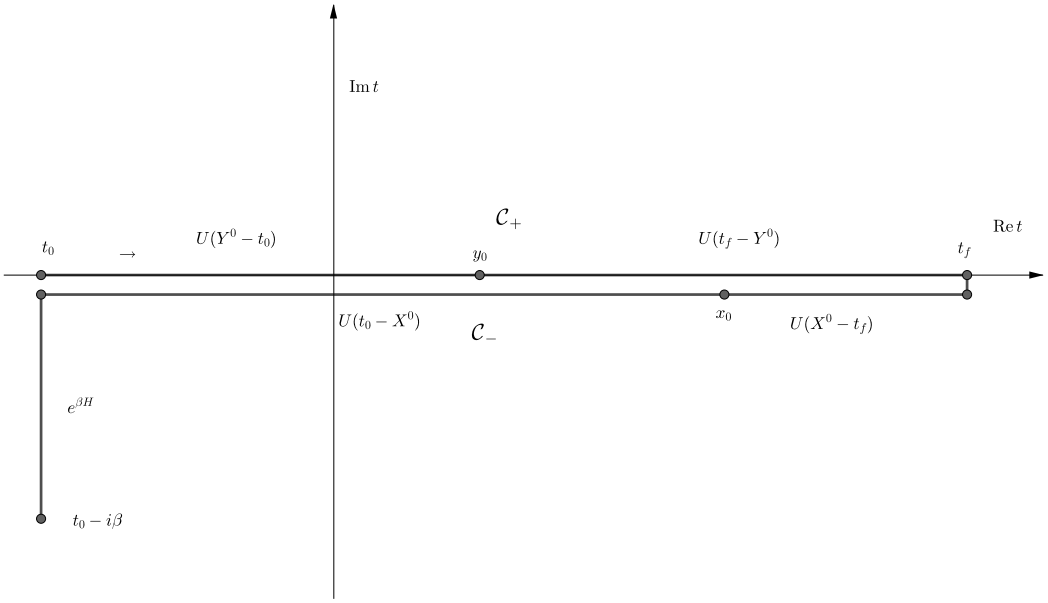

Figure 2.1.: Complex time-path for the propagator $D^>(X,Y)$

is the time-evolution operator, which evolves a state in time, $|\psi(t)\rangle = U(t)\,|\psi(0)\rangle$. Therefore

$$D^>(X,Y) = \mathrm{Tr}\left(\mathcal{D}\phi(X)\phi(Y)\right) = \mathrm{Tr}\left(\mathcal{D}e^{i(X^0-t_0)H}\phi(t_0,\mathbf{x})e^{i(Y^0-X^0)H}\phi(t_0,\mathbf{y})e^{-i(Y^0-t_0)H}\right), \tag{2.37}$$

where we can insert $\mathbb{I} = \sum_m |m,t\rangle\langle m,t|$,

$$\begin{aligned} D^>(X,Y) = \sum_{m,n,o,p,q} &\langle m,t_0|\,\mathcal{D}\,|n,t_0\rangle\,\langle n,t_0|\,U(t_0-X^0)\,|o,X^0\rangle\,\langle o,X^0|\,\phi(t_0,\mathbf{x})\,|p,X^0\rangle \\ \times &\langle p,X^0|\,U(X^0-Y^0)\,|q,Y^0\rangle\,\langle q,Y^0|\,\phi(t_0,\mathbf{y})\,|r,Y^0\rangle\,\langle r,Y^0|\,U(Y^0-t_0)\,|m,t_0\rangle\,. \end{aligned} \tag{2.38}$$

The time evolution from state $|m,t_0\rangle$ to $|r,Y^0\rangle$ can be written as a path integral,

$$\langle r|\,U(Y^0-t_0)\,|m\rangle = \int_{|m,t_0\rangle}^{|r,Y^0\rangle} \mathcal{D}e^{\,i\int_{t_0}^{Y^0}\mathrm{d}t\int\mathrm{d}^3\mathbf{x}\mathcal{L}(X)}. \tag{2.39}$$

We can then plug these time-evolution operators together along a path, using the multiplicative property $U(t_1)U(t_2) = U(t_1+t_2)$. We first go on $\mathcal{C}_+$ from an initial time t_0 to a final time t_f, which must be greater than X^0 and Y^0, then we go back to the initial time t_0 on the time-path $\mathcal{C}_-$. The extension of the time-path to t_f is possible because $U(X^0-y_0) = U(x_0-t_f)U(t_f-Y^0)$.

We can interpret $\mathcal{D} = e^{\beta H}$ as a time-evolution operator with an imaginary time, therefore in this case we extend the time-contour integral to $-i\beta$, see also figure 2.1 for the integration contour, for a more detailed description of the time path we refer to [28].

We can then give a more precise definition of the path integral along this time-path (see [20]):

We introduce two different sets of fields ("field doubling") ϕ_1 and ϕ_2 on the different time-paths $\mathcal{C}_+$ and $\mathcal{C}_-$. In thermal equilibrium we have additional fields ϕ_E on the time-path from t_0 to $t_0 - i\beta$. The full path integral partition function can then be written as

$$Z = \int \mathcal{D}\phi_E e^{iS[\phi_E]} \int \mathcal{D}\phi_1 \mathcal{D}\phi_2 e^{i[S[\phi_1]-S[\phi_2]]}. \tag{2.40}$$

In the path integral, the 1-fields and 2-fields do not mix, so we have 1-vertices, where only 1-fields meet and 2-vertices for 2-fields only. But these 1-vertices and 2-vertices can be connected by propagators.

We can then obtain four different correlation functions depending on the fields we choose,

$$\langle \phi_1(X)\phi_1(Y)\rangle = D(X,Y) \tag{2.41}$$

is the "normal" full (time-ordered) propagator, because the path-integral automatically produces a time-ordering along the contour. Similarly,

$$\langle \phi_1(X)\phi_2(Y)\rangle = D^<(X,Y), \tag{2.42}$$

because the path-integral automatically orders $\hat{\phi}_1(X)\hat{\phi}_2(Y) \to \hat{\phi}_2(Y)\hat{\phi}_1(X)$, because the time-argument of any 2-field is later on the time-path than any time-argument of any possible 1-field.

These propagators can be arranged in a matrix,

$$\mathbf{D}(X,Y) = \begin{pmatrix} \langle \phi_1(X)\phi_1(Y)\rangle & \langle \phi_1(X)\phi_2(Y)\rangle \\ \langle \phi_2(X)\phi_1(Y)\rangle & \langle \phi_2(X)\phi_2(Y)\rangle \end{pmatrix} = \begin{pmatrix} D(X,Y) & D^<(X,Y) \\ D^>(X,Y) & \bar{D}(X,Y) \end{pmatrix}. \tag{2.43}$$

Here, $\bar{D}(X,Y)$ denotes the anti time-ordered correlation function.

These propagators are actually not independent of each other[29], of course, the time-ordered $D(X,Y)$ and anti time-ordered $\bar{D}(X,Y)$ correlation functions can be expressed in terms of $D^>$ and $D^<$ with corresponding step functions.

Instead of working in the 1/2-basis, we can perform a linear transformation to arrive at the r/a basis[4] [20, 21, 29]

$$\phi_r = \frac{1}{2}(\phi_1 + \phi_2), \quad \phi_a = \phi_1 - \phi_2, \quad \phi_1 = \phi_r + \frac{1}{2}\phi_a, \quad \phi_2 = \phi_r - \frac{1}{2}\phi_a. \tag{2.44}$$

In this basis, we obtain vertices that mix the a- and r-fields, because we subtract the actions,

$$S[\phi_1] - S[\phi_2] = S\left[\phi_r + \frac{1}{2}\phi_a\right] - S\left[\phi_r - \frac{1}{2}\phi_a\right]. \tag{2.45}$$

For example, in our original Lagrangian (2.1) there is an interaction term

$$\bar{\psi}_1 \gamma^\mu (A_1)^c_\mu t^c \psi_1 - \bar{\psi}_2 \gamma^\mu (A_2)^c_\mu t^c \psi_2, \tag{2.46}$$

[4] The r/a basis is called physical representation in [29].

which becomes (we suppress again all indices other than r/a)

$$\bar{\psi}_r \not{A}_r \psi_a + \bar{\psi}_r \not{A}_a \psi_r + \bar{\psi}_a \not{A}_r \psi_r + \frac{1}{8} \bar{\psi}_a \not{A}_a \psi_a. \tag{2.47}$$

Due to the form of the transformation (2.44), we obtain only vertices with odd number of a-fields.

The propagators, e.g. D_{ar}, now also carry these field indices and we shall represent them pictorially by an arrow that points towards the r-field,

$$D_{ar}(x,y) = \quad a \longrightarrow r \ .$$

These propagators can be arranged in a matrix,

$$\mathbf{D}(X,Y) = \begin{pmatrix} D_{rr} & D_{ra} \\ D_{ar} & D_{aa} \end{pmatrix} = \begin{pmatrix} \frac{1}{2}\left(D^{>} + D^{<}\right) & D^{R} \\ D^{A} & 0 \end{pmatrix}. \tag{2.48}$$

The fact that $D_{aa} = 0$ reduces the number of diagrams one has to compute. Note also that we obtain in this basis the retarded (and advanced) propagators that we defined earlier.

The propagators can also be Fourier transformed,

$$\tilde{D}(P) = \int \mathrm{d}^4(X-Y)\, e^{-iP\cdot(X-Y)} D(X,Y). \tag{2.49}$$

For non-homogeneous systems this needs to be replaced by a Wigner transform, for details we refer to [28].

2.1.3. Self-energy

Up until now we have defined our propagators, but we have not actually talked about if we can easily calculate them. As it turns out, for an interacting theory (QCD for example) the path integral cannot be done in most cases. So what we usually do in physics when a problem is too difficult to solve is to reduce it to a problem we can solve: The free theory! Free meaning no interactions. It turns out that the path integral becomes Gaussian and can be done in that case, which gives the *free propagator* D_0. And for weak coupling we can apply perturbation theory to obtain the *full propagator* D and other more interesting quantities. The difference between those two quantities is in some sense - which we define below - given by the *self-energy*.

The self-energy $\Pi(x,y)$ is defined via the Dyson equation[5]

$$D^{-1}(X,Y) = D_0^{-1}(X,Y) + i\Pi(X,Y), \tag{2.50}$$

or, equivalently,

$$D(X,Y) = \frac{1}{D_0^{-1}(X,Y) + i\Pi(X,Y)}, \tag{2.51}$$

[5]There are different conventions on how the signs and factor is are defined. Here we quote the expression from [20].

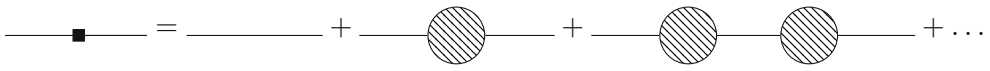

Figure 2.2.: The *full propagator* on the left-hand side is given by the sum of *free propagators* with insertions of *self-energies* (hatched blobs).

which provides a relation between the full propagator D, the free propagator D_0 and the self-energy Π. The fraction is a short notation for the geometric series

$$\begin{aligned} D(X,Y) = D_0(X,Y) &+ \int \mathrm{d}^4 Z_1\, \mathrm{d}^4 Z_2\, D_0(X,Z_1)\Pi(Z_1,Z_2)D_0(Z_2,Y) \\ &+ \int_{Z_1,Z_2,Z_3,Z_4} D_0(X,Z_1)\Pi(Z_1,Z_2)D_0(Z_2,Z_3)\Pi(Z_3,Z_4)D_0(Z_4,Y) + \dots, \end{aligned} \tag{2.52}$$

which represents repeated insertions of Π diagrams that are connected via free propagators. Pictorially, this equation is represented in figure 2.2. We integrate over all intermediate spacetime points and represent the individual pieces by diagrams. A propagator is represented by a line, a self-energy via a hatched blob.

On the other hand, let us think of the full propagator as the fully connected two-point function. We can build this function out of parts that are *one-particle irreducible*, meaning that we have to cut through at least two lines for them to fall apart. Those one-particle irreducible parts have to be connected by free propagators. By looking again at figure 2.2, we realize that the self-energy is given by the one-particle irreducible diagrams (to which we can attach two legs).

Similarly to the propagator, we can define $\Pi^>$ and $\Pi^<$,

$$\Pi(X,Y) = \Theta(X^0 - Y^0)\Pi^>(X,Y) + \Theta(Y^0 - X^0)\Pi^<(X,Y). \tag{2.53}$$

In the r/a basis, the in-medium self-energy $\tilde{\Pi}^>(k)$ is given by the *cutting rule* (see [21, 20],

$$\begin{aligned} \tilde{\Pi}^>(K) = \sum_n \frac{1}{n!} &\left(\prod_{j=1}^{n} \int \frac{\mathrm{d}^4 Q_j}{(2\pi)^4} \right) (2\pi)^4 \delta^4(Q_1 + \dots + Q_n - K) \\ &\times \mathcal{M}_{ar\dots r}(P; Q_1, \dots, Q_n)\mathcal{M}_{ar\dots r}(-P; -Q_1, \dots, -Q_n) \\ &\times \tilde{D}^>(Q_1) \dots \tilde{D}^>(Q_n) \end{aligned} \tag{2.54}$$

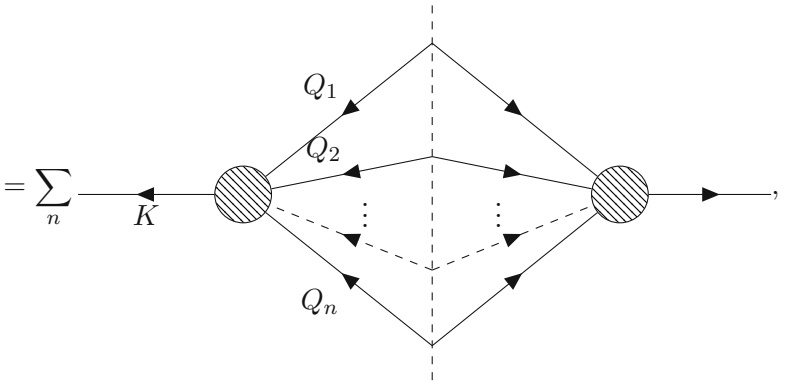

(2.55)

where $\mathcal{M}_{ar\ldots r}$ are *fully retarded amplitudes*, i.e. they represent a matrix element where we have exactly one a-index, the sum runs over all the propagators $\tilde{D}^{>}(Q_1)\ldots$ that are inserted between the two diagrams, or alternatively, over all the lines that are *cut* and then replaced by $\tilde{D}^{>}(Q_1)\ldots$.

2.1.4. Perturbative expansion and hard thermal loops

Because we cannot solve QCD exactly, we need to use perturbation theory, which works if the coupling g is small enough. Luckily, for QCD, this is the case for high enough temperatures, which is a property called *asymptotic freedom*. We can then expand all quantities of interest in terms of free propagators D_0 and obtain corrections that are proportional to the coupling g, g^2, ... This procedure is usually done in a loop expansion, because every vertex comes with a factor g or g^2 and thus increases the order in perturbation theory.

It turns out, however, that some diagrams that seem to be of higher order in the coupling constant will actually have the same magnitude as tree-level diagrams for non zero temperature [25]. This is due to hard thermal loops (HTL), important contributions when the internal momentum is hard ($\sim T$) and the external lines are soft ($\sim gT$). One needs to include the HTL self-energy in the propagator, for the retarded propagator, this reads [20]

$$D^R(P) = \frac{1}{[D_0^R(P)]^{-1} + i\Pi^R(P)}, \tag{2.56}$$

where Π should be evaluated in the HTL limit, which means that one has to expand for soft external momenta $Q \sim gT \ll P \sim T$.

The resulting HTL propagators G_R in strict Coulomb gauge are given by [20]

$$D_R^{00}(Q) = \frac{i}{q^2 + m_D^2\left(1 - \frac{\omega}{2q}\ln\left(\frac{\omega+q+i\epsilon}{\omega-q+i\epsilon}\right)\right)}, \tag{2.57}$$

$$D_R^{ij}(Q) = \left(\delta^{ij} - \hat{q}^i\hat{q}^j\right)D_R^T(Q) = \left.\frac{i\left(\delta^{ij} - \hat{q}^i\hat{q}^j\right)}{\omega^2 - q^2 - \frac{m_D^2}{2}\left(\frac{\omega^2}{q^2} - \left(\frac{\omega^2}{q^2} - 1\right)\frac{\omega}{2q}\ln\frac{\omega+q}{\omega-q}\right)}\right|_{\omega=\omega+i\epsilon}, \tag{2.58}$$

where $\omega = Q^0$ and m_D is the leading-order *Debye mass*, which reads in general (also out of equilibrium) [3]

$$m_D^2 = \sum_s 2d_s g^2 \frac{C_s}{d_A}\int \frac{\mathrm{d}^3\mathbf{p}}{2p(2\pi)^3} f_s(\mathbf{p}), \tag{2.59}$$

where the sum runs over g (gluons) and all quark flavors in the plasma. d_s and C_s are the dimension and quadratic casimir of the corresponding representation of s, see (2.13).

The Debye mass reduces in thermal equilibrium to [15]

$$m_D^2 = \frac{g^2T^2}{3}\left(N_C + \frac{N_f}{2}\right). \tag{2.60}$$

The HTL self-energies can also be constructed directly from kinetic theory without using diagrammatic techniques, for a review see [28].

2.1.5. A contribution to the self-energy diagram

Let us look at a specific term appearing in the self-energy, according to the cutting rule (2.54),

$$\eta^{\sigma\epsilon}\Pi^{>}_{\sigma\epsilon}(P) \ni \frac{1}{6}\int \frac{\mathrm{d}^4Q_1\,\mathrm{d}^4Q_2\,\mathrm{d}^4Q_3}{(2\pi)^{12}} \times \tilde{D}^{>}_{\alpha\mu}(Q_1)\tilde{D}^{>}_{\beta\nu}(Q_2)\tilde{D}^{>}_{\gamma\rho}(Q_3)(2\pi)^4\delta^4(Q_1+Q_2+Q_3-P) \tag{2.61}$$

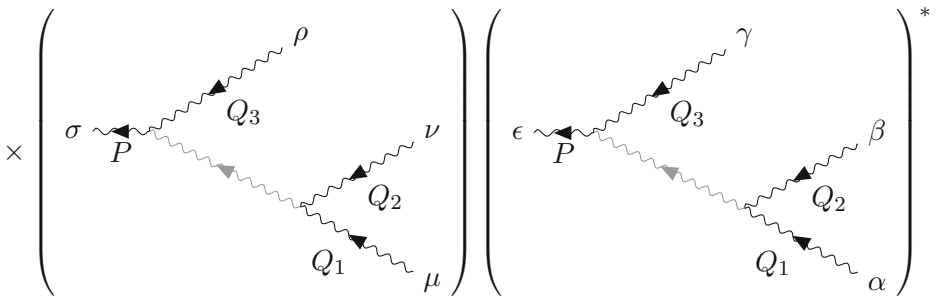

This is, for simplicity, a diagram consisting only of gluons. The arrows denote propagators in the r/a basis and the gray wavy-line in the middle is the only propagator that is not amputated when computing the amplitudes. In the r/a basis a propagator with one a and one r leg (or with one arrow) is a retarded propagator, in which we should also include the retarded HTL self-energy, (2.56).

Now we can still massage this expression a bit. Let us insert the Kadanoff-Baym ansatz[6] [30, 31],

$$\tilde{D}^{>}(Q_1) = \Big(1 \pm \tilde{f}(Q_1)\Big)\,\rho(Q_1), \tag{2.62}$$

where $\rho(Q_1)$ is called spectral function and $\tilde{f}(Q_1)$ will become the particle distribution, when Q_1 is on-shell. The upper sign is for bosons, the lower sign for fermions, which corresponds to Bose enhancement and Fermi blocking factors. In the quasiparticle approximation [28] we obtain

$$\rho(Q) = 2\pi\epsilon(Q^0)\delta\left((Q^0)^2 - E_{\mathbf{q}}^2\right) g(Q), \tag{2.63}$$

where $g(Q)$ might be an additional function of Q, e.g. for fermions [19] $g(Q) = \not{Q} + m$, for gluons (in Feynman gauge) $g(Q) = -\eta_{\mu\nu}$, and $\epsilon(Q^0) = \mathrm{sign}(Q^0)$. $E_{\mathbf{q}} > 0$ denotes the energy of the quasiparticle that depends on $\mathbf{q}$. We assume $E_{\mathbf{q}} = E_{-\mathbf{q}}$. Inserting this for the gluonic propagators in (2.62) means that we can write the two diagrams as $\frac{|\mathcal{M}|^2}{\nu}$, if we define $|\mathcal{M}|^2$ to be summed over all initial and final polarizations and colors. Therefore, for an ingoing particle with a definite spin and color state, we need to divide

[6] This is motivated by the fact that in thermal equilibrium we can use a thermal particle distribution. Note that here we are more general, $\tilde{f}(Q)$ does not have to be the Bose-Einstein or Fermi-Dirac distribution. This is a way to define the (time-dependent) particle distribution. In fact, these quantities can also be position-dependent, then the Fourier transform (2.49) should be replaced by a Wigner transform, see also [28].

by ν, which is defined as the number of spin times color states for the ingoing particle species. $|\mathcal{M}|^2$ is thus

$$|\mathcal{M}|^2 = \eta_{\alpha\mu}\eta_{\beta\nu}\eta_{\gamma\rho}\eta_{\sigma\epsilon} \tag{2.64}$$

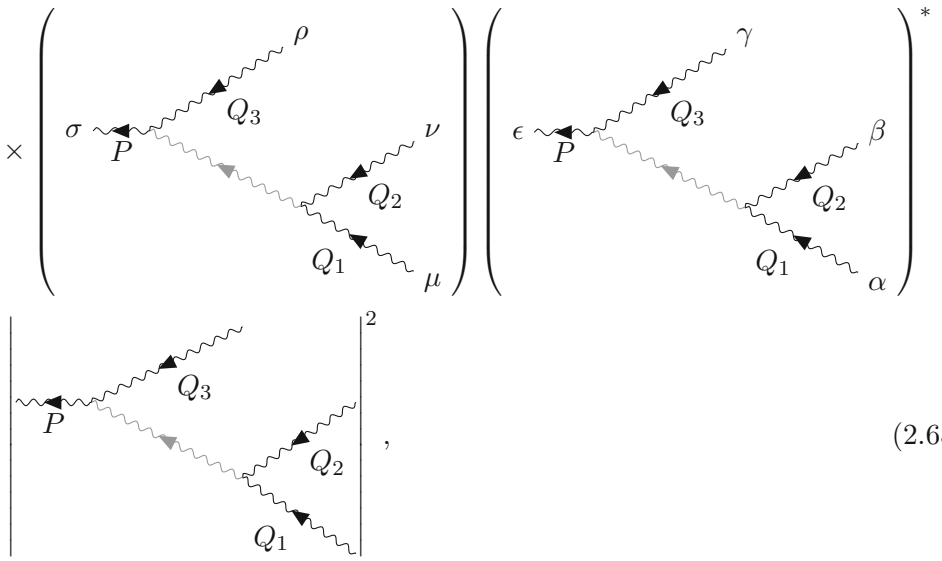

$$= \left| \begin{array}{l} \\ \\ \\ \\ \end{array} \right|^2 , \tag{2.65}$$

with the corresponding legs contracted and summed over all colors (and polarizations).

The delta function can be expanded,

$$\rho(Q) = 2\pi g(Q)\frac{1}{2E_{\mathbf{q}}}\left[\delta(Q^0 - E_{\mathbf{q}}) - \delta(Q^0 + E_{\mathbf{q}})\right], \tag{2.66}$$

with which we can write $\tilde{D}^>$ as

$$\tilde{D}^>(Q) = \rho(Q)\left[\Theta(Q^0)\left(1 \pm \tilde{f}(Q)\right) + \Theta(-Q^0)\left(1 \pm \tilde{f}(Q)\right)\right] \tag{2.67}$$

With

$$\tilde{D}^>(-Q) = \left(1 \pm \tilde{f}(-Q)\right)\rho(-Q) = \tilde{D}^<(Q) = \tilde{f}(Q)\rho(Q), \tag{2.68}$$

$$\rho(-Q) = -\rho(Q) \tag{2.69}$$

we obtain

$$\tilde{f}(Q) = -\left(1 \pm \tilde{f}(-Q)\right). \tag{2.70}$$

Inserting this into (2.67) yields

$$\tilde{D}^>(Q) = \rho(Q)\left[\Theta(Q^0)\left(1 \pm \tilde{f}(Q)\right) - \Theta(-Q^0)\tilde{f}(-Q)\right] \tag{2.71}$$

$$= 2\pi g(Q)\frac{1}{2E_{\mathbf{q}}}\left[\delta(Q^0 - E_{\mathbf{q}})\left(1 \pm \tilde{f}(Q)\right) + \delta(Q^0 + E_{\mathbf{q}})\tilde{f}(-Q)\right] \tag{2.72}$$

$$= 2\pi g(Q)\frac{1}{2E_{\mathbf{q}}}\left[\delta(Q^0 - E_{\mathbf{q}})\left(1 \pm f(\mathbf{q})\right) + \delta(Q^0 + E_{\mathbf{q}})f(-\mathbf{q})\right]. \tag{2.73}$$

Now the Q^0 component in all $\tilde{f}$ is always positive because of the delta function,

$$\delta(Q^0 - E_\mathbf{q})\tilde{f}(Q^0, \mathbf{q}) = \delta(Q^0 - E_\mathbf{q})\tilde{f}(E_\mathbf{q}, \mathbf{q}), \tag{2.74}$$

$$\delta(Q^0 + E_\mathbf{q})\tilde{f}(-Q^0, -\mathbf{q}) = \delta(Q^0 + E_\mathbf{q})\tilde{f}(E_\mathbf{q}, -\mathbf{q}). \tag{2.75}$$

This allows us to define

$$f_\mathbf{q} := f(\mathbf{q}) := \tilde{f}(E_\mathbf{q}, \mathbf{q}). \tag{2.76}$$

The Q^0 integrals in (2.62) can now be performed, where for every $\tilde{D}^>$ the delta function removes the Q^0 integral and yields two terms according to (2.73),

$$\begin{aligned}
&\frac{1}{6\nu}\int \frac{\mathrm{d}^3\mathbf{q}_1\,\mathrm{d}^3\mathbf{q}_2\,\mathrm{d}^3\mathbf{q}_3}{(2\pi)^9 2E_{\mathbf{q}_1}2E_{\mathbf{q}_2}2E_{\mathbf{q}_3}}(2\pi)^4\delta^3(\mathbf{q}_1+\mathbf{q}_2+\mathbf{q}_3-P)\,|\mathcal{M}|^2 \\
&\quad\times\Big\{\delta(E_{\mathbf{q}_1}+E_{\mathbf{q}_2}+E_{\mathbf{q}_3}-E_\mathbf{p})\,[(1\pm f_{\mathbf{q}_1})(1\pm f_{\mathbf{q}_2})(1\pm f_{\mathbf{q}_3})] \\
&\qquad+\delta(-E_{\mathbf{q}_1}+E_{\mathbf{q}_2}+E_{\mathbf{q}_3}-E_\mathbf{p})\,[f_{-\mathbf{q}_1}(1\pm f_{\mathbf{q}_2})(1\pm f_{\mathbf{q}_3})] \\
&\qquad+\text{ similar with } \mathbf{q}_1\leftrightarrow\mathbf{q}_2,\quad \mathbf{q}_1\leftrightarrow\mathbf{q}_3 \\
&\qquad+\delta(-E_{\mathbf{q}_1}-E_{\mathbf{q}_2}+E_{\mathbf{q}_3}-E_\mathbf{p})\,[f_{-\mathbf{q}_1}f_{-\mathbf{q}_2}(1\pm f_{\mathbf{q}_3})] \\
&\qquad+\text{ similar with } \mathbf{q}_2\leftrightarrow\mathbf{q}_3,\quad \mathbf{q}_1\leftrightarrow\mathbf{q}_3 \\
&\quad\delta(-E_{\mathbf{q}_1}-E_{\mathbf{q}_2}-E_{\mathbf{q}_3}-E_\mathbf{p})\,[f_{-\mathbf{q}_1}f_{-\mathbf{q}_2}f_{-\mathbf{q}_3}]\Big\}
\end{aligned} \tag{2.77}$$

$$\begin{aligned}
&=\frac{1}{6\nu}\int \frac{\mathrm{d}^3\mathbf{q}_1\,\mathrm{d}^3\mathbf{q}_2\,\mathrm{d}^3\mathbf{q}_3}{(2\pi)^9 2E_{\mathbf{q}_1}2E_{\mathbf{q}_2}2E_{\mathbf{q}_3}}(2\pi)^4\,|\mathcal{M}|^2 \\
&\quad\times\Big\{\delta^4(Q_1+Q_2+Q_3-P)\Big|_{(Q_i)^0=E_{\mathbf{q}_i}}\,[(1\pm f_{\mathbf{q}_1})(1\pm f_{\mathbf{q}_2})(1\pm f_{\mathbf{q}_3})] \\
&\qquad+\delta^4(-Q_1+Q_2+Q_3-P)\Big|_{(Q_i)^0=E_{\mathbf{q}_i}}\,[f_{\mathbf{q}_1}(1\pm f_{\mathbf{q}_2})(1\pm f_{\mathbf{q}_3})] \\
&\qquad+\text{ similar with } \mathbf{q}_1\leftrightarrow\mathbf{q}_2,\quad \mathbf{q}_1\leftrightarrow\mathbf{q}_3 \\
&\qquad+\delta^4(-Q_1-Q_2+Q_3-P)\Big|_{(Q_i)^0=E_{\mathbf{q}_i}}\,[f_{\mathbf{q}_1}f_{\mathbf{q}_2}(1\pm f_{\mathbf{q}_3})] \\
&\qquad+\text{ similar with } \mathbf{q}_2\leftrightarrow\mathbf{q}_3,\quad \mathbf{q}_1\leftrightarrow\mathbf{q}_3 \\
&\quad\delta^4(-Q_1-Q_2-Q_3-P)\Big|_{(Q_i)^0=E_{\mathbf{q}_i}}\,[f_{\mathbf{q}_1}f_{\mathbf{q}_2}f_{\mathbf{q}_3}]\Big\}
\end{aligned} \tag{2.78}$$

Energy-momentum conservation can only be fulfilled for the second delta function, which can be seen as follows:

The last term cannot contribute, because it contains $\delta(E_{\mathbf{q}_1}+E_{\mathbf{q}_2}+E_{\mathbf{q}_3}+E_\mathbf{p})$ and all $E>0$. For the first delta function, let us consider for a moment P to have a small mass m. Then we can boost into its rest frame to obtain

$$P = Q_1 + Q_2 + Q_3 \tag{2.79}$$

$$\begin{pmatrix} m \\ 0 \end{pmatrix} = \begin{pmatrix} E_{\mathbf{q}_1} \\ \mathbf{q}_1 \end{pmatrix} + \begin{pmatrix} E_{\mathbf{q}_2} \\ \mathbf{q}_2 \end{pmatrix} + \begin{pmatrix} E_{\mathbf{q}_3} \\ \mathbf{q}_3 \end{pmatrix}, \tag{2.80}$$

which can never be fulfilled, because $E_{\mathbf{q}_i} \geq m$. For massless particles this could in principle be fulfilled, if all particles are collinear, however since they acquire a small thermal mass, this argument should hold.

We thus obtain

$$= \frac{1}{2\nu}\int \frac{\mathrm{d}^3\mathbf{q}_1\,\mathrm{d}^3\mathbf{q}_2\,\mathrm{d}^3\mathbf{q}_3}{(2\pi)^9 2E_{\mathbf{q}_1}2E_{\mathbf{q}_2}2E_{\mathbf{q}_3}}(2\pi)^4\,|\mathcal{M}|^2 \times \delta^4(-Q_1+Q_2+Q_3-P)\Big|_{(Q_i)^0=E_{\mathbf{q}_i}}\,[f_{\mathbf{q}_1}(1\pm f_{\mathbf{q}_2})(1\pm f_{\mathbf{q}_3})] \quad . \tag{2.81}$$

2.2. Effective kinetic theory

In this section we give a brief introduction to the effective kinetic theory (EKT) developed in [3]. A brief one-page overview, including also the isotropic screening prescription [12] we use can also be found in [13]. Although we do not consider the time-evolution of particle distribution functions, which is described by EKT, we do use the elastic collision term introduced in Section 2.2.2, and for completeness we provide a complete introduction to the EKT, including also the inelastic collision term.

2.2.1. Overview

In the effective kinetic theory (EKT) description [3] of the quark-gluon plasma, quarks and gluons are represented by their phase-space density or distribution functions $f_s(\mathbf{x},\mathbf{p},t)$ for a single helicity and color state, where s labels the different species (quark flavors and gluons). The time-evolution of these distribution functions is given by a Boltzmann equation,

$$\left(\frac{\partial}{\partial t}+\mathbf{v}\cdot\nabla_x\right)f_s = -C_s[f], \tag{2.82}$$

where $C_s[f]$ is called the collision term, which can be split into two parts, elastic $2\leftrightarrow 2$ processes and effective collinear "$1\leftrightarrow 2$" processes,

$$C_s[f] = C_s^{2\leftrightarrow 2}[f] + C_s^{\text{"}1\leftrightarrow 2\text{"}}[f]. \tag{2.83}$$

We will describe those two terms individually in the following sections.

2.2.2. $2\leftrightarrow 2$ collision term

The first term is given by

$$C_a^{2\leftrightarrow 2}[f](\mathbf{p}) = \frac{1}{4|\mathbf{p}|\nu_a}\sum_{bcd}\int_{\mathbf{kp'k'}}\left|\mathcal{M}_{cd}^{ab}(\mathbf{p},\mathbf{k};\mathbf{p'k'})\right|^2(2\pi)^4\delta^4(P+K-P'-K') \Big\{f^a(\mathbf{p})f^b(\mathbf{k})\left[1\pm f^c(\mathbf{p'})\right]\left[1\pm f^d(\mathbf{k'})\right] - f^c(\mathbf{p'})f^d(\mathbf{k'})\left[1\pm f^a(\mathbf{p})\right]\left[1\pm f^b(\mathbf{k})\right]\Big\}, \tag{2.84}$$

which represents a loss and gain term, respectively, and $\nu_s = 2d_R$ is the number of spin times color states for a given (quasi-)particle species. The particles are ultra-relativistic, i.e. $P^2=0$ or $P^0=|\mathbf{p}|=p$. The integral measures are defined as

$$\int_{\mathbf{k}} := \int_{\mathbb{R}^3}\frac{\mathrm{d}^3\mathbf{k}}{(2\pi)^3 2k}. \tag{2.85}$$

$ab \leftrightarrow cd$	$\left\|\mathcal{M}_{cd}^{ab}\right\|^2 / g^4$
$q_1q_2 \leftrightarrow q_1q_2$, $q_1\bar{q}_2 \leftrightarrow q_1\bar{q}_2$, $\bar{q}_1q_2 \leftrightarrow \bar{q}_1q_2$, $\bar{q}_1\bar{q}_2 \leftrightarrow \bar{q}_1\bar{q}_2$	$8\frac{d_F^2C_F^2}{d_A}\left(\frac{s^2+u^2}{\underline{t^2}}\right)$
$q_1q_1 \leftrightarrow q_1q_1$, $\bar{q}_1\bar{q}_1 \leftrightarrow \bar{q}_1\bar{q}_1$	$8\frac{d_F^2C_F^2}{d_A}\left(\frac{s^2+u^2}{\underline{t^2}}+\frac{s^2+t^2}{\underline{u^2}}\right)+16d_FC_F\left(C_F-\frac{C_A}{2}\right)\frac{s^2}{tu}$
$q_1\bar{q}_1 \leftrightarrow q_1\bar{q}_1$	$8\frac{d_F^2C_F^2}{d_A}\left(\frac{s^2+u^2}{\underline{t^2}}+\frac{t^2+u^2}{s^2}\right)+16d_FC_F\left(C_F-\frac{C_A}{2}\right)\frac{u^2}{st}$
$q_1\bar{q}_1 \leftrightarrow q_2\bar{q}_2$	$8\frac{d_F^2C_F^2}{d_A}\left(\frac{t^2+u^2}{s^2}\right)$
$q_1\bar{q}_1 \leftrightarrow gg$	$8d_FC_F^2\left(\frac{u}{\underline{t}}+\frac{t}{\underline{u}}\right)-8d_FC_FC_A\left(\frac{t^2+u^2}{s^2}\right)$
$q_1g \leftrightarrow q_1g$, $\bar{q}_1g \leftrightarrow \bar{q}_1g$	$-8d_FC_F^2\left(\frac{u}{s}+\frac{s}{\underline{u}}\right)+8d_FC_FC_A\left(\frac{s^2+u^2}{\underline{t^2}}\right)$
$gg \leftrightarrow gg$	$16d_AC_A^2\left(3-\frac{su}{\underline{t^2}}-\frac{st}{\underline{u^2}}-\frac{tu}{s^2}\right)$

Table 2.1.: Matrix elements from [3]. Singly-underlined denominators indicate infrared-sensitive contributions from soft gluon exchange, double-underlined denominators from soft fermion exchange. The constants d_F, C_F, d_A, C_A are given in (2.13).

The matrix elements $\left|\mathcal{M}_{cd}^{ab}\right|^2$ correspond to elastic 2-particle scattering processes and are summed over the spins and colors of all incoming and outgoing particles. They obey certain symmetry relations given in [3], out of which we will later need

$$\left|\mathcal{M}_{cd}^{ab}(\mathbf{p},\mathbf{k};\mathbf{p}',\mathbf{k}')\right|^2 = \left|\mathcal{M}_{dc}^{ab}(\mathbf{p},\mathbf{k};\mathbf{k}',\mathbf{p}')\right|^2. \tag{2.86}$$

The matrix elements for the relevant scattering processes in vacuum are given in Table 2.1. They are functions of the so-called *Mandelstam variables*

$$s = -(P+K)^2, \qquad t = -(P'-P)^2, \qquad u = -(K'-P)^2. \tag{2.87}$$

However, since a Quark-Gluon Plasma certainly differs from vacuum, these matrix elements must be modified to include medium-dependent corrections. For leading order, it turns out that these matrix elements are sufficient, except for the singly or doubly underlined ones. In those matrix elements, medium-dependent self-energy corrections need to be taken into account. A singly underlined denominator indicates a correction for an internal virtual (soft) gluon, whereas a doubly underlined denominator for an internal virtual (soft) fermion. We will only need to consider the singly underlined terms, and we will do so in the following section.

2.2.3. Isotropic screening

As we have seen before, the free particle propagator is modified due to interactions with the many-body system, which are quantified by the self-energy. We must therefore replace it by the full propagator. In the EKT description this amounts to [3]

$$\frac{su}{t^2} = \frac{1}{4} - \frac{1}{4}\frac{(s-u)^2}{t^2} \to \left| D^R(P-P')_{\mu\nu}(P+P')^\mu(K+K')^\nu \right|^2 . \tag{2.88}$$

where D^R is the HTL *retarded* propagator, given by (2.57) and (2.58).

This prescription only becomes important when the momentum of the virtual particle Q^2 becomes small with respect to Π^R, otherwise we can use the free propagator, $D_0^R(Q)$, instead. Therefore, we only need to incorporate this screening prescription in the underlined terms in Table 2.1.

The reason that the retarded propagator (and not some other propagator) appears here is because the in-media gain and loss rates in (2.84) are proportional to $\Pi^<$ and $\Pi^>$, respectively [19], where for gluons we need to take e.g. $g^{\mu\nu}\Pi^<_{\mu\nu}$ and for fermions e.g. $\mathrm{Tr}\left[\not{P}\Pi^>\right]$. As an example, we have calculated one of those terms contributing to the loss term in (2.84) in (2.81), where we have seen via the cutting rule (2.54) that the propagator that appears in the matrix element (2.65) must be a retarded propagator. (2.81) has also the correct Bose enhancement and Fermi blocking factor incorporated.

Instead of incorporating the hard-thermal-loop (HTL) self-energy, we use a different method presented in [12], which is leading order accurate for isotropic distributions and amounts to replacing

$$q^2 t \to t(q^2 + 2\xi^2 m^2), \tag{2.89}$$

where $\xi = e^{5/6}/\sqrt{8} \approx 0.8135$ and m is the gluonic effective mass [3], which for a gluonic plasma reads

$$m^2 = 2\lambda \int \frac{\mathrm{d}^3 p}{(2\pi)^3} \frac{f(\mathbf{p})}{|\mathbf{p}|}, \tag{2.90}$$

with $\lambda = g^2 N_C$. We can also represent this via the Debye mass, $m_D^2 = 2m^2$, as we can easily compare with (2.59).

Example of how the screening is implemented

Let us illustrate this procedure by an example. Consider a matrix element $\sim -\frac{su}{t^2}$. As we will show later (cf. (3.193)), we can write this, for $k, p \gg q, \omega$, as

$$-\frac{su}{t^2} = \frac{4p^2k^2(1-\cos\phi)^2 t^2}{t^2 q^4}. \tag{2.91}$$

Applying our regularization procedure (2.89) yields

$$-\frac{su}{t^2} = \frac{4p^2k^2(1-\cos\phi)^2}{(q^2+\xi^2 m_D^2)^2}. \tag{2.92}$$

Actually, we could have also replaced $q^4 \to q^2(q^2 + \tilde{\xi}^2 m_D^2)$ with another constant $\tilde{\xi}$. Every replacement that exhibits the same behavior is equally valid, albeit with a different constant ξ.

The exact HTL result for this matrix element would be, following [3],

$$\frac{su}{t^2} = \frac{1}{4} - \frac{1}{4}\frac{(s-u)^2}{t^2} \to \left| D^R (P-P')_{\mu\nu} (P+P')^\mu (K+K')^\nu \right|^2 . \tag{2.93}$$

The matrix element must be gauge invariant, so we can perform the calculation in any gauge and use the retarded HTL propagator G_R in the strict Coulomb gauge (2.57) and (2.58).

We then obtain

$$\left| D_R^{\mu\nu}(Q)(2P+Q)_\mu (2K-Q)_\nu \right|^2 \tag{2.94}$$

$$= \Big| D_R^{00}(Q)(2p+\omega)(2k-\omega) \tag{2.95}$$

$$+ \left((2\mathbf{p}+\mathbf{q})\cdot(2\mathbf{k}-\mathbf{q}) - \frac{(\mathbf{q}\cdot(2\mathbf{p}+\mathbf{q}))\,(\mathbf{q}\cdot(2\mathbf{k}-\mathbf{q}))}{q^2} \right) D_R^T(Q) \Big|^2 . \tag{2.96}$$

Using the parametrization of (3.58), (3.59) and (3.60), and also (3.98b) and (3.98a), we obtain

$$\left| D_R^{00}(Q)(2p+\omega)(2k-\omega) + 4pk(\sin\theta_{pq}\sin\theta_{kq}\cos\phi_{kq}) D_R^T(Q) \right|^2 \tag{2.97}$$

$$= \left| D_R^{00}(Q) \right|^2 (2p+\omega)^2 (2k-\omega)^2 \tag{2.98}$$

$$+ 16p^2k^2 \left(1 - \left(\frac{\omega}{q} + \frac{t}{2pq} \right)^2 \right) \left(1 - \left(\frac{\omega}{q} - \frac{t}{2kq} \right)^2 \right) \cos^2\phi \left| D_R^T(Q) \right|^2 + \cos\phi \ldots ,$$

which for $p, k \gg q, \omega \gg m_D$ has exactly the same behavior as (2.91), because $\left| D_R^{00}(Q) \right|^2 \to \frac{1}{q^4}$ and $\left| D_R^T(Q) \right|^2 \to \frac{1}{(\omega^2-q^2)^2}$. This is the reason, why we could replace the full HTL matrix element by the simpler one. Note that we integrate over $\mathrm{d}\phi$, so we need not consider the term $\sim \cos\phi$.

In the collision term we always integrate over q, ω. For small ω, we can expand the distribution functions for small ω as in [12] and then obtain the condition that this integral should vanish:

$$\int_{-\infty}^{\infty} \mathrm{d}\omega\, \omega^2 \int_{|\omega|}^{\infty} \mathrm{d}q \int_0^{2\pi} \mathrm{d}\phi \left(\left| \mathcal{M}^2_{\xi,m_D} \right|^{\text{Approx HTL}}_{k,p\gg q} - \left| \mathcal{M}^2_{m_D} \right|^{\text{Exact HTL}}_{k,p\gg q} \right) \tag{2.99}$$

If we split the ω-integral in $\int_{|\omega|>a} \mathrm{d}\omega$ and $\int_{|\omega|<a} \mathrm{d}\omega$, with $a \gg m_D$, then for the first case, those two terms cancel each other, as we have shown before that they are identical in this limit. And this is also the leading order behavior of the integrated matrix element. Thus all further terms are of lower order. The integrated matrix element thus behaves as $\int \frac{1}{\omega^n} + \text{const}$, where the constant is given by the low-ω region, i.e. by the region where our approximated matrix element differs from the "exact" HTL matrix element. For the exact element the constant can only be given by a function $f(m_D)$, whereas for the approximated matrix element $g(\xi m_D)$. We can then adjust the value of ξ, effectively rescaling the mass, such that $g(\xi m_D) = f(m_D)$, which leads to the value reported above for ξ, see (2.89).

2.2.4. Effective "1 ↔ 2" collision term

$C_f^{\text{"1}\leftrightarrow\text{2"}}$ does not only describe a $1 \leftrightarrow 2$ particle process, but also includes $1+N \leftrightarrow 2+N$ processes and has the form [3]

$$\begin{aligned} C_a^{\text{"1}\leftrightarrow\text{2"}}[f] = \frac{(2\pi)^3}{2p^2\nu_a} \sum_{b,c} \int_0^\infty \mathrm{d}p'\, \mathrm{d}k'\, \delta(p-p'-k')\gamma_{bc}^a(\mathbf{p};p'\hat{\mathbf{p}},k'\hat{\mathbf{p}}) \\ \times \left\{ f_a(\mathbf{p}) \left[1 \pm f_b(p'\hat{\mathbf{p}})\right] \left[1 \pm f_c(k'\hat{\mathbf{p}})\right] - f_b(p'\hat{\mathbf{p}}) f_c(k'\hat{\mathbf{p}}) \left[1 \pm f_a(\mathbf{p})\right] \right\} \\ + \frac{(2\pi)^3}{p^2\nu_a} \sum_{b,c} \int_0^\infty \mathrm{d}k\, \mathrm{d}p'\, \delta(p+k-p')\gamma_{ab}^c(p'\hat{\mathbf{p}};\mathbf{p},k\hat{\mathbf{p}}) \\ \times \left\{ f_a(\mathbf{p}) f_b(k\hat{\mathbf{p}}) \left[1 \pm f_c(p'\hat{\mathbf{p}})\right] - f_c(p'\hat{\mathbf{p}}) \left[1 \pm f_a(\mathbf{p})\right] \left[1 \pm f_b(k\hat{\mathbf{p}})\right] \right\}, \end{aligned} \tag{2.100}$$

where γ_{bc}^a now represents the differential splitting/joining rates and includes all the phase space integrations and the summation over N.

γ_{bc}^a can be calculated as follows: Let $\hat{\mathbf{n}}$ be a unit vector in the direction of propagation of the splitting/merging. Then

$$\gamma_{qg}^q(p\hat{\mathbf{n}};p'\hat{\mathbf{n}},k\hat{\mathbf{n}}) = \gamma_{\bar{q}g}^{\bar{q}}(p\hat{\mathbf{n}};p'\hat{\mathbf{n}},k\hat{\mathbf{n}}) = \frac{p'^2+p^2}{p'^2p^2k^3}\mathcal{F}_q^{\hat{\mathbf{n}}}(p,p',k), \tag{2.101}$$

$$\gamma_{q\bar{q}}^g(p\hat{\mathbf{n}};p'\hat{\mathbf{n}},k\hat{\mathbf{n}}) = \frac{k^2+p'^2}{k^2p'^2p^3}\mathcal{F}_q^{\hat{\mathbf{n}}}(k,-p',p), \tag{2.102}$$

$$\gamma_{gg}^g(p\hat{\mathbf{n}};p'\hat{\mathbf{n}},k\hat{\mathbf{n}}) = \frac{p'^4+p^4+k^4}{p'^3p^3k^3}\mathcal{F}_g^{\hat{\mathbf{n}}}(p,p',k), \tag{2.103}$$

where

$$\mathcal{F}_s^{\hat{\mathbf{n}}}(p',p,k) := \frac{d_sC_s\alpha}{2(2\pi)^3}\int \frac{\mathrm{d}^2h}{(2\pi)^2} 2\mathbf{h}\cdot\mathrm{Re}\,\mathbf{F}_s^{\hat{\mathbf{n}}}(\mathbf{h};p',p,k). \tag{2.104}$$

α is given by (2.16), $\mathbf{h}$ is a two-dimensional vector perpendicular to $\hat{\mathbf{n}}$, and $\mathbf{F}_s^{\hat{\mathbf{n}}}$ is the solution to the linear integral equation

$$\begin{aligned} 2\mathbf{h} = i\delta E(\mathbf{h};p',p,k)\mathbf{F}_s^{\hat{\mathbf{n}}}(\mathbf{h};p',p,k) + g^2\int \frac{\mathrm{d}^4Q}{(2\pi)^4} 2\pi\delta\left(v_{\hat{\mathbf{n}}}\cdot Q\right) v_{\hat{\mathbf{n}}}^\mu v_{\hat{\mathbf{n}}}^\nu \langle A_\mu(Q)[A_\nu(Q)]^*\rangle \\ \times \left\{ \left(C_s - \frac{1}{2}C_A\right)\left[\mathbf{F}_s^{\hat{\mathbf{n}}}(\mathbf{h};p',p,k) - \mathbf{F}_s^{\hat{\mathbf{n}}}(\mathbf{h}-k\mathbf{q}_\perp;p',p,k)\right] \right. \\ + \frac{1}{2}C_A\left[\mathbf{F}_s^{\hat{\mathbf{n}}}(\mathbf{h};p',p,k) - \mathbf{F}_s^{\hat{\mathbf{n}}}(\mathbf{h}+p'\mathbf{q}_\perp;p',p,k)\right] \\ \left. + \frac{1}{2}C_A\left[\mathbf{F}_s^{\hat{\mathbf{n}}}(\mathbf{h};p',p,k) - \mathbf{F}_s^{\hat{\mathbf{n}}}(\mathbf{h}-p\mathbf{q}_\perp;p',p,k)\right] \right\}. \end{aligned} \tag{2.105}$$

$v_{\hat{\mathbf{n}}} = (1,\hat{\mathbf{n}})$ and $\mathbf{q}_\perp$ is the part of $\mathbf{q}$ perpendicular to $\hat{\mathbf{n}}$, and d_s, C_s given by (2.13).

δE is defined as

$$\delta E(\mathbf{h};p',p,k) = \frac{m_{\text{eff},g}^2}{2k} + \frac{m_{\text{eff},s}^2}{2p} - \frac{m_{\text{eff},s}^2}{2p'} + \frac{\mathbf{h}^2}{2pkp'}, \tag{2.106}$$

where the effective mass $m_{\text{eff},g}$ of gluons and fermions $m_{\text{eff},s}$ are given by

$$m_{\text{eff},g}^2 = \sum_s 2\nu_s \frac{g^2 C_s}{d_A} \int \frac{\mathrm{d}^3\mathbf{p}}{2p(2\pi)^3} f_s(\mathbf{p}), \tag{2.107}$$

$$m_{\text{eff,s}}^2 = 2g^2 C_F \int \frac{\mathrm{d}^3\mathbf{p}}{2p(2\pi)^3} \left[2f_g(\mathbf{p}) + f_s(\mathbf{p}) + f_{\bar{s}}(\mathbf{p})\right]. \tag{2.108}$$

Finally, $\langle A_\mu(Q)[A_\nu(Q)]^*\rangle$ is the Fourier transform of the (non-equlibrium) HTL approximation to the Wightman gauge field correlator and is given by

$$\langle A_\mu(Q)[A_\nu(Q)]^*\rangle = D^{\text{Ret}}_{\mu\alpha}(Q)\Pi_{12}^{\alpha\beta}(Q)[D^{\text{Ret}}_{\nu\beta}(Q)]^*. \tag{2.109}$$

For consistency with the previous isotropic screening, we make the same assumption here, which enables us to evaluate

$$\begin{aligned} g^2 \int \frac{\mathrm{d}^4 Q}{(2\pi)^4} 2\pi\delta\left(v_{\hat{\mathbf{n}}}\cdot Q\right) v^\mu_{\hat{\mathbf{n}}} v^\nu_{\hat{\mathbf{n}}} \langle A_\mu(Q)[A_n(Q)]^*\rangle h(\mathbf{q}_\perp) \\ = g^2 T_* \int \frac{\mathrm{d}^2\mathbf{q}_\perp}{(2\pi)^2} \left(\frac{1}{\mathbf{q}_\perp^2} - \frac{1}{\mathbf{q}_\perp^2 + m_D^2}\right) h(\mathbf{q}_\perp), \end{aligned} \tag{2.110}$$

with

$$T_* = \frac{\sum_s \nu_s \frac{g^2 C_s}{d_A} \int \frac{\mathrm{d}^3\mathbf{p}}{(2\pi)^3} \frac{f_s(\mathbf{p})}{p}}{\frac{1}{2}\sum_s \nu_s \frac{g^2 C_s}{d_A} \int \frac{\mathrm{d}^3\mathbf{p}}{(2\pi)^3} f_s(\mathbf{p}) \left[1 \pm f(\mathbf{p})\right]}. \tag{2.111}$$

We only consider a gluonic plasma, which means that we do not have any quarks in the plasma, which allows us to simplify these expressions to obtain (see also [12, 13])

$$\begin{aligned} 2\mathbf{h} = i\delta E(\mathbf{h};p',p,k)\mathbf{F}_g^{\hat{\mathbf{n}}}(\mathbf{h};p',p,k) + g^2 T_* \int \frac{\mathrm{d}^2\mathbf{q}_\perp}{(2\pi)^2} \left(\frac{1}{\mathbf{q}_\perp^2} - \frac{1}{\mathbf{q}_\perp^2 + m_D^2}\right) \\ \times \frac{C_A}{2} \left\{3\mathbf{F}_g^{\hat{\mathbf{n}}}(\mathbf{h}) - F_g^{\hat{\mathbf{n}}}(\mathbf{h} - k\mathbf{q}_\perp) - F_g^{\hat{\mathbf{n}}}(\mathbf{h} + p'\mathbf{q}_\perp) - F_g^{\hat{\mathbf{n}}}(\mathbf{h} - p\mathbf{q}_\perp)\right\}. \end{aligned} \tag{2.112}$$

2.2.5. Expansion term

For heavy-ion collisions we also should take into account expansion along the beam axis. We assume that our distribution function does not depend on x, y, but can depend on z. In the Boltzmann equation, (2.82), we then have a term

$$v^z \frac{\partial f}{\partial z}. \tag{2.113}$$

We will now show that this reduces under the assumption of boost invariance and at $z = 0$ to [32]

$$v^z \frac{\partial f}{\partial z} = -\frac{p^z}{t}\frac{\partial f}{\partial p^z}. \tag{2.114}$$

To show this, we follow [32] and consider the distribution function to be dependent on t, z, $\mathbf{p}$, i.e. $f(t, z, \mathbf{p}_\perp, p_z)$. We then apply a Lorentz boost, parametrized [33] by the rapidity η,

$$\begin{pmatrix} t \\ z \end{pmatrix} = \begin{pmatrix} \cosh\eta & \sinh\eta \\ \sinh\eta & \cosh\eta \end{pmatrix} \begin{pmatrix} \tilde{t} \\ \tilde{z} \end{pmatrix}, \tag{2.115}$$

where $\tilde{t}$, $\tilde{z}$ are the components of the position vector in a different basis. The same transformation applies to the 4-momentum, which yields

$$t = \tilde{t}\cosh\eta + \tilde{z}\sinh\eta \qquad z = \tilde{t}\sinh\eta + \tilde{z}\cosh\eta \tag{2.116}$$

$$p^0 = \tilde{p}^0\cosh\eta + \tilde{p}^z\sinh\eta \qquad p^z = \tilde{p}^0\sinh\eta + \tilde{p}^z\cosh\eta \tag{2.117}$$

With boost invariance we mean that

$$\left.\frac{\partial f}{\partial \eta}\right|_{\eta=0,\, z=0} = 0 \tag{2.118}$$

This yields

$$\begin{aligned} \frac{\partial f}{\partial \eta} = &\left(\tilde{p}^0\cosh\eta + \tilde{p}^z\sinh\eta\right)\frac{\partial f}{\partial p^z} \\ &+ \left(\tilde{t}\sinh\eta + \tilde{z}\cosh\eta\right)\frac{\partial f}{\partial t} \\ &+ \left(\tilde{t}\cosh\eta + \tilde{z}\sinh\eta\right)\frac{\partial f}{\partial z} = 0, \end{aligned} \tag{2.119}$$

which at $\eta = z = 0$ reduces to

$$t\frac{\partial f}{\partial z} = -p^0\frac{\partial f}{\partial p^z} \tag{2.120}$$

Using[7] $v_z = \frac{p^z}{p^0}$, we obtain (2.114).

The Boltzmann equation (2.82) then reads

$$\frac{\partial f_s}{\partial t} = -C_s[f] + \frac{p^z}{t}\frac{\partial f}{\partial p^z}, \tag{2.121}$$

and we can formally define a new collision term,

$$C_s^{\exp}[f] = -\frac{p^z}{t}\frac{\partial f}{\partial p^z}, \tag{2.122}$$

which captures the expansion of the system.

2.3. Monte Carlo integration

The numerical evaluation of multi-dimensional integrals can become quite costly when using a deterministic method of numerical integration, e.g. a trapezoidal rule [34]

$$\int_{x_0}^{x_{N-1}} f(x)\,\mathrm{d}x \approx h\left[\frac{1}{2}f(x_0) + f(x_1) + f(x_2) + \cdots + f(x_{N-2}) + \frac{1}{2}f(x_{N-1})\right], \tag{2.123}$$

[7] This follows immediately from $E = m\gamma$ and $\mathbf{p} = m\gamma\mathbf{v}$ in relativistic kinematics, see e.g. [26].

where the integration interval (x_0, x_{N-1}) is discretized using N evenly spaced points x_i with $h = x_{i+1} - x_i$.

The *Monte carlo method* uses random samples from our integration region.

We can calculate an integral of a function f over a multidimensional volume V via [34]

$$\int f \, \mathrm{d}V \approx V\langle f \rangle, \tag{2.124}$$

with $\langle \dots \rangle$ denoting the arithmetic mean over the N randomly chosen and uniformly distributed sample points x_i,

$$\langle f \rangle = \frac{1}{N} \sum_{i=0}^{N-1} f(x_i). \tag{2.125}$$

If we have a function f that is strongly peaked in a small region and almost zero elsewhere, drawing samples x_i from a uniform distribution is very inefficient, since most samples that are drawn randomly do not contribute much. We can then generalize (2.124) for *importance sampling*, where we draw our samples from a probability density p satisfying

$$\int p \, \mathrm{d}V = 1. \tag{2.126}$$

Our integral can then be approximated as

$$\int f \, \mathrm{d}V = \int \frac{f}{p} p \, \mathrm{d}V \approx \left\langle \frac{f}{p} \right\rangle, \tag{2.127}$$

with samples drawn from p and the volume factor yields 1 because of the normalization.

We can also generalize this, such that the probability distribution does not need to be normalized to 1. Consider now a one-dimensional integral,

$$I = \int_a^b f(x) \, \mathrm{d}x = \int_a^b h(x) g(x) \, \mathrm{d}x \, . \tag{2.128}$$

We can perform a change of variables to $g(x) \, \mathrm{d}x = \mathrm{d}y$, with

$$y(x) = y_0 + \int g(x) \, \mathrm{d}x \, . \tag{2.129}$$

Then our integral becomes

$$I = \int_{y(a)}^{y(b)} h\left(x(y)\right) \mathrm{d}y \approx \left(y(b) - y(a)\right) \frac{1}{N} \sum_{i=0}^{N-1} h(x(y_i)), \tag{2.130}$$

with y_i from a uniform distribution from $(y(a), y(b))$. This is exactly the same as before with $V = y(b) - y(a)$ and $h(x) = \frac{f(x)}{g(x)}$.

In principle, this formula is exact and should work for any $g(x) \neq 0$ such that $y(x)$ of (2.129) is invertible, but the convergence can be rather slow if $g(x)$ is not chosen appropriately. The best case is that we can choose a $g(x)$ such that $h(x) = 1$, then

(2.130) is exact. In this case, of course, it is best to perform the integral analytically. The best choice of $g(x)$ is such that $h(x)$ becomes approximately constant.

For an example of how (2.130) can be used in practice, we refer to Section 4.2.1.

Because this method is based on random numbers, it will deviate from the "exact" value of the integral. An exact estimation of the error is difficult since it depends on the specific integrand, but it can be estimated to be proportional to $\frac{1}{\sqrt{N}}$, where N is the number of samples [34].

3. A formula for $\hat{q}$

In this Chapter we derive a formula for $\hat{q}$ based on the effective kinetic theory description introduced in 2.2. In the derivation we consider a plasma consisting of both quarks and gluons. Likewise for the jet we make no restriction, both a high energy gluon and quark is considered. The jet direction is parametrized by an angle θ_p to account for different jet directions in an expanding plasma. In Section 3.11 we will show that this formula produces known analytical results in the soft limit in thermal equilibrium.

3.1. Definition of $\hat{q}$

We use the definition of $\hat{q}$ from [8],

$$\hat{q}(p) = \int_{q_\perp < \Lambda_\perp} \mathrm{d}^2 q_\perp \, q_\perp^2 \frac{\mathrm{d}\Gamma_{\mathrm{el}}}{\mathrm{d}^2 q_\perp}, \tag{3.1}$$

with Γ_{el} being the rate of elastic collisions of a high energetic jet particle with plasma particles and $q_\perp$ is the transferred transverse momentum in such a single collision.

We use the expression (2.84) from [3, 15] for the $2 \leftrightarrow 2$ Collision operator,

$$\begin{aligned} C_a^{2\leftrightarrow 2}[f](\mathbf{p}) = \frac{1}{4|\mathbf{p}|\nu_a} \sum_{bcd} \int_{\mathbf{kp'k'}} \left|\mathcal{M}_{cd}^{ab}(\mathbf{p},\mathbf{k};\mathbf{p'k'})\right|^2 (2\pi)^4 \delta^4(P + K - P' - K') \\ \Big\{ f^a(\mathbf{p}) f^b(\mathbf{k}) \left[1 \pm f^c(\mathbf{p'})\right] \left[1 \pm f^d(\mathbf{k'})\right] \\ - f^c(\mathbf{p'}) f^d(\mathbf{k'}) \left[1 \pm f^a(\mathbf{p})\right] \left[1 \pm f^b(\mathbf{k})\right] \Big\}, \end{aligned} \tag{3.2}$$

which consists of a loss and a gain term. The first term thus must be proportional to the decay rate (or rate of elastic collisions). The proportionality constant is exactly one, which we will now make plausible.

We start with a textbook [35] expression for the Boltzmann equation,

$$\frac{\partial f}{\partial t} + \mathbf{v} \cdot \nabla f = C(f), \tag{3.3}$$

$$C(f) = \int w(\tilde{\mathbf{k}'}, \tilde{\mathbf{k}_1'}; \tilde{\mathbf{k}}, \tilde{\mathbf{k}_1})(f' f_1' - f f_1) \, \mathrm{d}^3\tilde{\mathbf{k}_1} \, \mathrm{d}^3\tilde{\mathbf{k}'} \, \mathrm{d}^3\tilde{\mathbf{k}_1'}, \tag{3.4}$$

which is a classical (and non-relativistic) expression (no Bose enhancement or Fermi blocking factors are present, no Lorentz-invariant integration measure), but this can be generalized to quantum particles in a straightforward way. We use a condensed notation, in which f' is dependent on $\tilde{\mathbf{k}'}$. w contains an energy and momentum conserving delta function.

The quantity $w(\tilde{\mathbf{k}}', \tilde{\mathbf{k}}_1'; \tilde{\mathbf{k}}, \tilde{\mathbf{k}}_1)$ is related to the differential cross section via

$$\mathrm{d}\sigma = \frac{w(\tilde{\mathbf{k}}', \tilde{\mathbf{k}}_1'; \tilde{\mathbf{k}}, \tilde{\mathbf{k}}_1)}{|\mathbf{v} - \mathbf{v}_1|} \mathrm{d}^3\tilde{\mathbf{k}}_1' \, \mathrm{d}^3\tilde{\mathbf{k}}_2' \,, \tag{3.5}$$

which describes the collision of two molecules with $\tilde{\mathbf{k}}$ in a given range $\mathrm{d}\tilde{\mathbf{k}}$ (similarly for $\tilde{\mathbf{k}}_1$) that scatter into $\mathrm{d}\tilde{\mathbf{k}}'$ (similarly $\tilde{\mathbf{k}}_1'$).

This is, of course, all done in a non relativistic way, so we will compare this to a textbook treatment of cross section and decay rates [24]. The differential cross section is given by

$$\mathrm{d}\sigma = \frac{1}{(2E_{\mathbf{k}_1})(2E_{\mathbf{k}_2})|\mathbf{v}_1 - \mathbf{v}_2|} |\mathcal{M}|^2 (2\pi)^4 \delta^4(K_1 + K_2 - K_1' - K_2') \frac{\mathrm{d}^3\mathbf{k}_1'}{2E_{\mathbf{k}_1'}(2\pi)^3} \frac{\mathrm{d}^3\mathbf{k}_2'}{2E_{\mathbf{k}_2'}(2\pi)^3}. \tag{3.6}$$

We can now compare this to the non-relativistic expression,

$$w = \frac{|\mathcal{M}|^2 (2\pi)^4 \delta^4(K_1 + K_2 - K_1' - K_2')}{(2E_{\mathbf{k}_1})(2E_{\mathbf{k}_2})(2E_{\mathbf{k}_1'})(2E_{\mathbf{k}_2'})}, \tag{3.7}$$

where we used that $\mathrm{d}^3\tilde{\mathbf{k}} = \frac{\mathrm{d}^3\mathbf{k}}{(2\pi)^3}$ due to different conventions.

This is just the change from a transition matrix element to a Lorentz-invariant matrix element [36].

Comparing with (3.2), we find[1]

$$|\mathcal{M}|^2 = \frac{\left|\mathcal{M}_{cd}^{ab}(\mathbf{p}, \mathbf{k}; \mathbf{p}', \mathbf{k}')\right|^2}{2\nu}. \tag{3.8}$$

The decay rate for a decay in two particles in vacuum is given by [24]

$$\mathrm{d}\Gamma_{\mathrm{vac}}^{1\to 2} = \frac{1}{2E_{\mathbf{p}}} |\mathcal{M}|^2 (2\pi)^4 \delta^4(P - K - K' - P') \frac{\mathrm{d}^3\mathbf{k}'}{2E_{\mathbf{k}'}(2\pi)^3} \frac{\mathrm{d}^3\mathbf{p}'}{2E_{\mathbf{p}'}(2\pi)^3}, \tag{3.9}$$

which we integrate over $\frac{\mathrm{d}^3\mathbf{k}}{2E_{\mathbf{k}}(2\pi)^3}$ with the probability of finding a particle in state $\mathbf{k}$, $f(\mathbf{k})$, and add Bose enhancement and Fermi blocking factors for the final states:

$$\begin{aligned}\mathrm{d}\Gamma = \frac{1}{2E_{\mathbf{p}}} |\mathcal{M}|^2 (2\pi)^4 \delta^4(P - K - K' - P') \frac{\mathrm{d}^3\mathbf{k}}{2E_{\mathbf{k}}(2\pi)^3} \frac{\mathrm{d}^3\mathbf{k}'}{2E_{\mathbf{k}'}(2\pi)^3} \frac{\mathrm{d}^3\mathbf{p}'}{2E_{\mathbf{p}'}(2\pi)^3} \\ \times f(\mathbf{k}) \left[1 \pm f(\mathbf{k}')\right] \left[1 \pm f(\mathbf{p}')\right]\end{aligned} \tag{3.10}$$

We now insert (3.8) to obtain[2]

$$\begin{aligned}\Gamma = \frac{1}{4p\nu_a} \sum_{bcd} \int_{\mathbf{kp'k'}} (2\pi)^4 \delta^4(P + K - P' - K') \\ \left|\mathcal{M}_{cd}^{ab}(\mathbf{p}, \mathbf{k}; \mathbf{p}', \mathbf{k}')\right|^2 f^b(\mathbf{k}) \left[1 \pm f^d(\mathbf{k}')\right] \left[1 \pm f^c(\mathbf{p}')\right].\end{aligned} \tag{3.11}$$

[1] We can do this for every term in the sum over b, c, d, that means for a specific combination a, b, c, d.

[2] A more precise procedure would be to take the decay rate as [19] $\Gamma = \frac{1}{2p}\Pi^<(P)_{\mu\nu}\eta^{\mu\nu}$, together with (2.81), which yields the same result. This is also equivalent to taking only the loss term in (3.2) and setting $f(\mathbf{p}) = 1$, i.e. having one jet particle.

Note that this expression is symmetric under the exchange $\mathbf{p}' \leftrightarrow \mathbf{k}'$ and $c \leftrightarrow d$. Adding something to the integral like $\mathbf{q}_\perp^2$ breaks this symmetry! (Unless we define $p' > k'$) Now there are two possibilities to proceed further:

1. Always define $p' > k'$, which can always be done since we can just rename $p' \leftrightarrow k'$ if $p' < k'$. This yields a factor 2 because we integrate over p' and k', thus

$$\int_{k'p'} g(k', p') = \int_{k'p'} g(k', p')\theta(k' - p') + \int_{k'p'} g(k', p')\theta(p' - k') \tag{3.12}$$

$$= 2\int_{k'p'} g(k', p')\theta(p' - k'), \tag{3.13}$$

   with $g(k', p') = g(p', k')$. However, then we need to be careful about the matrix elements, because we obtain more than those shown in Table 2.1. We then always have the lower momentum particle in $k' \simeq d$-index. Thus if we consider $qg \to qg$, this becomes $qg \to gq$ for $p' < k'$ (before renaming) and $qg \to qg$ for $p' > k'$. If the c and d species are identical, e.g. $gg \to gg$, this provides no further complication. This option basically means that we define the jet as the outgoing particle with larger momentum.

2. Do not define $p' > k'$ but leave them arbitrary. Then we do not always have $p' > k'$. So far everything was symmetric under the replacement $p' \leftrightarrow k'$ and $c \leftrightarrow d$. However, for $k' > p'$, t and u switch places and now u becomes the smallest one.

We choose the former[3] and *define* $p' > k'$, or, viewed differently, rename $p' \leftrightarrow k'$ if $p' < k'$. This yields a factor 2, and additional matrix elements, see section 3.5.

Using the symmetry (2.86) of the matrix element,

$$\left|\mathcal{M}_{cd}^{ab}(\mathbf{p}, \mathbf{k}; \mathbf{p}', \mathbf{k}')\right|^2 = \left|\mathcal{M}_{dc}^{ab}(\mathbf{p}, \mathbf{k}; \mathbf{k}', \mathbf{p}')\right|^2, \tag{3.14}$$

we can rename $\mathbf{k}' \leftrightarrow \mathbf{p}'$, which yields the first term. Thus via this procedure we call $\mathbf{p}'$ the "hard" outgoing momentum and obtain a factor 2,

$$\Gamma = \frac{1}{2p\nu_a} \sum_{bcd} \int_{\substack{\mathbf{kp'k'} \\ p'>k'}} (2\pi)^4 \delta^4(P + K - P' - K') \left|\mathcal{M}_{cd}^{ab}(\mathbf{p}, \mathbf{k}; \mathbf{p}', \mathbf{k}')\right|^2 f^b(\mathbf{k}) \left[1 \pm f^d(\mathbf{k}')\right]. \tag{3.15}$$

By assumption the jet has a very large momentum, such that by energy conservation $p + k = p' + k'$ with $p' > k'$ the outgoing state with momentum p' is unoccupied, i.e. $f(p') = 0$.

Thus, with $\mathbf{q} = \mathbf{p}' - \mathbf{p}$, $\mathbf{q}_\perp = \mathbf{p}'_\perp - \mathbf{p}_\perp$,

$$\hat{q} = \frac{1}{2p\nu_a} \sum_{bcd} \int_{\substack{\mathbf{kp'k'} \\ p'>k'}} q_\perp^2 (2\pi)^4 \delta^4(P + K - P' - K') \left|\mathcal{M}_{cd}^{ab}(\mathbf{p}, \mathbf{k}; \mathbf{p}', \mathbf{k}')\right|^2 f^b(\mathbf{k}) \left[1 \pm f^d(\mathbf{k}')\right], \tag{3.16}$$

[3] $\hat{q}$ is most often defined in a way that the outgoing jet particle has still very large momentum [15, 8].

which we can rewrite using 4-dimensional integrals,

$$\hat{q} = \frac{1}{2p\nu_a}\sum_{bcd}\int \frac{\mathrm{d}^4K\,\mathrm{d}^4P'\,\mathrm{d}^4K'}{(2\pi)^5} q_\perp^2\,\delta^4(P+K-P'-K')\left|\mathcal{M}^{ab}_{cd}(\mathbf{p},\mathbf{k};\mathbf{p}',\mathbf{k}')\right|^2 \\ \times\,\delta(K^2)\delta(P'^2)\delta(K'^2)\Theta(K^0)\Theta(P'^0)\Theta(K'^0)f^b(\mathbf{k})\left[1\pm f^d(\mathbf{k}')\right]\Theta(p'-k') \tag{3.17}$$

$$\hat{q} = \frac{1}{2p\nu_a}\sum_{bcd}\int \frac{\mathrm{d}^4K\,\mathrm{d}^4P'}{(2\pi)^5} q_\perp^2\left|\mathcal{M}^{ab}_{cd}(\mathbf{p},\mathbf{k};\mathbf{p}',\mathbf{k}')\right|^2\Theta(p'-k') \\ \times\,\delta(K^2)\delta(P'^2)\delta(K'^2)\Theta(K^0)\Theta(P'^0)\Theta(K'^0)f^b(\mathbf{k})\left[1\pm f^d(\mathbf{k}')\right], \tag{3.18}$$

where we integrated out the delta function. To ease notation we still write K' or $\mathbf{k}'$ as a short notation for $P+K-P'$ or $\mathbf{p}+\mathbf{k}-\mathbf{p}'$. We will proceed similarly as in [37]. Now let's introduce $Q^\mu = (\omega,\mathbf{q})^\mu$ via

$$Q = P'-P \quad\Leftrightarrow\quad \mathbf{q} = \mathbf{p}'-\mathbf{p} = \mathbf{k}-\mathbf{k}' \tag{3.19}$$

$$\omega = p'-p = k-k'. \tag{3.20}$$

Then[4] $\mathrm{d}^4K\mathrm{d}^4P' = \mathrm{d}^4K\mathrm{d}^4Q$ and thus

$$\hat{q} = \frac{1}{2p\nu_a}\sum_{bcd}\int \frac{\mathrm{d}^4K\,\mathrm{d}^4Q}{(2\pi)^5} q_\perp^2\left|\mathcal{M}^{ab}_{cd}(\mathbf{p},\mathbf{k};\mathbf{p}',\mathbf{k}')\right|^2\Theta(p'-k') \\ \times\,\delta(K^2)\delta\left((P+Q)^2\right)\delta\left((K-Q)^2\right)\Theta(K^0)\Theta(P^0+\omega)\Theta(K^0-\omega)f^b(\mathbf{k})\left[1\pm f^d(\mathbf{k}')\right]. \tag{3.21}$$

Note that Q is not light-like, i.e. $Q^2 = -\omega^2+q^2 \neq 0$. The delta functions can be rewritten as

$$\delta\left((P+Q)^2\right)\delta\left((K-Q)^2\right) = \delta\left(Q^2+2P\cdot Q\right)\delta\left(Q^2-2K\cdot Q\right), \tag{3.22}$$

where we have used the lightlikeness of the momenta P and K, i.e. $P^2 = K^2 = 0$. We can now write the arguments of the delta function with 3-momenta, which yields the same result in any metric convention (The factor -1 is irrelevant since $\delta(x) = \delta(-x)$).

Thus we obtain

$$\delta(-\omega^2+q^2-2\omega p+2pq\cos\theta_{pq})\delta(-\omega^2+q^2+2\omega k-2kq\cos\theta_{kq}) \tag{3.23}$$

$$= \frac{1}{4pkq^2}\delta\left(\cos\theta_{pq}-\frac{\omega}{q}-\frac{\omega^2-q^2}{2pq}\right)\delta\left(\cos\theta_{kq}-\frac{\omega}{q}+\frac{\omega^2-q^2}{2kq}\right). \tag{3.24}$$

Because of this expression we decide to perform the q integral in a coordinate frame in which θ_{pq} is its polar angle and the k integral in a frame in which θ_{kq} is its polar angle. The delta function only contributes if its argument becomes zero, which restricts the

[4] We could have also decided to integrate out P' first. Then we would have $\mathrm{d}^4K\mathrm{d}^4K' = -\mathrm{d}^4K\mathrm{d}^4Q$, but the minus sign cancels with the shifted integration boundaries, $\int_{-\infty}^{\infty}\mathrm{d}K'^1 = -\int_{\infty}^{-\infty}\mathrm{d}Q^1$ for a fixed k, which then yields the same result.

integration region. First we consider the first delta function. Because the cosine can only take values between -1 and 1, we obtain the condition

$$-1 < \frac{\omega}{q} + \frac{\omega^2 - q^2}{2pq} < 1 \tag{3.25}$$

$$-2pq < 2\omega p + \omega^2 - q^2 < 2pq \tag{3.26}$$

$$\omega^2 - q^2 + 2p(\omega + q) > 0 > \omega^2 - q^2 + 2p(\omega - q) \tag{3.27}$$

$$(\omega + q)(\omega - q + 2p) > 0 > (\omega - q)(\omega + q + 2p) \tag{3.28}$$

Let us first look at the left-hand side.

$$\omega + q > 0: \qquad \omega - q + 2p > 0 \iff p > \frac{q - \omega}{2} \tag{3.29}$$

$$\omega + q < 0: \qquad \omega - q + 2p < 0 \iff p < \frac{q - \omega}{2}. \tag{3.30}$$

For the right-hand side we obtain

$$\omega > q: \qquad \omega + q + 2p < 0 \iff p < \frac{-\omega - q}{2} \tag{3.31}$$

$$\omega < q: \qquad \omega + q + 2p > 0 \iff p > \frac{-\omega - q}{2}. \tag{3.32}$$

From the step function $\Theta(\omega + p)$ we obtain $\omega + p > 0$. We know that $q > 0$ and $p > 0$ by construction. In (3.31), however, we obtain $p < \frac{-\omega - q}{2}$, which is negative for $\omega > q$. This is in contradiction to $p > 0$ and thus we conclude that $\omega < q$. In (3.30) we have $p < \frac{q-\omega}{2} \overset{q<-\omega}{<} -\omega$. This is in contradiction with the $\Theta(\omega + p)$ function, thus we know that $\omega > -q$. By comparing (3.29) and (3.32), we observe that (3.32), $p > \frac{-q}{2} - \frac{\omega}{2}$ is always fulfilled if (3.29) holds, $p > \frac{q}{2} - \frac{\omega}{2}$. Thus we obtain from the first δ function the conditions

$$|\omega| < q \qquad\qquad p > \frac{q - \omega}{2}. \tag{3.33}$$

We now repeat this procedure for the second delta function in (3.24): We obtain the condition

$$-1 < \frac{\omega}{q} - \frac{\omega^2 - q^2}{2kq} < 1 \tag{3.34}$$

$$-2kq < 2\omega k - \omega^2 + q^2 < 2kq \tag{3.35}$$

$$-\omega^2 + q^2 + 2k(\omega + q) > 0 > -\omega^2 + q^2 + 2k(\omega - q) \tag{3.36}$$

$$(\omega + q)(-\omega + q + 2k) > 0 > (\omega - q)(-\omega - q + 2k) \tag{3.37}$$

Let us first look at the left-hand side. We know already from before that $\omega + q > 0$, thus

$$\omega + q > 0: \qquad -\omega + q + 2k > 0 \iff k > \frac{\omega - q}{2} \tag{3.38}$$

For the right-hand side with $\omega < q$ we obtain

$$\omega < q: \qquad -\omega - q + 2k > 0 \iff k > \frac{\omega + q}{2}. \tag{3.39}$$

By comparing (3.38) and (3.39), we observe that (3.39) is the stronger restriction that already includes (3.38). Thus we obtain from the delta functions the conditions

$$|\omega| < q, \qquad p > \frac{q-\omega}{2}, \qquad k > \frac{q+\omega}{2}. \tag{3.40}$$

Now we can integrate out the K^0 integral in (3.21), $\int \mathrm{d}K^0\, \delta(K^2)\Theta(K^0) = \frac{1}{2k}$, where $k = |\mathbf{k}|$, and we obtain

$$\begin{aligned}\hat{q} = \frac{1}{16p^2\nu_a}\sum_{bcd}\int \frac{\mathrm{d}^3\mathbf{k}\,\mathrm{d}^3\mathbf{q}\,\mathrm{d}\omega}{(2\pi)^5 q^2 k^2} q_\perp^2 \left|\mathcal{M}^{ab}_{cd}(\mathbf{p},\mathbf{k};\mathbf{p}',\mathbf{k}')\right|^2 \\ \times \delta\left(\cos\theta_{pq} - \frac{\omega}{q} - \frac{\omega^2-q^2}{2pq}\right)\delta\left(\cos\theta_{kq} - \frac{\omega}{q} + \frac{\omega^2-q^2}{2kq}\right)\Theta(p'-k') \\ \times \Theta\left(p - \frac{q-\omega}{2}\right)\Theta\left(k - \frac{q+\omega}{2}\right)\Theta(q-|\omega|) f^b(\mathbf{k})\left[1 \pm f^d(\mathbf{k}')\right].\end{aligned} \tag{3.41}$$

From the step function we obtain restrictions for our integration variables q, ω, k that can be expressed in different sets of integration bounds:

$$\int_0^\infty \mathrm{d}q \int_{-q}^{q} \mathrm{d}\omega \int_{\frac{q+\omega}{2}}^\infty \mathrm{d}k\, \Theta\left(p - \frac{q-\omega}{2}\right)\Theta(p'-k') \tag{3.42}$$

$$= \int_0^\infty \mathrm{d}q \int_{\max(-q,q-2p)}^{q} \mathrm{d}\omega \int_{\frac{q+\omega}{2}}^\infty \mathrm{d}k\, \Theta(p-k+2\omega) \tag{3.43}$$

$$= \int_0^\infty \mathrm{d}q \int_{\max(-q,q-2p)}^{q} \mathrm{d}\omega \int_{\frac{q+\omega}{2}}^{p+2\omega} \mathrm{d}k \tag{3.44}$$

We also need the upper boundary of the k-integral to be always bigger than the lower boundary, which yields $\omega > \frac{1}{3}(q-2p)$, and thus

$$\boxed{\int_0^\infty \mathrm{d}q \int_{\max\left(-q,q-2p,\frac{1}{3}(q-2p)\right)}^{q} \mathrm{d}\omega \int_{\frac{q+\omega}{2}}^{p+2\omega} \mathrm{d}k}. \tag{3.45}$$

Another set of integration bounds is

$$\int_0^\infty \mathrm{d}k \int_{-\infty}^\infty \mathrm{d}\omega \int_{|\omega|}^\infty \mathrm{d}q\, \Theta\left(p - \frac{q-\omega}{2}\right)\Theta\left(k - \frac{q+\omega}{2}\right)\Theta(p'-k') \tag{3.46}$$

$$= \int_0^\infty \mathrm{d}k \int_{-\infty}^\infty \mathrm{d}\omega \int_{|\omega|}^{\min(p+p',k+k')} \mathrm{d}q\, \Theta(p'-k') \tag{3.47}$$

$$= \int_0^\infty \mathrm{d}k \int_{-\frac{p-k}{2}}^\infty \mathrm{d}\omega \int_{|\omega|}^{\min(p+p',k+k')} \mathrm{d}q \tag{3.48}$$

We also need the q-integral boundaries to be consistent, i.e. $\min(p+p', k+k') > |\omega|$. If (i) $p+p' = 2p+\omega < 2k-\omega = k+k' \iff \omega < k-p$, we obtain (ii) $2p+\omega > |\omega|$, which for $\omega > 0$ is already fulfilled and otherwise yields $\omega > -p$. If (i), $\omega < k-p$, is not fulfilled, i.e. if $\omega > k-p$, but then $\omega > -p$ automatically, since $k > 0$. Similarly, if $2k-\omega < 2p+\omega \iff \omega > k-p$, we obtain $2k-\omega > |\omega|$, which is always true for $\omega < 0$ and otherwise yields $\omega < k$. Again, if the initial condition does not hold and we have instead $\omega < k-p$, this condition is always fulfilled.

Thus

$$\int_0^\infty \mathrm{d}k \int_{\max\left(-\frac{p-k}{2},-p\right)}^{k} \mathrm{d}\omega \int_{|\omega|}^{\min(p+p',k+k')} \mathrm{d}q\,. \tag{3.49}$$

Actually, the lower boundary of the ω-integral is always $-\frac{p-k}{2}$, and thus

$$\boxed{\int_0^\infty \mathrm{d}k \int_{-\frac{p-k}{2}}^{k} \mathrm{d}\omega \int_{|\omega|}^{\min(p+p',k+k')} \mathrm{d}q} \tag{3.50}$$

or

$$\boxed{\int_0^\infty \mathrm{d}k \int_{0}^{\frac{p-k}{2}} \mathrm{d}k' \int_{|k-k'|}^{\min(p+p',k+k')} \mathrm{d}q}. \tag{3.51}$$

We will use these different sets of integration bounds, (3.45), (3.50) and (3.51), frequently.

3.2. Coordinate systems

Now we need to choose the coordinate systems in which we want to evaluate these integrals. Since we have delta functions containing θ_{pq} and θ_{kq} it makes sense to use coordinate systems in which we integrate over θ_{pq} and θ_{kq}. We choose coordinate frames as in appendix A of [37]. In our code, we store the phase-space distribution functions $f(\mathbf{k})$ in a specific frame, let us call it "lab frame", see figure 3.1 for an overview of the different frames. The $\mathbf{q}$ integration is done in the "p-frame", while the $\mathbf{k}$ integration is done in the "q-frame". We write the coordinates with respect to a specific frame in a vector $\mathbf{p}_1$, where the subscript labels the frame. The vector $\mathbf{p}$ in the lab frame has no y-component because we assume cylindrical symmetry. We thus have

$$\mathbf{p}_1 = p(\sin\theta_p, 0, \cos\theta_p) \tag{3.52}$$
$$\mathbf{q}_1 = q(\sin\theta_q\cos\phi_q, \sin\theta_q\sin\phi_q, \cos\theta_q) \tag{3.53}$$
$$\mathbf{k}_1 = k(\sin\theta_k\cos\phi_k, \sin\theta_k\sin\phi_k, \cos\theta_k) \tag{3.54}$$
$$\mathbf{p}_2 = p(0, 0, 1) \tag{3.55}$$
$$\mathbf{q}_2 = q(\sin\theta_{pq}\cos\tilde{\phi}_{pq}, \sin\theta_{pq}\sin\tilde{\phi}_{pq}, \cos\theta_{pq}) \tag{3.56}$$
$$\mathbf{k}_2 = k(\sin\theta_{pk}\cos\phi_{pk}, \sin\theta_{pk}\sin\phi_{pk}, \cos\theta_{pk}) \tag{3.57}$$
$$\mathbf{p}_3 = p(\sin\theta_{pq}, 0, \cos\theta_{pq}) \tag{3.58}$$
$$\mathbf{q}_3 = q(0, 0, 1) \tag{3.59}$$
$$\mathbf{k}_3 = k(\sin\theta_{kq}\cos\phi_{kq}, \sin\theta_{kq}\sin\phi_{kq}, \cos\theta_{kq}). \tag{3.60}$$

We put a tilde on $\tilde{\phi}_{pq}$ to emphasize that it is not the same as ϕ_{pq} in [13].

The relations between the different angles can be derived as follows: We construct first the coordinate transformation between the different frames and then use those to obtain the relations between the different angles.

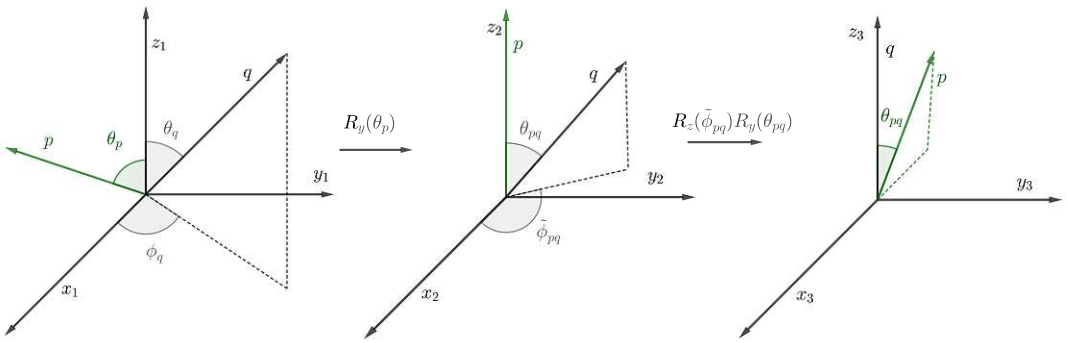

Figure 3.1.: The integration frames. The first frame (1) is called the "lab frame". In this frame all vectors are parametrized by polar and azimuthal angles that only contain one subscript, e.g. the vector $\mathbf{q}$ is uniquely determined by its length q and the angles θ_q and ϕ_q. We perform a rotation around the y axis to obtain the second frame, "p-frame", in which the $\mathbf{p}$ vector points into the z direction. The vector $\mathbf{q}$ is determined by θ_{pq} and $\tilde{\phi}_{pq}$. The third frame, "q-frame", is obtained by applying a rotation to the "p-frame" such that $\mathbf{q}$ points in the z direction and $\mathbf{p}$ lies in the $x-z$ plane.

A coordinate transformation between orthonormal bases is a linear transformation that is represented by an orthogonal matrix that can be defined by transforming the basis vectors, $\mathbf{e}_i \to \mathbf{e}'_j$,

$$\mathbf{e}'_i = T_i{}^j \mathbf{e}_j = S^j{}_i \mathbf{e}_j. \tag{3.61}$$

The coordinates[5] then transform inverse,

$$v = v^{j'} \mathbf{e}'_j = v^{j'} S^k{}_j \mathbf{e}_k = v^k \mathbf{e}_k, \tag{3.62}$$

and thus

$$v^k = S^k{}_j v'^j \tag{3.63}$$

$$v^{k'} = \left(S^{-1}\right)^k{}_j v^j. \tag{3.64}$$

Because we have orthonormal bases[6] in Euclidean space, we can write this in matrix notation simply as[7]

$$S = T^T, \qquad v = Sv', \qquad v' = S^T v = Tv. \tag{3.65}$$

[5] Here, v denotes an abstract vector of a vector space and v^j its components in a specific basis.

[6] Otherwise we would have to proceed with more care as $R^{-1} = R^T$ is only true for orthogonal matrices.

[7] The superscript T means transposition, i.e. $\left(A^T\right)_{ij} = A_{ji}$.

We shall label the rotation matrices as R, $R = T$, they read

$$R_x(\alpha) = \begin{pmatrix} 1 & 0 & 0 \\ 0 & \cos\alpha & \sin\alpha \\ 0 & -\sin\alpha & \cos\alpha \end{pmatrix}, \tag{3.66}$$

$$R_y(\alpha) = \begin{pmatrix} \cos\alpha & 0 & -\sin\alpha \\ 0 & 1 & 0 \\ \sin\alpha & 0 & \cos\alpha \end{pmatrix}, \tag{3.67}$$

$$R_z(\alpha) = \begin{pmatrix} \cos\alpha & \sin\alpha & 0 \\ -\sin\alpha & \cos\alpha & 0 \\ 0 & 0 & 1 \end{pmatrix}. \tag{3.68}$$

The components of vectors transform in a frame change as

$$\mathbf{v}_2 = A\mathbf{v}_1, \qquad A = R_y(\theta_p), \tag{3.69}$$

$$\mathbf{v}_3 = B\mathbf{v}_2, \qquad B = R_y(\theta_{pq})R_z(\tilde{\phi}_{pq}). \tag{3.70}$$

The transformation matrices read

$$A = \begin{pmatrix} \cos\theta_p & 0 & -\sin\theta_p \\ 0 & 1 & 0 \\ \sin\theta_p & 0 & \cos\theta_p \end{pmatrix}, \tag{3.71}$$

$$B = \begin{pmatrix} \cos\theta_{pq}\cos\tilde{\phi}_{pq} & \cos\theta_{pq}\sin\tilde{\phi}_{pq} & -\sin\theta_{pq} \\ -\sin\tilde{\phi}_{pq} & \cos\tilde{\phi}_{pq} & 0 \\ \cos\tilde{\phi}_{pq}\sin\theta_{pq} & \sin\theta_{pq}\sin\tilde{\phi}_{pq} & \cos\theta_{pq} \end{pmatrix} \tag{3.72}$$

We are also interested in anisotropic systems, thus we implement an anisotropic version [5, 14] of $\hat{q}$, where we need all the components. For the definition of $q_\perp$ and the components of $\hat{q}$, we have two possibilities:

- Define it in the p-frame,

$$q_x = (\mathbf{q}_2)_x \qquad = q\sin\theta_{pq}\cos\tilde{\phi}_{pq} \tag{3.73}$$

$$q_y = (\mathbf{q}_2)_y \qquad = q\sin\theta_{pq}\sin\tilde{\phi}_{pq} \tag{3.74}$$

$$q_z = (\mathbf{q}_2)_z \qquad = q\cos\theta_{pq} \tag{3.75}$$

  Then the components of $\hat{q}$ are always defined relative to p, thus the labels q_x do not refer to the x-axis in the "lab-frame".

- Define it in the "lab-frame", but then we need to express the angles in terms of θ_{pq} and $\tilde{\phi}_{pq}$,

$$\mathbf{q}_1 = A^T\mathbf{q}_2 = q\begin{pmatrix} \cos\theta_p\sin\theta_{pq}\cos\tilde{\phi}_{pq} + \sin\theta_p\cos\theta_{pq} \\ \sin\theta_{pq}\sin\tilde{\phi}_{pq} \\ -\sin\theta_p\sin\theta_{pq}\cos\tilde{\phi}_{pq} + \cos\theta_p\cos\theta_{pq} \end{pmatrix}. \tag{3.76}$$

Because $\hat{q}$ measures the momentum broadening transverse to the jet, it makes more sense to define it in the p-frame. The only caveat is that the x in q_x means something different than in the code.

Actually, one can easily transform between those two definitions: Let us define

$$\hat{q}_1^{ij} = \frac{1}{\nu_a}\frac{1}{2^9\pi^5}\sum_{bcd}\int_0^{2\pi} \mathrm{d}\tilde{\phi}_{pq}\int_0^{2\pi}\mathrm{d}\phi_{kq}\int_0^{\infty}\mathrm{d}k\int_{-\frac{p-k}{2}}^{k}\mathrm{d}\omega\int_{|\omega|}^{\min(p+p',k+k')}\mathrm{d}q$$
$$q_1^i q_1^j \frac{|M_{cd}^{ab}|^2}{p^2} f_b(k,v_k)\left(1 \pm f_d(k-\omega, v_{k'})\right) \tag{3.77}$$

$$\hat{q}_2^{ij} = \frac{1}{\nu_a}\frac{1}{2^9\pi^5}\sum_{bcd}\int_0^{2\pi} \mathrm{d}\tilde{\phi}_{pq}\int_0^{2\pi}\mathrm{d}\phi_{kq}\int_0^{\infty}\mathrm{d}k\int_{-\frac{p-k}{2}}^{k}\mathrm{d}\omega\int_{|\omega|}^{\min(p+p',k+k')}\mathrm{d}q$$
$$q_2^i q_2^j \frac{|M_{cd}^{ab}|^2}{p^2} f_b(k,v_k)\left(1 \pm f_d(k-\omega, v_{k'})\right) \tag{3.78}$$

With $q_2^i = A^i{}_j q_1^j$ we obtain

$$\hat{q}_2^{ij} = \frac{1}{\nu_a}\frac{1}{2^9\pi^5}\sum_{bcd}\int_0^{2\pi} \mathrm{d}\tilde{\phi}_{pq}\int_0^{2\pi}\mathrm{d}\phi_{kq}\int_0^{\infty}\mathrm{d}k\int_{-\frac{p-k}{2}}^{k}\mathrm{d}\omega\int_{|\omega|}^{\min(p+p',k+k')}\mathrm{d}q$$
$$A^i{}_l q_1^l A^j{}_m q_1^m \frac{|M_{cd}^{ab}|^2}{p^2} f_b(k,v_k)\left(1 \pm f_d(k-\omega, v_{k'})\right) \tag{3.79}$$

and thus

$$\hat{q}_2^{ij} = A^i{}_l A^j{}_m \hat{q}_1^{lm} = (A\hat{q}_1 A^T)^{ij}. \tag{3.80}$$

In our integration we only have $\tilde{\phi}_{pq}$, ϕ_{kq}, k, ω, q, so we need to express all other quantities in terms of them. $\cos\theta_{pq}$, for example, is actually set by the delta function, but we can also rederive it easily:

To do this, we first find that the Mandelstam variable t is given by $t = \omega^2 - q^2$ and consider

$$|\mathbf{k}'|^2 = |\mathbf{k} - \mathbf{q}|^2 = (k-\omega)^2 \tag{3.81}$$
$$q^2 - 2kq\cos\theta_{kq} = -2\omega k + \omega^2 \tag{3.82}$$
$$\cos\theta_{kq} = \frac{\omega}{q} - \frac{t}{2kq}. \tag{3.83}$$

Similarly, for $\mathbf{p}'$,

$$|\mathbf{p}'|^2 = |\mathbf{p} + \mathbf{q}|^2 = (p+\omega)^2 \tag{3.84}$$
$$q^2 + 2pq\cos\theta_{pq} = 2\omega p + \omega^2 \tag{3.85}$$
$$\cos\theta_{pq} = \frac{\omega}{q} + \frac{t}{2kq}. \tag{3.86}$$

We also need $\theta_{k'q}$,

$$|\mathbf{k}|^2 = |\mathbf{k}' + \mathbf{q}|^2 = (k'+\omega)^2 \tag{3.87}$$
$$q^2 + 2k'q\cos\theta_{pq} = 2\omega k' + \omega^2 \tag{3.88}$$
$$\cos\theta_{k'q} = \frac{\omega}{q} + \frac{t}{2k'q}. \tag{3.89}$$

In our expression for $\hat{q}$, we have $f(\mathbf{k})$ and $f(\mathbf{k}')$, which we store in the "lab-frame". Thus we need to figure out how to express θ_k and $\theta_{k'}$. The azimuthal angles ϕ_k and $\phi_{k'}$ are not needed since we assume cylindrical symmetry.

We thus need to compute

$$\mathbf{k}_1 = A^T B^T \mathbf{k}_3 = A^T B^T k \begin{pmatrix} \sin\theta_{kq}\cos\phi_{kq} \\ \sin\theta_{kq}\sin\phi_{kq} \\ \cos\theta_{kq} \end{pmatrix} \tag{3.90}$$

The components of $\mathbf{k}_1$ read

$$\begin{aligned} \frac{(\mathbf{k}_1)_x}{k} &= -\cos\theta_p \sin\phi_{kq} \sin\tilde{\phi}_{pq} \sin\theta_{kq} \\ &\quad + \cos\theta_{kq}\left(\cos\theta_{pq}\sin\theta_p + \cos\tilde{\phi}_{pq}\cos\theta_p\sin\theta_{pq}\right) \\ &\quad + \cos\phi_{kq}\sin\theta_{kq}\left(\cos\tilde{\phi}_{pq}\cos\theta_p\cos\theta_{pq} - \sin\theta_p\sin\theta_{pq}\right) \end{aligned} \tag{3.91}$$

$$\frac{(\mathbf{k}_1)_y}{k} = \cos\tilde{\phi}_{pq}\sin\phi_{kq}\sin\theta_{kq} + \cos\phi_{kq}\cos\theta_{pq}\sin\tilde{\phi}_{pq}\sin\theta_{kq} + \cos\theta_{kq}\sin\tilde{\phi}_{pq}\sin\theta_{pq} \tag{3.92}$$

$$\begin{aligned} \frac{(\mathbf{k}_1)_z}{k} &= \sin\phi_{kq}\sin\tilde{\phi}_{pq}\sin\theta_{kq}\sin\theta_p \\ &\quad + \cos\phi_{kq}\sin\theta_{kq}\left(-\cos\tilde{\phi}_{pq}\cos\theta_{pq}\sin\theta_p - \cos\theta_p\sin\theta_{pq}\right) \\ &\quad + \cos\theta_{kq}\left(\cos\theta_p\cos\theta_{pq} - \cos\tilde{\phi}_{pq}\sin\theta_p\sin\theta_{pq}\right) \end{aligned} \tag{3.93}$$

From $(\mathbf{k}_1)_z$ we can extract $\cos\theta_k$,

$$\begin{aligned} \cos\theta_k &= \sin\phi_{kq}\sin\tilde{\phi}_{pq}\sin\theta_{kq}\sin\theta_p \\ &\quad + \cos\phi_{kq}\sin\theta_{kq}\left(-\cos\tilde{\phi}_{pq}\cos\theta_{pq}\sin\theta_p - \cos\theta_p\sin\theta_{pq}\right) \\ &\quad + \cos\theta_{kq}\left(\cos\theta_p\cos\theta_{pq} - \cos\tilde{\phi}_{pq}\sin\theta_p\sin\theta_{pq}\right), \end{aligned} \tag{3.94}$$

which, for $\theta_p = \frac{\pi}{2}$ (jet transverse to direction of expansion), reduces to

$$\begin{aligned} \cos\theta_k &= \sin\phi_{kq}\sin\tilde{\phi}_{pq}\sin\theta_{kq} \\ &\quad - \cos\phi_{kq}\sin\theta_{kq}\cos\tilde{\phi}_{pq}\cos\theta_{pq} \\ &\quad - \cos\theta_{kq}\cos\tilde{\phi}_{pq}\sin\theta_{pq}. \end{aligned} \tag{3.95}$$

A similar formula holds for k', with $k \to k'$.

3.3. Formula for $\hat{q}$ for finite p

In summary, we obtain

$$\hat{q}_2^{ij} = \frac{1}{\nu_a}\frac{1}{2^9\pi^5}\sum_{bcd}\int_0^{2\pi}\mathrm{d}\tilde{\phi}_{pq}\int_0^{2\pi}\mathrm{d}\phi_{kq}\int_0^{\infty}\mathrm{d}k\int_{-\frac{p-k}{2}}^{k}\mathrm{d}\omega\int_{|\omega|}^{\min(2p+\omega,2k-\omega)}\mathrm{d}q \times q_2^i q_2^j\frac{|\mathcal{M}_{cd}^{ab}|^2}{p^2}f_b(k,v_k)\left(1\pm f_d(k-\omega,v_{k'})\right) \tag{3.96a}$$

$$\hat{q}_2^{ij} = \frac{1}{\nu_a}\frac{1}{2^9\pi^5}\sum_{bcd}\int_0^{2\pi}\mathrm{d}\tilde{\phi}_{pq}\int_0^{2\pi}\mathrm{d}\phi_{kq}\int_0^{\infty}\mathrm{d}k\int_0^{\frac{k+p}{2}}\mathrm{d}k'\int_{|k-k'|}^{\min(p+p',k+k')}\mathrm{d}q \times q_2^i q_2^j\frac{|\mathcal{M}_{cd}^{ab}|^2}{p^2}f_b(k,v_k)\left(1\pm f_d(k-\omega,v_{k'})\right), \tag{3.96b}$$

$$\hat{q}_2^{ij} = \frac{1}{\nu_a}\frac{1}{2^9\pi^5}\sum_{bcd}\int_0^{2\pi}\mathrm{d}\tilde{\phi}_{pq}\int_0^{2\pi}\mathrm{d}\phi_{kq}\int_0^{\infty}\mathrm{d}q\int_{\max\left(-q,q-2p\frac{q-2p}{3}\right)}^{q}\mathrm{d}\omega\int_{\frac{q+\omega}{2}}^{p+2\omega}\mathrm{d}k \times q_2^i q_2^j\frac{|\mathcal{M}_{cd}^{ab}|^2}{p^2}f_b(k,v_k)\left(1\pm f_d(k-\omega,v_{k'})\right). \tag{3.96c}$$

$$\hat{q} = q_2^{xx} + q_2^{yy} \tag{3.96d}$$

with $v_{(\dots)} = \cos\theta_{(\dots)}$, And the components q_i are defined as

$$q_2^x = q\sqrt{1-v_{pq}^2}\cos\tilde{\phi}_{pq}, \tag{3.97a}$$

$$q_2^y = q\sqrt{1-v_{pq}^2}\sin\tilde{\phi}_{pq}, \tag{3.97b}$$

$$q_2^z = qv_{pq}. \tag{3.97c}$$

The additional quantities are

$$v_{pq} = \frac{\omega}{q} + \frac{t}{2pq}, \tag{3.98a}$$

$$v_{kq} = \frac{\omega}{q} - \frac{t}{2kq}, \tag{3.98b}$$

$$v_{k'q} = \frac{\omega}{q} + \frac{t}{2k'q}, \tag{3.98c}$$

$$\begin{aligned} v_k = {} & \sin\phi_{kq}\sin\tilde{\phi}_{pq}\sqrt{1-v_{kq}^2}\sqrt{1-v_p^2} \\ & + \cos\phi_{kq}\sqrt{1-v_{kq}^2}\left(-\cos\tilde{\phi}_{pq}v_{pq}\sqrt{1-v_p^2} - v_p\sqrt{1-v_{pq}^2}\right) \\ & + v_{kq}\left(v_pv_{pq} - \cos\tilde{\phi}_{pq}\sqrt{1-v_p^2}\sqrt{1-v_{pq}^2}\right), \end{aligned} \tag{3.98d}$$

$$\begin{aligned} v_{k'} = {} & \sin\phi_{kq}\sin\tilde{\phi}_{pq}\sqrt{1-v_{k'q}^2}\sqrt{1-v_p^2} \\ & + \cos\phi_{kq}\sqrt{1-v_{k'q}^2}\left(-\cos\tilde{\phi}_{pq}v_{pq}\sqrt{1-v_p^2} - v_p\sqrt{1-v_{pq}^2}\right) \\ & + v_{k'q}\left(v_pv_{pq} - \cos\tilde{\phi}_{pq}\sqrt{1-v_p^2}\sqrt{1-v_{pq}^2}\right), \end{aligned} \tag{3.98e}$$

$$p' = p + \omega, \tag{3.98f}$$
$$k' = k - \omega, \tag{3.98g}$$
$$t = \omega^2 - q^2, \tag{3.98h}$$
$$s = -\frac{t}{2q^2}\left((p+p')(k+k') + q^2 - \sqrt{(4pp'+t)(4k'k+t)}\cos(\phi_{kq})\right), \tag{3.98i}$$
$$u = \frac{t}{2q^2}\left((p+p')(k+k') - q^2 - \sqrt{(4pp'+t)(4k'k+t)}\cos(\phi_{kq})\right), \tag{3.98j}$$

and $\nu_a = 2d_R$, where d_R is the dimension of the representation of the jet particle. $\phi_{k'q} = \phi_{kq}$ because they are defined in a coordinate frame in which $q = q(0,0,1)$ and $\mathbf{k}' = \mathbf{k} - \mathbf{q}$. In (3.96a), (3.96b) and (3.96c) the upper sign is to be used when the d particle is a boson (gluon), the lower sign if it is a fermion (quark). The expressions for u, s can be found in [37] and in Appendix A.

We will use these different parametrizations, (3.96a), (3.96b) and (3.96c), which are all equivalent, as a sanity check, because they should all give the same results.

3.4. Symmetries of $\hat{q}_2^{ij}$

If the particle distribution $f(k, v_k)$ is spherically symmetric, i.e. does not depend on v_k, the mixed components of $\hat{q}_2^{ij}$ vanish, i.e.

$$\hat{q}^{xy} = \hat{q}^{xz} = \hat{q}^{yz} = 0. \tag{3.99}$$

This is because the only $\tilde{\phi}$-dependence comes from q_2^i and $\int_0^{2\pi} \mathrm{d}\tilde{\phi}_{pq} \cos\tilde{\phi}_{pq} \sin\tilde{\phi}_{pq} = 0$.

We can even take it a step further and generalize this for general $f(k, v_k)$. Let us look at a general function dependent only on the angles

$$\int_0^{2\pi} \mathrm{d}\tilde{\phi}_{pq} \int_0^{2\pi} \mathrm{d}\phi_{kq}\, f\left(\tilde{\phi}_{pq}, \phi_{kq}\right) = \int_{-\pi}^{\pi} \mathrm{d}\tilde{\phi}_{pq} \int_{-\pi}^{\pi} \mathrm{d}\phi_{kq}\, f\left(\tilde{\phi}_{pq}, \phi_{kq}\right). \tag{3.100}$$

Then we can split the $\tilde{\phi}_{pq}$-integral to arrive at

$$\int_{-\pi}^{0} \mathrm{d}\tilde{\phi}_{pq} \int_{-\pi}^{\pi} \mathrm{d}\phi_{kq}\, f\left(\tilde{\phi}_{pq}, \phi_{kq}\right) + \int_{0}^{\pi} \mathrm{d}\tilde{\phi}_{pq} \int_{-\pi}^{\pi} \mathrm{d}\phi_{kq}\, f\left(\tilde{\phi}_{pq}, \phi_{kq}\right). \tag{3.101}$$

In the first term, we perform a change of integration variables, $\tilde{\phi}_{pq} \to -\tilde{\phi}_{pq}$, $\phi_{kq} \to -\phi_{kq}$,

$$\int_{0}^{\pi} \mathrm{d}\tilde{\phi}_{pq} \int_{-\pi}^{\pi} \mathrm{d}\phi_{kq} \left[f\left(-\tilde{\phi}_{pq}, -\phi_{kq}\right) + f\left(\tilde{\phi}_{pq}, \phi_{kq}\right)\right]. \tag{3.102}$$

In the expression for $\hat{q}_2^{ij}$, ϕ_{kq} and $\tilde{\phi}_{pq}$ only appear in $v_k\left(\phi_{kq}, \tilde{\phi}_{pq}\right)$, $v_{k'}\left(\phi_{kq}, \tilde{\phi}_{pq}\right)$, in $q_2^x \sim \cos\tilde{\phi}_{pq}$, and $q_2^y \sim \sin\tilde{\phi}_{pq}$in the matrix elements via $s\,(\cos\phi_{kq})$ and $u\,(\cos\phi_{kq})$. Because the cosine is an even function $\phi_{kq} \to -\phi_{kq}$ does not change s and u. Similarly, v_k and $v_{k'}$ are not changed by simultaneously replacing $\phi_{pq} \to -\tilde{\phi}_{pq}$ and $\phi_{kq} \to \phi_{kq}$, because the cosines are, again, even, and the only odd functions, $\sin\phi_{kq} \sin\tilde{\phi}_{pq}$ appear in pairs, resulting in an even expression. The only change happens in $q_2^y \to -q_2^y$, which results in

$$\hat{q}_2^{xy} = \hat{q}_2^{yz} = 0. \tag{3.103}$$

3.5. Matrix elements

We have started with the matrix elements in Table 2.1, however, we chose $p' > k'$, which breaks the symmetry that is present in [3]. Consider e.g. the process $q_1 g \leftrightarrow q_1 g$. Let us assign the incoming quark q_1 momentum p, the incoming gluon g momentum k, the outgoing quark q_1 momentum p' and the outgoing gluon momentum k'. In [3] there is no restriction for k' and p', but if we define $p' > k'$ we must make a distinction whether the quark or the gluon has the larger outgoing momentum. In table 2.1 there is no explicit matrix element for $q_1 g \leftrightarrow g q_1$, because in the symmetric way one can always relabel $p' \leftrightarrow k'$ and $c \leftrightarrow d$, which yields the same. In our case, however, we can have $q_1 g \leftrightarrow q_1 g$ corresponding to a incoming quark with momentum p scattering of a gluon with momentum k, where the outgoing quark has momentum p', which is larger than the outgoing gluon momentum k'. If the outgoing gluon has larger momentum, we label it p' and thus we call the process then $q_1 g \leftrightarrow g q_1$.

In table 2.1 the Mandelstam variables s, t, u are defined with respect to a, b, c, d,

$$s = -(P + K)^2, \qquad t = -(P' - P)^2, \qquad u = (K' - P)^2. \tag{3.104}$$

In our case, in the process $q_1 g \leftrightarrow q_1 g$, where the gluon has a larger momentum, we relabel $P' \leftrightarrow K'$ and thus obtain the substitution

$$s \to s, \qquad t \to u, \qquad u \to t. \tag{3.105}$$

The matrix elements are then given in Table 3.1.

We use again a regulator ξ_0 for the $\frac{1}{t^2}$ matrix elements, as explained in Section 2.2.3. We will find, however, that this ξ_0 will be different than the one used in Section 2.2.3. This is because previously the matching condition was formulated in such a way that the longitudinal momentum diffusion is reproduced in the soft limit, and here we use the transverse momentum diffusion. We will elaborate more on this in Section 3.11.

3.6. p dependence of $\hat{q}$

In all our calculations before we always considered the jet momentum to be much larger than all other momentum scales of the plasma. Now let us take this assumption to its extreme limit and consider $p \to \infty$. Then, of course, all matrix elements $\frac{\left|\mathcal{M}^{ab}_{cd}(s,t,u)\right|^2}{p^2}$ vanish unless they are at least proportional to p^2.

Let us now consider the Mandelstam variables individually, starting with $t = \omega^2 - q^2$,

$ab \leftrightarrow cd$	$\left\|\mathcal{M}_{cd}^{ab}\right\|^2/g^4$
$q_1q_2 \leftrightarrow q_1q_2$, $q_1\bar{q}_2 \leftrightarrow q_1\bar{q}_2$, $\bar{q}_1q_2 \leftrightarrow \bar{q}_1q_2$, $\bar{q}_1\bar{q}_2 \leftrightarrow \bar{q}_1\bar{q}_2$	$8\frac{d_F^2C_F^2}{d_A}\left(\frac{s^2+u^2}{\underline{t^2}}\right)$
$q_1q_2 \leftrightarrow q_2q_1$, $q_1\bar{q}_2 \leftrightarrow \bar{q}_2q_1$, $\bar{q}_1q_2 \leftrightarrow q_2\bar{q}_1$, $\bar{q}_1\bar{q}_2 \leftrightarrow \bar{q}_2\bar{q}_1$	$8\frac{d_F^2C_F^2}{d_A}\left(\frac{s^2+t^2}{u^2}\right)$
$q_1q_1 \leftrightarrow q_1q_1$, $\bar{q}_1\bar{q}_1 \leftrightarrow \bar{q}_1\bar{q}_1$	$8\frac{d_F^2C_F^2}{d_A}\left(\frac{s^2+u^2}{\underline{t^2}}+\frac{s^2+t^2}{u^2}\right)+16d_FC_F\left(C_F-\frac{C_A}{2}\right)\frac{s^2}{tu}$
$q_1\bar{q}_1 \leftrightarrow q_1\bar{q}_1$	$8\frac{d_F^2C_F^2}{d_A}\left(\frac{s^2+u^2}{\underline{t^2}}+\frac{t^2+u^2}{s^2}\right)+16d_FC_F\left(C_F-\frac{C_A}{2}\right)\frac{u^2}{st}$
$q_1\bar{q}_1 \leftrightarrow \bar{q}_1q_1$	$8\frac{d_F^2C_F^2}{d_A}\left(\frac{s^2+t^2}{u^2}+\frac{u^2+t^2}{s^2}\right)+16d_FC_F\left(C_F-\frac{C_A}{2}\right)\frac{t^2}{su}$
$q_1\bar{q}_1 \leftrightarrow q_2\bar{q}_2$, $q_1\bar{q}_1 \leftrightarrow \bar{q}_2q_2$	$8\frac{d_F^2C_F^2}{d_A}\left(\frac{t^2+u^2}{s^2}\right)$
$q_1\bar{q}_1 \leftrightarrow gg$	$8d_FC_F^2\left(\frac{u}{\underline{t}}+\frac{t}{u}\right)-8d_FC_FC_A\left(\frac{t^2+u^2}{s^2}\right)$
$q_1g \leftrightarrow q_1g$, $\bar{q}_1g \leftrightarrow \bar{q}_1g$	$-8d_FC_F^2\left(\frac{u}{s}+\frac{s}{u}\right)+8d_FC_FC_A\left(\frac{s^2+u^2}{\underline{t^2}}\right)$
$q_1g \leftrightarrow gq_1$, $\bar{q}_1g \leftrightarrow g\bar{q}_1$	$-8d_FC_F^2\left(\frac{t}{s}+\frac{s}{\underline{t}}\right)+8d_FC_FC_A\left(\frac{s^2+t^2}{u^2}\right)$
$gg \leftrightarrow gg$	$16d_AC_A^2\left(3-\frac{su}{\underline{t^2}}-\frac{st}{u^2}-\frac{tu}{s^2}\right)$

Table 3.1.: Matrix elements for $\hat{q}$, obtained from the matrix elements from Table 2.1 by changing $c \leftrightarrow d$ and $t \leftrightarrow u$. Singly-underlined denominators indicate infrared-sensitive contributions from soft gluon exchange, double-underlined denominators from soft fermion exchange. Note that - in contrast to [3] - only denominators with t are underlined. This is because the problematic regions are those where either $-t$ or $-u$ is small while s is large [3]. However, for big enough incoming jet momentum p, $-u \sim s$, so only regions with small t can be problematic.

which is much smaller than p. For s we expand

$$s = -\frac{t}{2q^2}\left((p+p')(k+k') + q^2 - \sqrt{(4pp'+t)(4k'k+t)}\cos(\phi_{kq})\right) \tag{3.106}$$

$$= -\frac{t}{2q^2}\left((2p+\omega)(2k-\omega) - q^2 - \sqrt{(4p(p+\omega)+t)(4(k-\omega)k+t)}\cos\phi_{kq}\right) \tag{3.107}$$

$$= -\frac{t}{2q^2}\left(2p(2k-\omega) + \omega(2k-\omega) - q^2 - \sqrt{(4p^2+4p\omega+t)((2k-\omega)^2-q^2)}\cos\phi_{kq}\right) \tag{3.108}$$

$$= -\frac{t}{2q^2}2p\Bigg[(2k-\omega) + \frac{\omega(2k-\omega)-q^2}{2p} \tag{3.109}$$

$$- \sqrt{(2k-\omega)^2 - q^2 + \frac{\omega}{p}((2k-\omega)^2-q^2) + \frac{t}{4p^2}\left((2k-\omega)^2-q^2\right)}\cos\phi_{kq}\Bigg]$$

$$= -\frac{t}{2q^2}2p\Bigg[(2k-\omega)\left(1+\frac{\omega}{2p} - \frac{q^2}{2p(2k-\omega)}\right) \tag{3.110}$$

$$- \sqrt{(2k-\omega)^2-q^2}\cdot\sqrt{1+\frac{\omega}{p}+\frac{t}{4p^2}}\cos\phi_{kq}\Bigg]$$

Now we need to find out if the terms $\sim \frac{1}{p}$ are indeed small when $p \to \infty$. The naïve way to proceed would be to write

$$s = -\frac{pt}{q^2}\left[(2k-\omega) - \sqrt{(2k-\omega)^2-q^2}\cos\phi_{kq} + \mathcal{O}\left(\frac{1}{p}\right)\right], \tag{3.111}$$

but are these $\mathcal{O}\left(\frac{1}{p}\right)$ terms really $\sim \frac{1}{p}$ in the expression for $\hat{q}$?

Let us define κ as the maximum momentum present in our plasma, i.e. $f(\mathbf{k}) = 0 \quad \forall k > \kappa$. Then we take a look at ω/p. From the parametrization of the integral boundaries, (3.45), we know that $0 < k < \kappa$, $-\frac{p-k}{2} < \omega < k$. For positive ω, this is obviously fine, since $p \gg \kappa$ and thus $\frac{\omega}{p} < \frac{k}{p} \ll 1$. For $\omega < 0$, however, we seemingly run into troubles, since

$$\left|\frac{\omega}{p}\right| = \frac{-\omega}{p} < \frac{p-k}{2p} = \frac{1}{2} - \frac{k}{2p}, \tag{3.112}$$

and thus the first term is independent of p, so we cannot make $\left|\frac{\omega}{p}\right|$ arbitrarily small by increasing p. Maybe, however, it works out under the integral, eventually, but for this let us consider the whole matrix element. The gluonic matrix element, $gg \to gg$, reads

$$\left|\mathcal{M}^{ab}_{cd}\right|^2/g^4 = 16 d_A C_A^2\left(3 - \frac{su}{t^2} - \frac{st}{u^2} - \frac{tu}{s^2}\right). \tag{3.113}$$

Due to our choice of our regularization (see section 2.2.3), the t-channel matrix element is changed, which yields

$$\left|\mathcal{M}^{gg}_{gg}\right|^2/g^4 = 16 d_A C_A^2\left(3 - \frac{su}{t^2}\frac{q^4}{(q^2+\tilde{m}^2)^2} - \frac{st}{u^2} - \frac{tu}{s^2}\right). \tag{3.114}$$

In the expression for $\hat{q}$, we need $\left|\mathcal{M}^{ab}_{cd}\right|^2/(g^4p^2)$. Let us expand this expression in $1/p$, then the leading order term should be independent of p and the next-to-leading-order (NLO) term should be $\sim\frac{1}{p}$. In s and u, p appears explicitly, thus they are at leading order $\sim p$. Then, for the first terms in the $\frac{1}{p}$-expansion of the matrix element, we can neglect all terms except for su/t^2. Any explicit[8] p-dependence can only come from the su term, thus it is sufficient to consider su.

$$su = -\frac{t^2p^2}{q^4}\left[(2k-\omega)\left(1+\frac{\omega}{2p}-\frac{q^2}{2p(2k-\omega)}\right)-\sqrt{(2k-\omega)^2-q^2}\left(1+\frac{\omega}{p}+\frac{\omega^2-q^2}{4p^2}\right)^{1/2}\cos\phi_{kq}\right]$$
$$\left[(2k-\omega)\left(1+\frac{\omega}{2p}+\frac{q^2}{2p(2k-\omega)}\right)-\sqrt{(2k-\omega)^2-q^2}\left(1+\frac{\omega}{p}+\frac{\omega^2-q^2}{4p^2}\right)^{1/2}\cos\phi_{kq}\right] \tag{3.115}$$

$$= -\frac{t^2p^2}{q^4}\left[(2k-\omega)\left(1+\frac{\omega}{2p}-\frac{q^2}{2p(2k-\omega)}\right)-\sqrt{(2k-\omega)^2-q^2}\left(1+\frac{\omega}{2p}+\ldots\right)\cos\phi_{kq}\right]$$
$$\left[(2k-\omega)\left(1+\frac{\omega}{2p}+\frac{q^2}{2p(2k-\omega)}\right)-\sqrt{(2k-\omega)^2-q^2}\left(1+\frac{\omega}{2p}+\ldots\right)\cos\phi_{kq}\right] \tag{3.116}$$

$$\approx -\frac{t^2p^2}{q^4}\left(2k-\omega-\sqrt{(2k-\omega)^2-q^2}\cos\phi_{kq}\right)^2 \tag{3.117}$$
$$-\frac{\omega t^2p}{q^4}\left(2k-\omega-\sqrt{(2k-\omega)^2-q^2}\cos\phi_{kq}\right)^2$$

Thus we obtain for the matrix element

$$\left|\mathcal{M}^{gg}_{gg}\right|^2/p^2 = 16d_AC_A^2\frac{\left(2k-\omega-\sqrt{(2k-\omega)^2-q^2}\cos\phi_{kq}\right)^2}{(q^2+\tilde{m}^2)^2}\left(1+\frac{\omega}{p}+\mathcal{O}\left(\frac{1}{p^2}\right)\right). \tag{3.118}$$

We now want to determine the behavior of[9]

$$\hat{q} = \frac{1}{\nu_a}\frac{1}{2^9\pi^5}\sum_{bcd}\int_0^{2\pi}\mathrm{d}\tilde{\phi}_{pq}\int_0^{2\pi}\mathrm{d}\phi_{kq}\int_0^{\infty}\mathrm{d}k\int_{-\frac{p-k}{2}}^{k}\mathrm{d}\omega\int_{|\omega|}^{\min(p+p',k+k')}\mathrm{d}q$$
$$(q^2-\omega^2)\frac{|\mathcal{M}^{ab}_{cd}|^2}{p^2}f_b(k,v_k)\left(1\pm f_d(k-\omega,v_{k'})\right) \tag{3.119}$$

with the matrix element given in (3.118). First, we observe that the distribution function $f_b(k,v_k)$ provides a natural upper boundary on the k-integral. Let us assume, for simplicity, that the distribution function is of the form

$$f(k) = N\Theta(\kappa-k), \tag{3.120}$$

[8] With explicit we mean that the p-dependence is already in the matrix element. In principle, after the integration, we could also obtain a p-dependence without any explicit p-dependence in the matrix element.

[9] We use $v_{pq}=\frac{\omega}{q}$, which is justified for large p, see also (3.163).

i.e. $f(k) = 0 \quad \forall k > \kappa$. Physically, κ is the maximum momentum of a particle in our plasma.

By assumption, the jet momentum $p \gg \kappa$. Thus the minimum of $(p + p', k + k') = (2p + \omega, 2k - \omega)$ is always $2k - \omega$, because

$$2k - \omega < 2p + \omega \tag{3.121}$$

$$\omega > k - p \tag{3.122}$$

is always fulfilled via the lower boundary of the ω-integral, $\omega > \frac{k-p}{2}$.

The second distribution function, $f_d(k - \omega)$ enforces $k - \omega < \kappa$ and thus yields a lower bound for the ω-integral, $\omega > k - \kappa$. But any p-dependence of the integral (that was not there in the matrix element) can only come from the lower boundary of the ω-integral. Therefore, $f_d(k - \omega)$ does not contribute to the p-dependence.

The p-dependence of $\hat{q}$ can therefore be inferred from

$$\hat{q} \sim I(p) = \int_{-\frac{p-k}{2}}^{k} \mathrm{d}\omega \int_{|\omega|}^{2k-\omega} \mathrm{d}q\, A(q, \omega, k, p, \phi_{kq}, \tilde{m}), \tag{3.123}$$

$$A(q, \omega, k, p, \phi_{kq}, \tilde{m}) = (q^2 - \omega^2) \frac{\left|\mathcal{M}^{gg}_{gg}\right|^2}{p^2}. \tag{3.124}$$

The p-dependence of $\hat{q}$ can either come from the lower boundary of the ω-integral or a p-dependence of A. We can expand A in p,

$$A(p) = A_0 + A_1 \frac{1}{p} + \mathcal{O}\left(\frac{1}{p^2}\right), \tag{3.125}$$

where A_0 and A_1 do no depend on p, but still depend on $q, \omega, k, \phi_{kq}, \tilde{m}$, but for the ease of notation we do not write this dependence explicitly. Comparing with (3.118), we obtain

$$A_0 = 16 g^2 d_A C_A^2 (q^2 - \omega^2) \frac{\left(2k - \omega - \sqrt{(2k-\omega)^2 - q^2}\right)^2}{(q^2 + \tilde{m}^2)^2}, \tag{3.126}$$

$$A_1 = \omega A_0. \tag{3.127}$$

We now split the ω-integral,

$$I(p) = I^c(p) + I^p(p), \tag{3.128}$$

$$I^c(p) = \int_{-\xi}^{k} \mathrm{d}\omega \int_{|\omega|}^{2k-\omega} \mathrm{d}q\, A(q, \omega, k, p, \phi_{kq}, \tilde{m}), \tag{3.129}$$

$$I^p(p) = \int_{-\frac{p-k}{2}}^{-\xi} \mathrm{d}\omega \int_{-\omega}^{2k-\omega} \mathrm{d}q\, A(q, \omega, k, p, \phi_{kq}, \tilde{m}), \tag{3.130}$$

with

$$k \ll \xi \ll p. \tag{3.131}$$

Because of our expansion of A in p, (3.125), we can perform the limit $p \to \infty$ for I^c, leaving ξ fixed. I^c is then independent of p, or constant, therefore labelled with the index c. For large p, any p-dependence to $\hat{q}$ can only come from I^p.

Inserting (3.125) into the definitions of I^c and I^p, we obtain an expansion of I^c and I^p in p,

$$I^c(p) = I_0^c + \frac{1}{p} I_1^c + \dots, \tag{3.132}$$

$$I_0^c = \int_{-\xi}^{k} \mathrm{d}\omega \int_{|\omega|}^{2k-\omega} \mathrm{d}q\, A_0(q,\omega,k,\phi_{kq},\tilde{m}), \tag{3.133}$$

$$I_1^c = \int_{-\xi}^{k} \mathrm{d}\omega \int_{|\omega|}^{2k-\omega} \mathrm{d}q\, A_1(q,\omega,k,\phi_{kq},\tilde{m}), \tag{3.134}$$

$$I^p(p) = I_0^p(p) + \frac{1}{p} I_1^p(p) + \dots, \tag{3.135}$$

$$I_0^p = \int_{-\frac{p-k}{2}}^{-\xi} \mathrm{d}\omega \int_{-\omega}^{2k-\omega} \mathrm{d}q\, A_0(q,\omega,k,\phi_{kq},\tilde{m}), \tag{3.136}$$

$$I_1^p = \int_{-\frac{p-k}{2}}^{-\xi} \mathrm{d}\omega \int_{-\omega}^{2k-\omega} \mathrm{d}q\, A_1(q,\omega,k,\phi_{kq},\tilde{m}), \tag{3.137}$$

and also

$$I(p) = I_0(p) + \frac{1}{p} I_1(p) + \dots. \tag{3.138}$$

From (3.132) we can see immediately that for $p \to \infty$ $I^c(p)$ becomes independent of p, because I_1^c does not depend on p. The $p \to \infty$ asymptotic behavior of $I(p) = I^c(p) + I^p(p)$ comes, therefore, only from $I^p(p)$.

3.7. Analysis of the integrand

We shall now analyse a general integrand of the form in (3.135), e.g. I_0^p or I_1^p. Let us define a general I_{nm},

$$I_{nm}(p) = \int_{-\frac{p-k}{2}}^{-\xi} \mathrm{d}\omega \int_{-\omega}^{2k-\omega} \mathrm{d}q\, A_{nm}(q,\omega), \tag{3.139}$$

for

$$A_{nm}(q,\omega) = q^n \omega^m, \quad n \neq -1. \tag{3.140}$$

To get rid of additional minus signs, we define $x = -\omega$,

$$I_{nm}(p) = (-1)^m \int_{\xi}^{\frac{p-k}{2}} \mathrm{d}x \int_{x}^{2k+x} \mathrm{d}q\, q^n x^m, \tag{3.141}$$

$$\overset{n\neq -1}{=} \frac{(-1)^m}{n+1} \int_{\xi}^{\frac{p-k}{2}} \mathrm{d}x\, x^m \left[(2k+x)^{n+1} - x^{n+1} \right]. \tag{3.142}$$

It will be useful for later to also go to next-to-leading order. We expand the first term in a power series using the Binomial series [38],

$$(x+y)^r = \sum_{k=0}^{\infty} \binom{r}{k} x^{r-k} y^k, \quad x, y \in \mathbb{R}, \quad |x| > |y|, \quad r \in \mathbb{C}. \tag{3.143}$$

We thus obtain

$$I_{nm} = \frac{(-1)^m}{n+1} \int_\xi^{\frac{p-k}{2}} \mathrm{d}x\, x^m \left[\sum_{j=0}^{\infty} \binom{n+1}{j} x^{n+1-j} (2k)^j - x^{n+1} \right]. \tag{3.144}$$

The first term with $j = 0$ cancels, so we can start the sum at $j = 1$,

$$I_{nm} = \frac{(-1)^m}{n+1} \int_\xi^{\frac{p-k}{2}} \mathrm{d}x \sum_{j=1}^{\infty} \binom{n+1}{j} x^{n+m+1-j} (2k)^j, \tag{3.145}$$

$$= \frac{(-1)^m}{n+1} \left(\sum_{\substack{j=1 \\ j\neq n+m+2}}^{\infty} \binom{n+1}{j} \frac{x^{n+m+2-j}}{n+m+2-j} \Bigg|_{x=\xi}^{\frac{p-k}{2}} (2k)^j + \binom{n+1}{n+m+2} \ln\left(\frac{p-k}{2\xi}\right) (2k)^{n+m+2} \right). \tag{3.146}$$

We only want to get the leading (and next-to-leading) order behavior in p, thus we need not consider the lower boundary $x = \xi$, and we only need to take into account the leading terms, i.e. the terms with the largest exponents in p. The largest exponent is obtained for $j = 1$, for which the (generalized) binomial coefficient yields $n + 1$. As hinted earlier, it will be useful to also consider the next-to-leading order (NLO) terms. We obtain

$$I_{nm}^{LO} = \begin{cases} \frac{(-1)^m (2k)}{n+m+1} \left(\frac{p}{2}\right)^{n+m+1}, & n+m+1 \neq 0 \\ (-1)^m (2k) \ln(p) + \text{const}, & n+m+1 = 0 \end{cases} \tag{3.147}$$

$$I_{nm}^{NLO} = \begin{cases} \frac{(-1)^m (2k)^2}{(n+1)(n+m)} \binom{n+1}{2} \left(\frac{p}{2}\right)^{n+m}, & n+m \neq 0 \\ \frac{(-1)^m}{n+1} \binom{n+1}{2} (2k)^2 \ln(p) + \text{const}, & n+m = 0. \end{cases} \tag{3.148}$$

$$\tag{3.149}$$

Now we need to find out n and m for our specific integrand of I_0^p, A_0:

$$A_0 = 16 d_A C_A^2 (q^2 - \omega^2) \frac{\left(2k - \omega - \sqrt{(2k-\omega)^2 - q^2}\right)^2}{(q^2 + \tilde{m}^2)^2} \tag{3.150}$$

$$= 16 d_A C_A^2 (q^2 - \omega^2) \frac{\omega^2 \left(1 - \frac{2k}{\omega} + \sqrt{\frac{4k^2 - 4k\omega + \omega^2 - q^2}{\omega^2}}\right)^2}{q^4 \left(1 + \frac{\tilde{m}^2}{q^2}\right)^2}. \tag{3.151}$$

By assumption $|\omega| > \xi \gg k$ and $q > |\omega|$, thus $\frac{2k}{\omega} \to 0$, $\frac{4k(k-\omega)}{\omega^2} \to 0$ and $\frac{q^2-\omega^2}{\omega^2} < \frac{(2k-\omega)^2-\omega^2}{\omega^2} = \frac{4k(k-\omega)}{\omega^2} \to 0$ for big enough ξ.

We then have $A_0 = \alpha \left(\frac{\omega^2}{q^2} - \frac{\omega^4}{q^4}\right)$, $\alpha = 16 d_A C_A$, thus

$$I_0^p(p) = \alpha \left(I_{-2,2} - I_{-4,4}\right). \tag{3.152}$$

The leading order term depends only on $n+m$ and $(-1)^m$, and behaves like p^{n+m+1}. A closer look, however, reveals that the leading order terms cancel and we need to take into account the NLO terms,

$$I_{-2,2} - I_{-4,4} = \frac{(-1)^2}{-1}\binom{-1}{2}(2k)^2\ln(p) - \frac{(-1)^4}{-3}\binom{-3}{2}(2k)^2\ln(p), \tag{3.153}$$

thus

$$I_0^p(p) \sim \ln(p), \tag{3.154}$$

$$I_0(p) = a + b\ln(p) + \mathcal{O}\left(\frac{1}{p}\right). \tag{3.155}$$

which diverges logarithmically.

For I_1^p we find

$$I_1^p(p) = \alpha\left(I_{-2,3} - I_{-4,4}\right), \tag{3.156}$$

$$I_{-2,3} = \frac{(-1)^3(2k)}{2}\left(\frac{p}{2}\right)^2 + \frac{(-1)^3}{(-1)(1)}\binom{-1}{2}(2k)^2\frac{p}{2} \tag{3.157}$$

$$I_{-4,5} = \frac{(-1)^5(2k)}{2}\left(\frac{p}{2}\right)^2 + \frac{(-1)^5}{(-3)(1)}\binom{-3}{2}(2k)^2\frac{p}{2} \tag{3.158}$$

and thus

$$I_1^p(p) \sim p \tag{3.159}$$

$$I_1(p) = c + ep + \mathcal{O}\left(\frac{1}{p}\right). \tag{3.160}$$

Taking only the leading order term is a good approximation if $\frac{I_1(p)}{p} \ll I_0(p)$, which we can now easily show:

$$\frac{\frac{I_1}{p}}{I_0} = \frac{\frac{1}{p}(ep+c)}{b\ln(p)+a} = \frac{e\left(1+\frac{c}{ep}\right)}{b\ln(p)\left(1+\frac{a}{b\ln(p)}\right)} \sim \frac{1}{\ln(p)} \tag{3.161}$$

We have now learned two important facts:

- For $p \to \infty$, $\hat{q}$ is given by its leading order contribution in p
- $\hat{q}$ grows logarithmically with p.

Actually, it is not always the case that the NLO term is negligible. If we consider $A_0 = q^n\omega^m$ with $n+m > 0$, $A_1 = \omega A_0$, we obtain $I_0 \sim p^{n+m+1}$ and $I_1 \sim p^{n+m+2}$ and thus

$$\frac{\frac{1}{p}I_1}{I_0} = \frac{\frac{1}{p}\left(ap^{n+m+2}+b\right)}{cp^{n+m+1}+e} \sim \frac{a}{c} + \mathcal{O}\left(\frac{1}{p}\right),$$

which means that the NLO term does not get smaller than a/c with larger p. Luckily, for our case, these leading order terms cancel and we effectively obtain $n+m<0$, so we have convergence. This example is to show that an expansion in $1/p$ of A does not necessarily mean that all higher-order terms do not contribute.

3.8. UV-cutoff for $q_\perp$

In the previous section we have seen that $\hat{q}$ exhibits a logarithmic divergence in the limit of $p \to \infty$. Therefore, we need to impose some cutoff, which is typically [8, 9] implemented as a $q_\perp$-cutoff.

We only consider processes up to a maximum $q_\perp < \Lambda_\perp$,

$$q_\perp = q\sqrt{1 - v_{pq}^2} = q\sqrt{1 - \frac{\omega^2}{q^2} - \frac{\omega^2 - q^2}{2pq}} < \Lambda_\perp. \tag{3.162}$$

For $p \to \infty$,

$$\frac{q^2 - \omega^2}{2pq} < \frac{4k(k-\omega)}{2pq} = 2\underbrace{\frac{k}{p}}_{\ll 1}\frac{k}{q} - 2\underbrace{\frac{k}{p}}_{\ll 1}\underbrace{\frac{\omega}{q}}_{\in[-1,1]}. \tag{3.163}$$

The second term clearly becomes 0 for $p \to \infty$. The first term $\to 0$ for $q \neq 0$. Let us look at the case $q = 0$ separately. From (3.45) we see immediately that $q > |\omega|$, and thus $q \to 0$ can only happen for $\omega = 0$. Then,

$$\lim_{q\to 0} \frac{\omega^2 - q^2}{2pq}\bigg|_{\omega=0} = \lim_{q\to 0} \frac{-q^2}{2pq} = 0. \tag{3.164}$$

For $p \to \infty$, the $q_\perp$-cutoff can therefore be implemented by requiring

$$q^2 - \omega^2 < \Lambda_\perp^2. \tag{3.165}$$

We can implement this in the different parametrizations, (3.45), (3.50) and (3.51). For (3.50) and (3.51), this can easily be implemented via

$$\hat{q} \sim \int_0^\infty \mathrm{d}k \int_0^\infty \mathrm{d}k' \int_{|k-k'|}^{\min\left(k+k', \sqrt{(k-k')^2+\Lambda_\perp^2}\right)} \mathrm{d}q \tag{3.166}$$

and

$$\hat{q} \sim \int_0^\infty \mathrm{d}k \int_{-\infty}^{k} \mathrm{d}\omega \int_{|\omega|}^{\min\left(2k-\omega, \sqrt{\omega^2+\Lambda_\perp^2}\right)} \mathrm{d}q\,. \tag{3.167}$$

For (3.45) we need to implement the condition (3.165) in the ω-integral, $\omega^2 > q^2 - \Lambda_\perp^2$. If $q < \Lambda_\perp$, this leads to no new condition, but if $q > \Lambda_\perp$, we need to have a lower boundary for $|\omega|$, which we write symbolically as

$$\hat{q} \sim \left(\int_0^{\Lambda_\perp} \mathrm{d}q \int_{-q}^{q} \mathrm{d}\omega + \int_{\Lambda_\perp}^\infty \mathrm{d}q \left[\int_{-q}^{-\sqrt{q^2-\Lambda_\perp^2}} \mathrm{d}\omega + \int_{\sqrt{q^2-\Lambda_\perp^2}}^{q} \mathrm{d}\omega\right]\right) \int_{\frac{q+\omega}{2}}^\infty \mathrm{d}k\,. \tag{3.168}$$

3.9. $p \to \infty$ behavior of $\hat{q}$ with a $q_\perp$ cutoff

Previously, we have seen that $\hat{q}$ diverges for $p \to \infty$. We shall now show that, this is no longer the case for a $q_\perp$ cutoff.

We can now perform, again, a similar analysis of the integrand as in (3.139), but with different integration boundaries,

$$I_{nm}(p) = \int_{-\frac{p-k}{2}}^{-\xi} \mathrm{d}\omega \int_{-\omega}^{\min(2k-\omega,\sqrt{\omega^2+\Lambda_\perp^2})} \mathrm{d}q\, A_{nm}(q,\omega). \tag{3.169}$$

Actually, we can simplify the minimum, because it is always the second item for ξ big enough,

$$\sqrt{\omega^2+\Lambda_\perp^2} < 2k-\omega \tag{3.170}$$

$$\omega^2+\Lambda_\perp^2 < 4k(k-\omega)+\omega^2 \tag{3.171}$$

$$-\omega > \frac{\Lambda_\perp^2}{4k} - k, \tag{3.172}$$

but since $-\omega > \xi$, we can just choose a ξ that is big enough such that this expression is fulfilled, i.e. if

$$\xi > \frac{\Lambda_\perp^2}{4k} - k. \tag{3.173}$$

Thus we may rewrite (3.169) to

$$I_{nm}(p) = \int_{-\frac{p-k}{2}}^{-\xi} \mathrm{d}\omega \int_{-\omega}^{\sqrt{\omega^2+\Lambda_\perp^2}} \mathrm{d}q\, q^n \omega^m \tag{3.174}$$

Similarly as before, with $x = -\omega$, we obtain

$$I_{nm}(p) = (-1)^m \int_{\xi}^{\frac{p-k}{2}} \mathrm{d}x \int_{x}^{\sqrt{x^2+\Lambda_\perp^2}} \mathrm{d}q\, q^n x^m, \tag{3.175}$$

$$\overset{n\neq -1}{=} \frac{(-1)^m}{n+1} \int_{\xi}^{\frac{p-k}{2}} \mathrm{d}x\, x^m \left[\left(x^2+\Lambda_\perp^2\right)^{\frac{n+1}{2}} - x^{n+1} \right]. \tag{3.176}$$

For the convergence of (3.143) we need to know if $\Lambda_\perp^2 < x^2$. From (3.173) we know that $\Lambda_\perp^2 < 4k\xi\left(1+\frac{k}{\xi}\right) \approx 4k\xi$ and thus $\Lambda_\perp^2/\xi^2 < \frac{4k}{\xi} \ll 1$, which makes $\Lambda_\perp < \xi$ and thus $\Lambda_\perp < x$.

$$I_{nm} = \frac{(-1)^m}{n+1} \int_{\xi}^{\frac{p-k}{2}} \mathrm{d}x\, x^m \left[\sum_{j=0}^{\infty} \binom{(n+1)/2}{j} x^{n+1-2j} (\Lambda_\perp)^{2j} - x^{n+1} \right] \tag{3.177}$$

$$= \frac{(-1)^m}{n+1} \int_{\xi}^{\frac{p-k}{2}} \mathrm{d}x \sum_{j=1}^{\infty} \binom{(n+1)/2}{j} x^{n+m+1-2j} (\Lambda_\perp)^{2j}, \tag{3.178}$$

$$= \frac{(-1)^m}{n+1} \Bigg[\sum_{\substack{j=1 \\ j\neq(n+m+2)/2}}^{\infty} \binom{(n+1)/2}{j} \frac{x^{n+m+2-2j}}{n+m+2-2j} \Bigg|_{x=\xi}^{\frac{p-k}{2}} \Lambda_\perp^{2j} + \binom{(n+1)/2}{(n+m+2)/2} \ln\left(\frac{p-k}{2\xi}\right) \Lambda_\perp^{n+m+2} \Bigg]. \tag{3.179}$$

We now obtain

$$I_{nm}^{LO} = \begin{cases} \frac{(-1)^m \Lambda_\perp^2}{2(n+m)} \left(\frac{p}{2}\right)^{n+m}, & n+m \neq 0 \\ (-1)^m \Lambda_\perp^2 \ln(p) + \text{const}, & n+m = 0 \end{cases} \tag{3.180}$$

$$I_{nm}^{NLO} = \begin{cases} \frac{(-1)^m \Lambda_\perp^4}{(n+1)(n+m-2)} \binom{(n+1)/2}{2} \left(\frac{p}{2}\right)^{n+m-2}, & n+m-2 \neq 0 \\ \frac{(-1)^m}{n+1} \binom{(n+1)/2}{2} \Lambda_\perp^4 \ln(p) + \text{const}, & n+m-2 = 0. \end{cases} \tag{3.181}$$

Therefore,

$$I_0^p(p) \sim \frac{1}{p^2}, \tag{3.182}$$

$$I_1^p(p) \sim \frac{1}{p}, \tag{3.183}$$

$$I_0(p) = a + \frac{b}{p^2} + \mathcal{O}\left(\frac{1}{p^3}\right), \tag{3.184}$$

$$I_1(p) = c + \frac{e}{p} + \mathcal{O}\left(\frac{1}{p^2}\right). \tag{3.185}$$

The leading order term to $\hat{q}$, $\sim I_0$ is then independent of p, the NLO term, $\sim \frac{I_1}{p} \to 0$, or, more precisely,

$$\frac{I_1/p}{I_0} = \frac{\frac{1}{p}\left(c + \frac{e}{p}\right)}{a + \frac{b}{p^2}} \sim \frac{1}{p}. \tag{3.186}$$

Thus, now $\hat{q}$ converges, and the NLO terms for finite p are also small.

3.10. $\hat{q}$ in the limit $p \to \infty$

Previously, we have seen that in the limit $p \to \infty$ we can take the leading order term in the expansion in p of the matrix element. The formula for $\hat{q}$ then reads

$$\hat{q}_2^{ij}(\Lambda_\perp) = \frac{1}{\nu_a}\frac{1}{2^9\pi^5}\sum_{bcd}\int_0^{2\pi}\mathrm{d}\tilde{\phi}_{pq}\int_0^{2\pi}\mathrm{d}\phi_{kq}\int_0^{\infty}\mathrm{d}k\int_{-\infty}^{k}\mathrm{d}\omega\int_{|\omega|}^{\min\left(2k-\omega,\sqrt{\omega^2+\Lambda_\perp^2}\right)}\mathrm{d}q \times q_2^i q_2^j \frac{|\mathcal{M}_{cd}^{ab}|^2}{p^2} f_b(k,v_k)\left(1 \pm f_d(k-\omega,v_{k'})\right), \tag{3.187a}$$

$$\hat{q}_2^{ij}(\Lambda_\perp) = \frac{1}{\nu_a}\frac{1}{2^9\pi^5}\sum_{bcd}\int_0^{2\pi}\mathrm{d}\tilde{\phi}_{pq}\int_0^{2\pi}\mathrm{d}\phi_{kq}\int_0^{\infty}\mathrm{d}k\int_0^{\infty}\mathrm{d}k'\int_{|k-k'|}^{\min\left(k+k',\sqrt{(k-k')^2+\Lambda_\perp^2}\right)}\mathrm{d}q \times q_2^i q_2^j \frac{|\mathcal{M}_{cd}^{ab}|^2}{p^2} f_b(k,v_k)\left(1 \pm f_d(k',v_{k'})\right), \tag{3.187b}$$

$$\hat{q}_2^{ij}(\Lambda_\perp) = \frac{1}{\nu_a}\frac{1}{2^9\pi^5}\sum_{bcd}\int_0^{2\pi}\mathrm{d}\tilde{\phi}_{pq}\int_0^{2\pi}\mathrm{d}\phi_{kq} \times \left(\int_0^{\Lambda_\perp}\mathrm{d}q\int_{-q}^{q}\mathrm{d}\omega + \int_{\Lambda_\perp}^{\infty}\mathrm{d}q\left[\int_{-q}^{-\sqrt{q^2-\Lambda_\perp^2}}\mathrm{d}\omega + \int_{\sqrt{q^2-\Lambda_\perp^2}}^{q}\mathrm{d}\omega\right]\right) \times \int_{\frac{q+\omega}{2}}^{\infty}\mathrm{d}k\, q_2^i q_2^j \frac{|\mathcal{M}_{cd}^{ab}|^2}{p^2} f_b(k,v_k)\left(1 \pm f_d(k-\omega,v_{k'})\right), \tag{3.187c}$$

$$\hat{q} = q_2^{xx} + q_2^{yy}, \tag{3.187d}$$

with

$$q_2^x = q\sqrt{1-v_{pq}^2}\cos\tilde{\phi}_{pq}, \tag{3.188a}$$

$$q_2^y = q\sqrt{1-v_{pq}^2}\sin\tilde{\phi}_{pq}, \tag{3.188b}$$

$$q_2^z = qv_{pq}, \tag{3.188c}$$

$$v_{pq} = \frac{\omega}{q}, \tag{3.188d}$$

$$v_{kq} = \frac{\omega}{q} - \frac{t}{2kq}, \tag{3.188e}$$

$$v_{k'q} = \frac{\omega}{q} + \frac{t}{2k'q}, \tag{3.188f}$$

$$\begin{aligned} v_k = {} & \sin\phi_{kq}\sin\tilde{\phi}_{pq}\sqrt{1-v_{kq}^2}\sqrt{1-v_p^2} \\ & + \cos\phi_{kq}\sqrt{1-v_{kq}^2}\left(-\cos\tilde{\phi}_{pq}v_{pq}\sqrt{1-v_p^2} - v_p\sqrt{1-v_{pq}^2}\right) \\ & + v_{kq}\left(v_pv_{pq} - \cos\tilde{\phi}_{pq}\sqrt{1-v_p^2}\sqrt{1-v_{pq}^2}\right), \end{aligned} \tag{3.188g}$$

$$\begin{aligned} v_{k'} = {} & \sin\phi_{kq}\sin\tilde{\phi}_{pq}\sqrt{1-v_{k'q}^2}\sqrt{1-v_p^2} \\ & + \cos\phi_{kq}\sqrt{1-v_{k'q}^2}\left(-\cos\tilde{\phi}_{pq}v_{pq}\sqrt{1-v_p^2} - v_p\sqrt{1-v_{pq}^2}\right) \\ & + v_{k'q}\left(v_pv_{pq} - \cos\tilde{\phi}_{pq}\sqrt{1-v_p^2}\sqrt{1-v_{pq}^2}\right), \end{aligned} \tag{3.188h}$$

$ab \leftrightarrow cd$	$\lim_{p\to\infty} \lvert M^{ab}_{cd}\rvert^2/(p^2 g^4)$
$q_1 q_i \leftrightarrow q_1 q_i$ $\bar{q}_1 q_i \leftrightarrow \bar{q}_1 q_i$ $q_1 \bar{q}_i \leftrightarrow q_1 \bar{q}_i$ $\bar{q}_1 \bar{q}_i \leftrightarrow \bar{q}_1 \bar{q}_i$	$16 \frac{d_F^2 C_F^2}{d_a} \frac{\left(2k-\omega-\sqrt{4(k-\omega)k+t}\cos(\phi_{kq})\right)^2}{(q^2+2\xi_0^2 m^2)^2}$
$q_1 g \leftrightarrow q_1 g$ $\bar{q}_1 g \leftrightarrow \bar{q}_1 g$	$16 d_F C_F C_A \frac{\left(2k-\omega-\sqrt{4(k-\omega)k+t}\cos(\phi_{kq})\right)^2}{(q^2+2\xi_0^2 m^2)^2}$
$gg \leftrightarrow gg$	$16 d_A C_A^2 \frac{\left(2k-\omega-\sqrt{4(k-\omega)k+t}\cos(\phi_{kq})\right)^2}{(q^2+2\xi_0^2 m^2)^2}$

Table 3.2.: Matrix elements for $\hat{q}$ in the limit $p \to \infty$.

$$k' = k - \omega, \tag{3.188i}$$

$$t = \omega^2 - q^2, \tag{3.188j}$$

$$s = -\frac{t}{q^2} p \left[2k\omega - \sqrt{4(k-\omega)k + t}\cos(\phi_{kq}) + \mathcal{O}\left(\frac{1}{p}\right)\right], \tag{3.188k}$$

$$u = -s + \mathcal{O}(1), \tag{3.188l}$$

and the only nonvanishing matrix elements with $\lim_{p\to\infty} \frac{|M|^2}{p^2}$ are given in Table 3.2. The upper sign, again, is for bosonic (gluons) d particles, the lower sign for fermionic particles (quarks). Previously, we have only shown the limiting behavior of $-\frac{su}{t^2}$ for $p \to \infty$, but the behavior of $\frac{s^2+u^2}{t^2}$ must be similar, since from $s + t + u = 0$ we can deduce

$$t^2 = (s+u)^2 = s^2 + 2us + u^2 \tag{3.189}$$

$$\frac{s^2+u^2}{t^2} = 1 - \frac{2us}{t^2}. \tag{3.190}$$

Note that we have some freedom of choice regarding the regularization in the denominator. All choices that reproduce the same behavior for $q, \omega \gg m_D$ are equally acceptable. We then need to fit the constant ξ_0 such that it reproduces the exact matrix element or known analytical results to leading order.

3.11. Soft limit

We now take the soft limit of the $\hat{q}$ formula in thermal equilibrium, i.e. the limit in which $\Lambda_\perp \ll T$, or $\Lambda_\perp \ll \kappa$, where κ denotes the largest momentum in our plasma. This restricts the maximum transverse momentum $q_\perp$ that can be transferred to the jet particle, but not its longitudinal momentum transfer. But we will make the additional assumption that also $\omega \ll \kappa$, which also restricts q.

Our assumptions are

$$\Lambda_\perp \ll T, \qquad \omega \ll T \qquad f_{b,d}(k) = \frac{1}{e^{k/T} \pm 1}. \tag{3.191}$$

We will denote the Bose-Einstein distribution as $n_{BE}(k) = (e^{k/T} - 1)^{-1}$ and the Fermi-Dirac distribution as $n_{FD}(k) = (e^{k/T} + 1)^{-1}$

Let us consider a generic process with a matrix element

$$\lim_{p\to\infty} \frac{\left|\mathcal{M}^{ab}_{cd}\right|^2}{p^2 g^4} = A \frac{\left(2k - \omega - \sqrt{4(k-\omega)k + t}\cos(\phi_{kq})\right)^2}{(q^2 + 2\xi_0^2 m^2)^2}, \tag{3.192}$$

where A is some constant.

With our approximations the matrix element becomes

$$\lim_{p\to\infty} \frac{\left|\mathcal{M}^{ab}_{cd}\right|^2}{p^2 g^4} \approx \frac{4k^2 A}{(q^2 + 2\xi_0^2 m^2)^2} \left(1 - \cos\phi_{kq}\right)^2. \tag{3.193}$$

We then obtain for $\hat{q}$

$$\begin{aligned}\hat{q}(\Lambda_\perp) = \frac{1}{\nu_a}\frac{1}{2^9\pi^5}\sum_{bcd}\int_0^{2\pi} \mathrm{d}\tilde{\phi}_{pq}\int_0^{2\pi}\mathrm{d}\phi_{kq}\int_0^\infty \mathrm{d}q\int_{-q}^{q}\mathrm{d}\omega\int_{\frac{q+\omega}{2}}^\infty \mathrm{d}k\,\Theta(q^2-\omega^2-\Lambda_\perp^2)\\ q^2\sin^2\theta_{pq}\frac{|\mathcal{M}^{ab}_{cd}|^2}{p^2} f_b(k,v_k)\left(1 \pm f_d(k-\omega, v_{k'})\right), \qquad (3.194)\\ \approx \frac{4A}{\nu_a}\frac{1}{2^9\pi^5}\int_0^{2\pi} \mathrm{d}\tilde{\phi}_{pq}\int_0^{2\pi}\mathrm{d}\phi_{kq}\int_0^\infty \mathrm{d}q\int_{-q}^{q}\mathrm{d}\omega\int_{\frac{q+\omega}{2}}^\infty \mathrm{d}k\,\Theta(q^2-\omega^2-\Lambda_\perp^2)\\ \frac{q_\perp^2\left(1-\cos\phi_{kq}\right)^2}{(q^2+2\xi_0^2m^2)^2}k^2 f_b(k,v_k)\left(1 \pm f_d(k-\omega, v_{k'})\right). \qquad (3.195)\end{aligned}$$

Currently, we integrate over the modulus of $\mathbf{q} = (\mathbf{q}_\perp, q_z)$. From the definition of q_z, (3.75), we see that for $p \to \infty$ we have

$$q_z = \omega. \tag{3.196}$$

Thus we can write

$$q^2 = q_\perp^2 + \omega^2, \tag{3.197}$$

with $q_\perp^2 = |\mathbf{q}_\perp|^2 = q_x^2 + q_y^2$. Note that the labels x, y, z are with respect to the direction of $\mathbf{p}$, i.e. in a frame in which $\mathbf{p}$ points in the z-direction. We now perform a change of integration variables from $(q, \tilde{\phi}_{pq}, \omega) \to (q_x, q_y, \omega)$. The transformation is given by (see (3.188a), (3.188b) and (3.188c)),

$$q_x = q\sqrt{1 - \frac{\omega^2}{q^2}}\cos\tilde{\phi}_{pq}, \tag{3.198}$$

$$q_y = q\sqrt{1 - \frac{\omega^2}{q^2}}\sin\tilde{\phi}_{pq}, \tag{3.199}$$

$$\omega = \omega. \tag{3.200}$$

We obtain a Jacobian factor of q,

$$\mathrm{d}q\,\mathrm{d}\tilde{\phi}_{pq}\,\mathrm{d}\omega = \frac{1}{q}\,\mathrm{d}q_x\,\mathrm{d}q_y\,\mathrm{d}\omega = \frac{1}{\sqrt{q_\perp^2 + \omega^2}}\,\mathrm{d}^2\mathbf{q}_\perp\,\mathrm{d}\omega. \tag{3.201}$$

The transformation yields

$$\hat{q}(\Lambda_\perp) = \frac{4A}{\nu_a}\frac{1}{2^9\pi^5}\int_0^{2\pi}\mathrm{d}\phi_{kq}\int_0^{\Lambda_\perp}\mathrm{d}^2\mathbf{q}_\perp\int_{-\infty}^{\infty}\mathrm{d}\omega\int_{\frac{q+\omega}{2}}^{\infty}\mathrm{d}k \\ \frac{q_\perp^2\left(1-\cos\phi_{kq}\right)^2}{\sqrt{q_\perp^2+\omega^2}\left(q_\perp^2+\omega^2+2\xi_0^2m^2\right)^2}k^2f_b(k)\left(1\pm f_d(k)\right), \tag{3.202}$$

where we have used that $f(k-\omega)\approx f(k)$. We have also implemented the integration intervals for ω, $-q=-\sqrt{q_\perp^2+\omega^2}<\omega<\sqrt{q_\perp^2+\omega^2}$, which yields no restriction to the ω-integral. Actually, our assumption was that ω is small, but we will check later that performing the integral from $-\infty$ to ∞ does not significantly change the result.

We have now several possibilities to proceed. As discussed in section 2.2.3, we have a certain freedom of how to implement the screening. We will check this fact here, again. For now, let us make a different choice for the regularization,

$$\frac{q_\perp^2}{\sqrt{q_\perp^2+\omega^2}\left(q_\perp^2+\omega^2+2\xi_0^2m^2\right)^2}\to\frac{q_\perp^4}{\left(q_\perp^2+\omega^2\right)^{5/2}\left(q_\perp^2+m_D^2\right)}. \tag{3.203}$$

This choice will be justified a posteriori, when we compare to known analytical results. There it will turn out that this mass m_D is indeed the Debye mass, and we can then via this change fit the value of ξ_0.

We can now shift the lower boundary of the k-integral to 0, a fact that we will later check, then the integral can be factorized,

$$\begin{aligned}\hat{q}(\Lambda_\perp) = \frac{4A}{\nu_a}\frac{1}{2^9\pi^5}&\int_0^{2\pi}\mathrm{d}\phi_{kq}\left(1-\cos\phi_{kq}\right)^2 \\ &\times\int_0^{\infty}\mathrm{d}k\,k^2f_b(k)\left(1\pm f_d(k)\right) \\ &\times\int_0^{\Lambda_\perp}\mathrm{d}^2\mathbf{q}_\perp\frac{q_\perp^4}{\left(q_\perp^2+m_D^2\right)}\int_{-\infty}^{\infty}\mathrm{d}\omega\frac{1}{\left(q_\perp^2+\omega^2\right)^{5/2}}\end{aligned} \tag{3.204}$$

The first integral can be easily evaluated, $\int_0^{2\pi}\mathrm{d}\phi_{kq}\left(1-\cos\phi_{kq}\right)^2=3\pi$. The second integral can also be analytically evaluated. For the case of gluons, we use for f the Bose-Einstein distribution function $n_{BE}(k)$, whereas for quarks, we use the Fermi-Dirac distribution, $n_{FD}(k)$:

$$\int_0^{\infty}\mathrm{d}k\,k^2n_{BE}(k)\left(1+n_{BE}(k)\right)=\int_0^{\infty}\mathrm{d}k\,\frac{k^2}{e^{\beta k}-1}\left(1+\frac{1}{e^{\beta k}-1}\right)=\frac{\pi^2T^3}{3} \tag{3.205}$$

$$\int_0^{\infty}\mathrm{d}k\,k^2n_{FD}(k)\left(1-n_{FD}(k)\right)=\int_0^{\infty}\mathrm{d}k\,\frac{k^2}{e^{\beta k}+1}\left(1-\frac{1}{e^{\beta k}+1}\right)=\frac{\pi^2T^3}{6} \tag{3.206}$$

Now let us look at the contribution from the lower boundary, i.e. let us split the integral,

$$\int_{\frac{q+\omega}{2}}^{\infty}f(k)\left(1\pm f(k)\right)=\int_0^{\infty}f(k)\left(1\pm f(k)\right)-\int_0^{\frac{q+\omega}{2}}f(k)\left(1\pm f(k)\right). \tag{3.207}$$

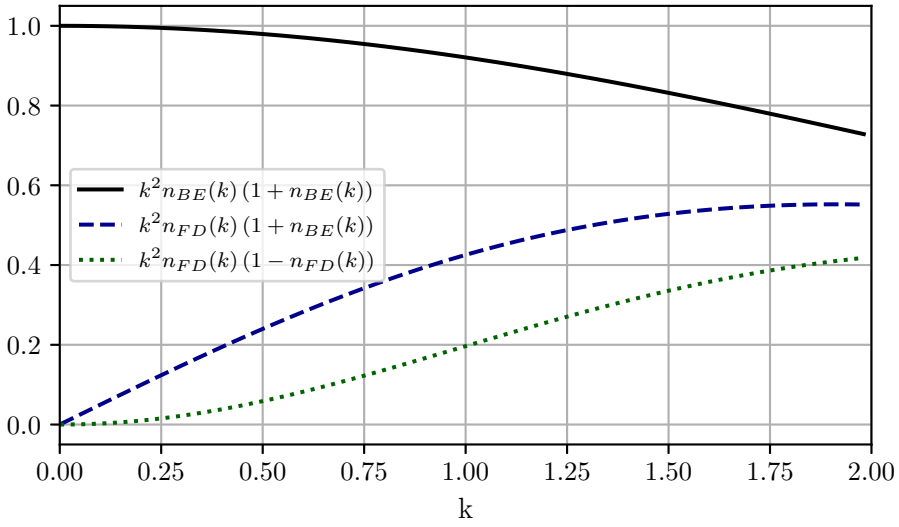

Figure 3.2.: Plot of the integrand $k^2 f(k)\,(1 \pm f(k))$ for $\beta = 1$. The cases $n_{FD}(k)(1+n_{BE}(k))$ and $n_{BE}(k)(1-n_{FD}(k))$ are identical. $n_{FD}(k)$ and $n_{BE}(k)$ denote the Fermi-Dirac and Bose-Einstein distribution, respectively.

In Figure 3.2 we plot the integrand for different distribution functions. We see that if at least b or d is fermionic, the low k-behavior does not contribute much. If the plasma particles are gluonic, we can approximate the integral

$$\int_0^a \mathrm{d}k\, f(k) \leq a f(k^*), \tag{3.208}$$

where k^* is the k value for which $f(k)$ reaches its maximum. For us this is the case at $k = 0$,

$$\lim_{k\to 0} \frac{k^2}{e^{\beta k}-1}\left(1-\frac{1}{e^{\beta k}-1}\right) = \lim_{k\to 0} \frac{k^2}{\beta k + \mathcal{O}(k^2)}\left(1-\frac{1}{\beta k + \mathcal{O}(k^2)}\right) = T^2. \tag{3.209}$$

The largest error we make by shifting the lower integration boundary to 0 is thus

$$\frac{T^2(q+\omega)}{2}, \tag{3.210}$$

which is always $\ll \frac{\pi^2 T^3}{3}$.

Now we turn to the ω-integral, which can be performed analytically and yields

$$\int_{-\infty}^{\infty} \mathrm{d}\omega\, \frac{1}{\left(q_\perp^2+\omega^2\right)^{5/2}} = \frac{4}{3q_\perp^4}. \tag{3.211}$$

As discussed before, our assumption $\omega \ll T$ actually forbids us to push the integration boundaries to $\pm\infty$, but we can analyse the integrand for different boundaries and we find no change of the integral value if the boundary is sufficiently large, see Figure 3.3. We thus obtain

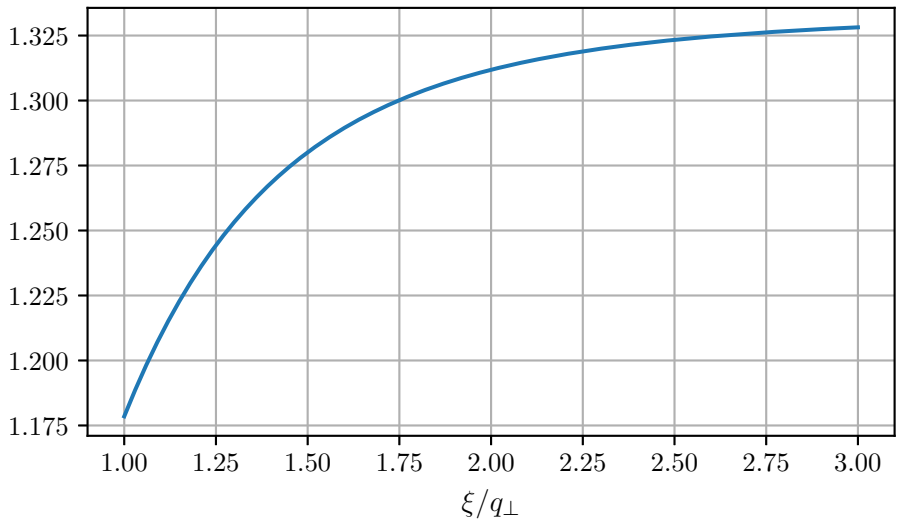

Figure 3.3.: Plot of the integral $\int_{-\xi}^{\xi} \mathrm{d}\omega \, \frac{1}{(q_\perp^2+\omega^2)^{5/2}}$ for different boundary values $\pm\xi$. For $\omega > q_\perp$, the integral roughly stays the same, which permits us to push the boundaries to $\pm\infty$.

$$\hat{q}(\Lambda_\perp) = \frac{A}{s\nu_a} \frac{T^3}{3 \cdot 2^5 \pi^2} \int_0^{\Lambda_\perp} \mathrm{d}^2\mathbf{q}_\perp \, \frac{1}{q_\perp^2 + m_D^2}, \tag{3.212}$$

with $s = 1$ for scattering off gluonic particles and $s = 2$ for fermionic particles. The integral can be performed,

$$\int_0^{\Lambda_\perp} \mathrm{d}^2\mathbf{q}_\perp \frac{1}{q_\perp^2 + m_D^2} = 2\pi \int_0^{\Lambda_\perp} \mathrm{d}q_\perp \, \frac{q_\perp}{q_\perp^2 + m_D^2} \tag{3.213}$$

$$= \pi \int_{m_D^2}^{\Lambda_\perp^2 + m_D^2} \mathrm{d}x \, \frac{1}{x} \tag{3.214}$$

$$= \pi \ln\left(\frac{\Lambda_\perp^2 + m_D^2}{m_D^2}\right) \approx 2\pi \ln\left(\frac{\Lambda_\perp}{m_D}\right). \tag{3.215}$$

We then arrive at

$$\hat{q} \approx \frac{AT^3}{3 \cdot 2^4 \pi s \nu_a} \ln\left(\frac{\Lambda_\perp}{m_D}\right). \tag{3.216}$$

Let us now start with a quark jet, thus $\nu_a = 2N_C$. We take the matrix elements from Table 3.2. We can thus either scatter with a quark or with a gluon. We have $2n_f$ quarks to scatter from (n_f quarks and n_f antiquarks), so this yields a factor $2n_f$,

$$\hat{q} = \left(\underbrace{\frac{16 d_F^2 C_F^2 g^4}{d_A}}_{A} \cdot 2n_F \cdot \frac{1}{3 \cdot 2^6 \pi N_C} + \underbrace{16 d_F C_F C_A g^4}_{A} \cdot \frac{1}{3 \cdot 2^5 \pi N_C} \right) T^3 \ln\left(\frac{\Lambda_\perp}{m_D}\right). \tag{3.217}$$

The Debye mass in thermal equilibrium is given by (2.60),

$$m_D^2 = g^2 T^2 \left(\frac{N_C}{3} + \frac{N_f}{6} \right). \tag{3.218}$$

We then use $d_F = C_A = N_C$, $C_F = \frac{d_A}{2N_C}$ and $d_A = N_C^2 - 1$ to arrive at

$$\hat{q} = \frac{T^3 g^4}{3 \cdot 2\pi N_C} \left(\frac{N_C^2 C_F n_F}{2N_C} + N_C^2 C_F \right) \ln\left(\frac{\Lambda_\perp}{m_D} \right) \tag{3.219}$$

$$= \frac{g^2 C_F T}{2\pi} \underbrace{g^2 T^2 \left(\frac{n_F}{6} + \frac{N_C}{3} \right)}_{m_D^2} \ln\left(\frac{\Lambda_\perp}{m_D} \right). \tag{3.220}$$

For a gluonic jet we have $\nu_a = 2d_A$,

$$\hat{q} = \left(\underbrace{16 d_F C_F C_A g^4}_{A} \cdot 2 n_F \cdot \frac{1}{3 \cdot 2^6 \pi d_A} + \underbrace{16 d_A C_A^2 g^4}_{A} \cdot \frac{1}{3 \cdot 2^5 \pi d_A} \right) T^3 \ln\left(\frac{\Lambda_\perp}{m_D} \right), \tag{3.221}$$

$$= T^3 g^4 \left(\frac{C_A d_A n_F}{3 \cdot 2^2 \pi d_A} + \frac{C_A N_C}{3 \cdot 2\pi} \right) \ln\left(\frac{\Lambda_\perp}{m_D} \right) \tag{3.222}$$

$$= \frac{g^2 C_A T}{2\pi} \underbrace{g^2 T^2 \left(\frac{n_F}{6} + \frac{N_C}{3} \right)}_{m_D^2} \ln\left(\frac{\Lambda_\perp}{m_D} \right). \tag{3.223}$$

This is the same as the known result [15, 8].

Instead of (3.203) we could have also chosen to calculate $\hat{q}$ in our original regularization. We can do this for arbitrary ξ_0 and we find that the choice $\xi_0 = 0.698$ correctly reproduces this soft limit result. This is in contrast to the original screening factor $\xi = 0.8135$. In fact, this soft limit result is only valid for $m_D \ll \Lambda_\perp \ll T$. We can only see this behavior in our simulation if the 't Hooft coupling λ is very small. Only then we can have a region with $m_D \ll \Lambda_\perp \ll T$. If we perform our simulations with ξ, we find that we obtain a similar behavior as in (3.223), but with a constant shift of about 8 %. If we use ξ_0 instead, we obtain the correct behavior, which we take as evidence that our prediction here for ξ_0 is valid.

The difference in $\xi \neq \xi_0$ is a result of the different matching procedure. In [12], effectively a matching of $\hat{q}_L$ is performed, which we can do as well when we replace $q_\perp^2 \to \omega^2$ in (3.195), then we obtain the same result. However, since we are interested in the transverse momentum transfer, it makes more sense to perform the matching in a way such that the transverse momentum is reproduced in the soft limit.

4. Implementation

We do not implement the effective kinetic theory description from scratch, but use the C++ code for the time evolution of the gluonic plasma corresponding to (2.82), described in [13].

The particle distribution function for gluons $f(\mathbf{p}) = f(p, v_p)$ is discretized on a 2D grid and the integrals in the collision term are evaluated using the Monte Carlo method, see Section 2.3. In our simulation we want our results to be insensitive to the number of grid points, which we check by varying this number.

To this existing code we append a routine that calculates $\hat{q}$ at different times, i.e. a routine that performs the integral (3.187a) numerically. We describe our implementation in this chapter.

4.1. Finite integral boundaries

4.1.1. Introducing k_{min} and k_{max}

In our code we store the distribution function only on a finite interval, i.e. only in the interval $k_{min} < k < k_{max}$. There are two possibilities to account for that

1. Sample according to (3.187a), (3.187b), (3.187c), and evaluate the expression to 0 if k or k' is out of range.

2. Already include the finite boundaries k_{min} and k_{max} in the integral boundaries, such that k, k' is already in the desired form.

In the first case we will have samples in our sampling region that yield zero and do not contribute to the integral.

In the second case, though a bit more tedious to work out, every sample will yield a contribution. Thus we stick to the second case.

For the Monte Carlo importance sampling, see Section 2.3, we need the probability density or volume factor, which is dependent on the exact boundaries of the integral. We thus cannot simply generate a random number and accept or reject it if it is in our integration region, because the weight depends on the integration boundaries.

We will consider the integrals[1] in the $p \to \infty$ limit,

$$I_1 = \int_0^\infty \mathrm{d}k \int_{-\infty}^{k} \mathrm{d}\omega \int_{|\omega|}^{2k-\omega} \mathrm{d}q \,, \tag{4.1}$$

$$I_{1b} = \int_0^\infty \mathrm{d}k \int_0^\infty \mathrm{d}k' \int_{|k-k'|}^{k+k'} \mathrm{d}q \,, \tag{4.2}$$

$$I_2 = \int_0^\infty \mathrm{d}q \int_{-q}^{q} \mathrm{d}\omega \int_{\frac{q+\omega}{2}}^\infty \mathrm{d}k \,. \tag{4.3}$$

[1] For the remaining integrals over the angles we do not need any additional boundaries k_{min}, k_{max}.

Now let us insert boundaries for numerical integration,

$$k_{min} < k < k_{max}, \qquad k_{min} < k' < k_{max}, \qquad k' = k - \omega. \tag{4.4}$$

For (4.2) this is most easily implemented as

$$\boxed{\int_{k_{min}}^{k_{max}} \mathrm{d}k \int_{k_{min}}^{k_{max}} \mathrm{d}k' \int_{|k-k'|}^{k+k'} \mathrm{d}q}. \tag{4.5}$$

For (4.1) we can implement this easily by $k_{min} < k - \omega < k_{max} \iff -k_{min} + k > \omega > -k_{max} + k$

$$\boxed{\int_{k_{min}}^{k_{max}} \mathrm{d}k \int_{k-k_{max}}^{k-k_{min}} \mathrm{d}\omega \int_{|\omega|}^{2k-\omega} \mathrm{d}q}. \tag{4.6}$$

For (4.3) we use $k_{min} < k < k_{max}$ to obtain

$$\int_0^\infty \mathrm{d}q \int_{-q}^{q} \mathrm{d}\omega \int_{\max\left(\frac{q+\omega}{2}, k_{min}\right)}^{k_{max}} \mathrm{d}k\,. \tag{4.7}$$

We then enforce $k_{min} < k - \omega < k_{max} \iff k_{min} + \omega < k < k_{max} + \omega$,

$$\int_0^\infty \mathrm{d}q \int_{-q}^{q} \mathrm{d}\omega \int_{\max\left(\frac{q+\omega}{2}, k_{min}, k_{min}+\omega\right)}^{\min(k_{max}, k_{max}+\omega)} \mathrm{d}k\,. \tag{4.8}$$

The k' condition also gives us a restriction for the ω integral, $k - k_{max} < \omega < k - k_{min} \to k_{min} - k_{max} < \omega < k_{max} - k_{min}$:

$$\int_0^\infty \mathrm{d}q \int_{\max(-q, k_{min}-k_{max})}^{\min(q, k_{max}-k_{min})} \mathrm{d}\omega \int_{\max\left(\frac{q+\omega}{2}, k_{min}, k_{min}+\omega\right)}^{\min(k_{max}, k_{max}+\omega)} \mathrm{d}k \tag{4.9}$$

Now we also need to enforce $\max\left(\frac{q+\omega}{2}, k_{min}, k_{min}+\omega\right) < \min(k_{max}, k_{max}+\omega)$,

$$\begin{cases} \omega > 0 \wedge \frac{q+\omega}{2} > \omega + k_{min}: & \omega < 2k_{max} - q \\ \omega > 0 \wedge \frac{q+\omega}{2} < \omega + k_{min}: & \omega < k_{max} - k_{min} \text{ already fulfilled} \\ \omega < 0 \wedge \frac{q+\omega}{2} > k_{min}: & \omega > q - 2k_{max} \\ \omega < 0 \wedge \frac{q+\omega}{2} < k_{min}: & \omega > k_{min} - k_{max} \text{ already fulfilled} \end{cases} \tag{4.10}$$

We thus need for $q > 2k_{min} + |\omega|$ that $q < 2k_{max} - |\omega|$, which gives an upper boundary on q, $q < 2k_{max}$. Additionally, for big enough q, such that this condition is fulfilled, we need additionally $\omega < 2k_{max} - q$ and $\omega > q - 2k_{max}$.

$$\boxed{\int_0^{2k_{max}} \mathrm{d}q \int_{\max(-q, k_{min}-k_{max}, q-2k_{max})}^{\min(q, k_{max}-k_{min}, 2k_{max}-q)} \mathrm{d}\omega \int_{\max\left(\frac{q+\omega}{2}, k_{min}, k_{min}+\omega\right)}^{\min(k_{max}, k_{max}+\omega)} \mathrm{d}k} \tag{4.11}$$

But could we also have cases in which this condition is not fulfilled, q is not big enough? I.e. where we impose the latter condition $|\omega| < 2k_{max} - q$ although we would not need it because $q < 2k_{min} + |\omega|$? Let us think of the case when we have the $2k_{max} - q$ boundary. This is the case if $q > k_{max} + k_{min}$. We would impose this condition wrongly if we could find an ω with $|\omega| > q - 2k_{min}$, but $|\omega| > q - 2k_{min} > k_{max} - k_{min}$, which we do not allow. Thus we can always impose the latter boundary.

4.1.2. $q_\perp$ cutoff for k_{min} and k_{max}

We take now (4.6) and implement the $q_\perp$ cutoff, $q^2 - \omega^2 < \Lambda_\perp^2$,

$$\boxed{\int_{k_{min}}^{k_{max}} \mathrm{d}k \int_{k_{min}}^{k_{max}} \mathrm{d}k' \int_{|k-k'|}^{\min(k+k', \sqrt{(k-k')^2+\Lambda_\perp^2})} \mathrm{d}q}\,. \tag{4.12}$$

Now we adapt (4.11),

$$\int_0^{2k_{max}} \mathrm{d}q \underbrace{\int_{\max(-q, k_{min}-k_{max}, q-2k_{max})}^{\min(q, k_{max}-k_{min}, 2k_{max}-q)} \mathrm{d}\omega}_{\text{if } q>\Lambda_\perp\colon \int_{\max(-q, k_{min}-k_{max}, q-2k_{max})}^{-\sqrt{q^2-\Lambda_\perp^2}} \mathrm{d}\omega + \int_{\sqrt{q^2-\Lambda_\perp^2}}^{\min(q, k_{max}-k_{min}, 2k_{max}-q)} \mathrm{d}\omega} \int_{\max\left(\frac{q+\omega}{2}, k_{min}, k_{min}+\omega\right)}^{\min(k_{max}, k_{max}+\omega)} \mathrm{d}k\,, \tag{4.13}$$

but we must ensure that for $q > \Lambda_\perp$ the upper boundaries of the ω integral are always larger than the lower boundaries. Thus we obtain, for $k_{max} - k_{min} < q < k_{max} + k_{min}$:

$$k_{max} - k_{min} > \sqrt{q^2 - \Lambda_\perp^2}, \tag{4.14}$$

$$(k_{max} - k_{min})^2 > q^2 - \Lambda_\perp^2 \tag{4.15}$$

$$q < \sqrt{(k_{max} - k_{min})^2 + \Lambda_\perp^2}. \tag{4.16}$$

This condition is also fulfilled in (4.12), which is a nice cross-check.

We also need $2k_{max} - q > \sqrt{q^2 - \Lambda_\perp^2}$, which gives an additional upper boundary for the q integral, $q < k_{max} + \frac{\Lambda_\perp^2}{4k_{max}}$.

We thus obtain, for arbitrary $\Lambda_\perp$,

$$\boxed{\begin{aligned}&\int_0^{\min\left(2k_{max}, k_{max}+\frac{\Lambda_\perp^2}{4k_{max}}, \sqrt{(k_{max}-k_{min})^2+\Lambda_\perp^2}\right)} \mathrm{d}q \\ &\qquad \underbrace{\int_{\max(-q, k_{min}-k_{max}, q-2k_{max})}^{\min(q, k_{max}-k_{min}, 2k_{max}-q)} \mathrm{d}\omega}_{\text{if } q>\Lambda_\perp\colon \int_{\max(-q, k_{min}-k_{max}, q-2k_{max})}^{-\sqrt{q^2-\Lambda_\perp^2}} \mathrm{d}\omega + \int_{\sqrt{q^2-\Lambda_\perp^2}}^{\min(q, k_{max}-k_{min}, 2k_{max}-q)} \mathrm{d}\omega} \\ &\qquad \int_{\max\left(\frac{q+\omega}{2}, k_{min}, k_{min}+\omega\right)}^{\min(k_{max}, k_{max}+\omega)} \mathrm{d}k\,.\end{aligned}} \tag{4.17}$$

One might ask if the upper boundaries on the q-integral are the most general, because we got them out of the conditions:

- For $k_{max} - k_{min} < q < k_{max} + k_{min}$ we need that $q < \sqrt{(k_{max} - k_{min})^2 + \Lambda_\perp^2}$
- For $q > k_{max} + k_{min}$ we need that $q < k_{max} + \frac{\Lambda_\perp^2}{4k_{max}}$.

It might be that by enforcing q to be smaller than both, we are too restrictive. We will find that this is not the case and the boundaries are fine.

To show this, we need to show that, if $q < k_{max} + k_{min}$ the minimum is always given by the square root, i.e. $\sqrt{(k_{max} - k_{min})^2 + \Lambda_\perp^2} < k_{max} + \frac{\Lambda_\perp^2}{4k_{max}}$. On the other hand, if $q > k_{max} + k_{min}$, then we need $\sqrt{(k_{max} - k_{min})^2 + \Lambda_\perp^2} > k_{max} + \frac{\Lambda_\perp^2}{4k_{max}}$.
This can indeed be shown:

- First assume that the upper q-boundary is given by the square root and that it is smaller than $k_{min} + k_{max}$,

$$\sqrt{(k_{max} - k_{min})^2 + \Lambda_\perp^2} < k_{min} + k_{max} \tag{4.18}$$
$$-2k_{max}k_{min} + \Lambda_\perp^2 < 2k_{max}k_{min} \tag{4.19}$$
$$\Lambda_\perp^2 < 4k_{max}k_{min}. \tag{4.20}$$

  We then need to show that the minimum comes always from the square root, which can easily be shown via

$$\sqrt{(k_{max} - k_{min})^2 + \Lambda_\perp^2} < k_{max} + \frac{\Lambda_\perp^2}{4k_{max}} \tag{4.21}$$
$$-2k_{min}k_{max} + k_{min}^2 + \Lambda_\perp^2 < \frac{1}{2}\Lambda_\perp^2 + \frac{\Lambda_\perp^4}{16k_{max}^2} \tag{4.22}$$
$$< \frac{1}{2}\Lambda_\perp^2 + \frac{16k_{max}^2 k_{min}^2}{16k_{max}^2} \tag{4.23}$$
$$\Lambda_\perp^2 < 4k_{max}k_{min}. \tag{4.24}$$

- Next, if the upper q-boundary is not given by the square root, i.e. if $k_{max}+k_{min} < q < k_{max} + \frac{\Lambda_\perp^2}{4k_{max}}$,

$$k_{max} + \frac{\Lambda_\perp^2}{4k_{max}} > k_{min} + k_{max} \tag{4.25}$$
$$\Lambda_\perp^2 > 4k_{min}k_{max}. \tag{4.26}$$

  Then the square root must not be smaller than the other term, which it indeed is, as we can see via

$$\sqrt{(k_{max} - k_{min})^2 + \Lambda_\perp^2} > k_{max} + \frac{\Lambda_\perp^2}{4k_{max}} \tag{4.27}$$
$$-2k_{min}k_{max} + k_{min}^2 + \Lambda_\perp^2 > \frac{1}{2}\Lambda_\perp^2 + \frac{\Lambda_\perp^4}{16k_{max}^2} \tag{4.28}$$
$$> \frac{1}{2}\Lambda_\perp^2 + \frac{16k_{max}^2 k_{min}^2}{16k_{max}^2} \tag{4.29}$$
$$\Lambda_\perp^2 > 4k_{max}k_{min}. \tag{4.30}$$

Thus the conditions and the minimum in the integral boundary match perfectly!

4.2. Phase-space sampling

The implementation of $\hat{q}$ in the code is done in the $p \to \infty$ limit using (3.187b) and its discretized version for k, k', q, (4.12); and (3.187c) and for k, ω, q (4.17). The integrals are evaluated using the *Monte Carlo* method with importance sampling, (2.130). As a cross-check, we also implemented a deterministic trapezoidal rule, (2.123), but this is rather slow.

For another cross-check, we implement both (4.12) and (4.17). The ω-sampling and, of course, the integral boundaries vary.

4.2.1. Sampling q

Because the matrix element is strongly peaked for small q, we need to use importance sampling, see (2.130), and we choose

$$g(q) = \frac{1}{(q+\tilde{m})^2}, \tag{4.31}$$

where $\tilde{m} = \xi_0 m_D$ is the rescaled mass, see Section 2.2.3. So we write the integral

$$\int_a^b \mathrm{d}q\, f(q) = \int_a^b \mathrm{d}q\, \frac{1}{(q+\tilde{m})^2} h(q), \tag{4.32}$$

with $h(q) = f(q)\,(q+\tilde{m})^2$.

From

$$\mathrm{d}y = \frac{\mathrm{d}q}{(q+\tilde{m})^2} \tag{4.33}$$

we obtain, see (2.129),

$$y(q) = y_0 - \frac{1}{q+\tilde{m}}. \tag{4.34}$$

With the choice $y_0 = \frac{1}{a+\tilde{m}}$ we can invert this expression,

$$q = \frac{1}{\frac{1}{a+\tilde{m}} - y} - \tilde{m}. \tag{4.35}$$

Thus,

$$\int_a^b \mathrm{d}q\, f(q) = \int_0^{\frac{1}{a+\tilde{m}} - \frac{1}{b+\tilde{m}}} \mathrm{d}y\, h(q(y)) \tag{4.36}$$

$$\approx \left[\frac{1}{a+\tilde{m}} - \frac{1}{b+\tilde{m}}\right] \frac{1}{N} \sum_{i=1}^{N} h(q(y_i)) \tag{4.37}$$

$$= \frac{b-a}{(a+\tilde{m})(b+\tilde{m})} \frac{1}{N} \sum_{i=1}^{N} f(q(y_i))\,(q(y_i)+\tilde{m})^2, \tag{4.38}$$

with $y_i \in \left(0, \frac{b-a}{(a+\tilde{m})(b+\tilde{m})}\right)$ sampled uniformly and $q(y) = \frac{1}{\frac{1}{a+\tilde{m}} - y} - \tilde{m}$.

4.2.2. Sampling k, k'

The particle distribution is peaked for small k, thus we sample from a probability distribution $\sim \frac{1}{k}$. We sample k this way in both (4.12) and (4.17) and k' in (4.12).

We use again (2.130) with

$$g(k) = \frac{1}{k}. \tag{4.39}$$

We write

$$\int_a^b \mathrm{d}k\, f(k) = \int_a^b \mathrm{d}k\, \frac{1}{k} h(k), \tag{4.40}$$

with $h(k) = kf(k)$.

From

$$\mathrm{d}r = \frac{\mathrm{d}k}{k} \tag{4.41}$$

we obtain, see (2.129),

$$r(k) = r_0 + \ln k \quad \overset{r_0 = -\ln a}{\Leftrightarrow} \quad k = ae^r. \tag{4.42}$$

Thus,

$$\int_a^b \mathrm{d}k\, f(k) \approx \ln \frac{b}{a} \frac{1}{N} \sum_{i=1}^{N} f(k(r_i))k(r_i), \tag{4.43}$$

with $r_i \in \left(0, \ln \frac{b}{a}\right)$ sampled uniformly and $k(r) = ae^r$.

4.2.3. Sampling ω, ϕ_{kq}, $\tilde{\phi}_{pq}$

For ω in (4.17), ϕ_{kq} and $\tilde{\phi}_{pq}$ we do not use importance sampling, $g(x) = 1$,

$$\int_a^b \mathrm{d}x\, f(x) \approx (b-a) \frac{1}{N} \sum_{i=1}^{N} f(x_i), \tag{4.44}$$

with $x_i \in (a, b)$ sampled uniformly.

4.3. Statistics and Plotting

Because the Monte Carlo method for evaluating the integrals is stochastic, it will be important to quantify the error or amount of fluctuations.

To do this, we perform the integration several times and then use the sample mean and standard error [39]:

We generate n values for the integral, I_i, then take the sample average $\bar{I}$ and sample variance s^2,

$$\bar{I} = \frac{\sum_{i=1}^{n} I_i}{n} \tag{4.45}$$

$$s^2 = \frac{\sum_{i=1}^{n} \left(I_i - \bar{I}\right)^2}{n-1}. \tag{4.46}$$

The standard error $\bar{\sigma}$ is then calculated as

$$\bar{\sigma} = \sqrt{\frac{s^2}{n}}. \tag{4.47}$$

The data analysis is done using the Python NumPy library [40] and the plots are generated with the Matplotlib package [41].

5. Results

In this section we give the numerical results of our implementation.

We assume a fully gluonic plasma, and also use a gluonic jet with $p \to \infty$. The value of $\hat{q}$ for a gluonic jet can easily be transferred to a quark jet by Casimir scaling. This can easily be seen from Table 3.2: The matrix elements for the two processes, $gg \leftrightarrow gg$ and $q_1 g \leftrightarrow q_1 g$ differ only by a multiplicative constant. The factor d_R cancels with $\nu_a = 2d_R$ in (3.187a), then they only differ in C_A, C_F, which provides exactly Casimir scaling: $\hat{q}_{\text{quark}} = \frac{C_F}{C_A}\hat{q}_{\text{gluonic}}$.

All simulations were done using a temperature $T = 1\,\text{GeV}$, but actually T gives the only energy scale in the plasma (apart from k_{min} and k_{max}, which should anyway be chosen in a way such that the result does not depend on them). Thus another way of thinking about this is that all results are scaled with respect to temperature, i.e. by changing $T = 1\,\text{GeV} \to 2\,\text{GeV}$ we change e.g. $\Lambda_\perp = 5\,\text{GeV} \to 10\,\text{GeV}$ and $\hat{q} = 0.5\,\text{GeV}^3 \to 4\,\text{GeV}^3$.

In the code I have implemented the anisotropic version of $\hat{q}$, $\hat{q}_{ij}$ from (3.187b) and (3.187c). We have checked that the two different integral parametrizations give the same results and that the off-diagonal elements $\hat{q}_{xy}$ vanish, as predicted from (3.103).

As a sanity check we compare the output of our code with something that has been analytically calculated: $\hat{q}$ in thermal equilibrium.

5.1. Thermal equilibrium

In thermal equlibrium, the particle distribution function of the gluonic plasma is given by the Bose-Einstein distribution

$$f(\mathbf{k}) = \frac{1}{e^{\beta|\mathbf{k}|} - 1}. \tag{5.1}$$

5.1.1. Analytical results

For $\hat{q}$ in thermal equilibrium, we compare our simulation with analytical results from [8]:

For $m_D \ll \Lambda_\perp \ll T$, Arnold and Xiao find

$$\hat{q}(\Lambda_\perp) \simeq \frac{g^2 T m_D^2 C_R}{2\pi} \ln\left(\frac{\Lambda_\perp}{m_D}\right) \tag{5.2}$$

and for $\Lambda_\perp \gg T$

$$\hat{q}(\Lambda_\perp) = C_R\left[\Xi_b \mathcal{I}_+(\Lambda_\perp) + \Xi_f \mathcal{I}_-(\Lambda_\perp)\right] \frac{g^4 T^3}{\pi^2} \tag{5.3}$$

with

$$\mathcal{I}_{\pm} \simeq \frac{\zeta_{\pm}(3)}{2\pi} \ln\left(\frac{\Lambda_{\perp}}{m_D}\right) + \Delta\mathcal{I}_{\pm}, \tag{5.4}$$

$$\Delta\mathcal{I}_{\pm} = \frac{\zeta_{\pm}(2) - \zeta_{\pm}(3)}{2\pi}\left[\ln\left(\frac{T}{m_D}\right) + \frac{1}{2} - \gamma_E + \ln 2\right] - \frac{\sigma_{+}}{2\pi}, \tag{5.5}$$

$$\sigma_{+} = 0.386043817389949\ldots, \qquad \sigma_{-} = 0.011216764589789, \tag{5.6}$$

where $\zeta_{+}(x) = \zeta(s)$ is the Riemann ζ function and

$$\zeta_{-}(s) = (1 - 2^{1-s})\zeta(s), \tag{5.7}$$

$$\Xi_b = 2t_A, \tag{5.8}$$

$$\Xi_f = 4N_f t_F, \tag{5.9}$$

and in the case of N_f-flavor QCD, $\Xi_b = 6$, $\Xi_f = 2N_f$. This result ignores running of the coupling constant, which can be accounted for using the replacements described in [8], but we also do not consider a running coupling constant in our EKT code. γ_E is the Euler-Mascheroni constant with numerical value [38, 42]

$$\gamma_E = 0.5772156649\ldots \tag{5.10}$$

and $\zeta(2)$ and $\zeta(3)$ are given by [42]

$$\zeta(2) = \frac{\pi^2}{6}, \qquad \zeta(3) = 1.2020569031\ldots. \tag{5.11}$$

It should be noted that Arnold and Xiao [8] make the assumption[1] that one can choose a momentum scale $\tilde{\Lambda}$ with $m_D \ll \tilde{\Lambda} \ll T$. This is only valid for small coupling λ.

5.1.2. Comparison

In thermal equilibrium, the collision term identically vanishes (without longitudinal expansion), thus we do not need to solve the kinetic equations for the distribution function numerically. The distribution function is initialized once and stays the same. Effectively, we only need to evaluate the integral (3.187a), (3.187b) or (3.187c). We use a finite k_{min} and k_{max} and a *Monte Carlo* method for evaluating the integral as described in Chapter 4. The results of the numerical integration procedure are then compared with the analytical results quoted in the previous section.

In Figure 5.1 we plot the results of our Monte Carlo integration for $\lambda = 0.01$, $T = 1\,\mathrm{GeV}$ for different $q_{\perp}$ cutoffs $\Lambda_{\perp}$.

Our integration results are compatible with (5.2) and (5.3), see Figure 5.1(a). In (b), (c) and (d) we plot the obtained value for $\hat{q}$ for different k_{min}, k_{max}. In (b) we observe that the results are all compatible with one another, whereas in (c) and (d) we look explicitly at the low and high $\Lambda_{\perp}$ behavior. As we might naïvely expect, changing k_{min}

[1] See (3.24) in [8]. We write $\tilde{\Lambda}$ instead of λ in [8], because in our case λ is reserved for the coupling $\lambda = g^2 N_C$, (2.17). The scale is introduced in the evaluation of the integral $\mathcal{I}_{\pm}(\Lambda_{\perp}) = \int_{q_{\perp}<\Lambda_{\perp}} \frac{\mathrm{d}^2\mathbf{q}_{\perp}}{(2\pi)^2} \frac{I_{\pm}(q_{\perp}/T)}{q_{\perp}^2+m_D^2} \approx \int_{q_{\perp}<\tilde{\Lambda}} \frac{\mathrm{d}^2\mathbf{q}_{\perp}}{(2\pi)^2} \frac{I_{\pm}(0)}{q_{\perp}^2+m_D^2} + \int_{\tilde{\Lambda}<q_{\perp}<\Lambda_{\perp}} \frac{\mathrm{d}^2\mathbf{q}_{\perp}}{(2\pi)^2} \frac{I_{\pm}(q_{\perp}/T)}{q_{\perp}^2}$.

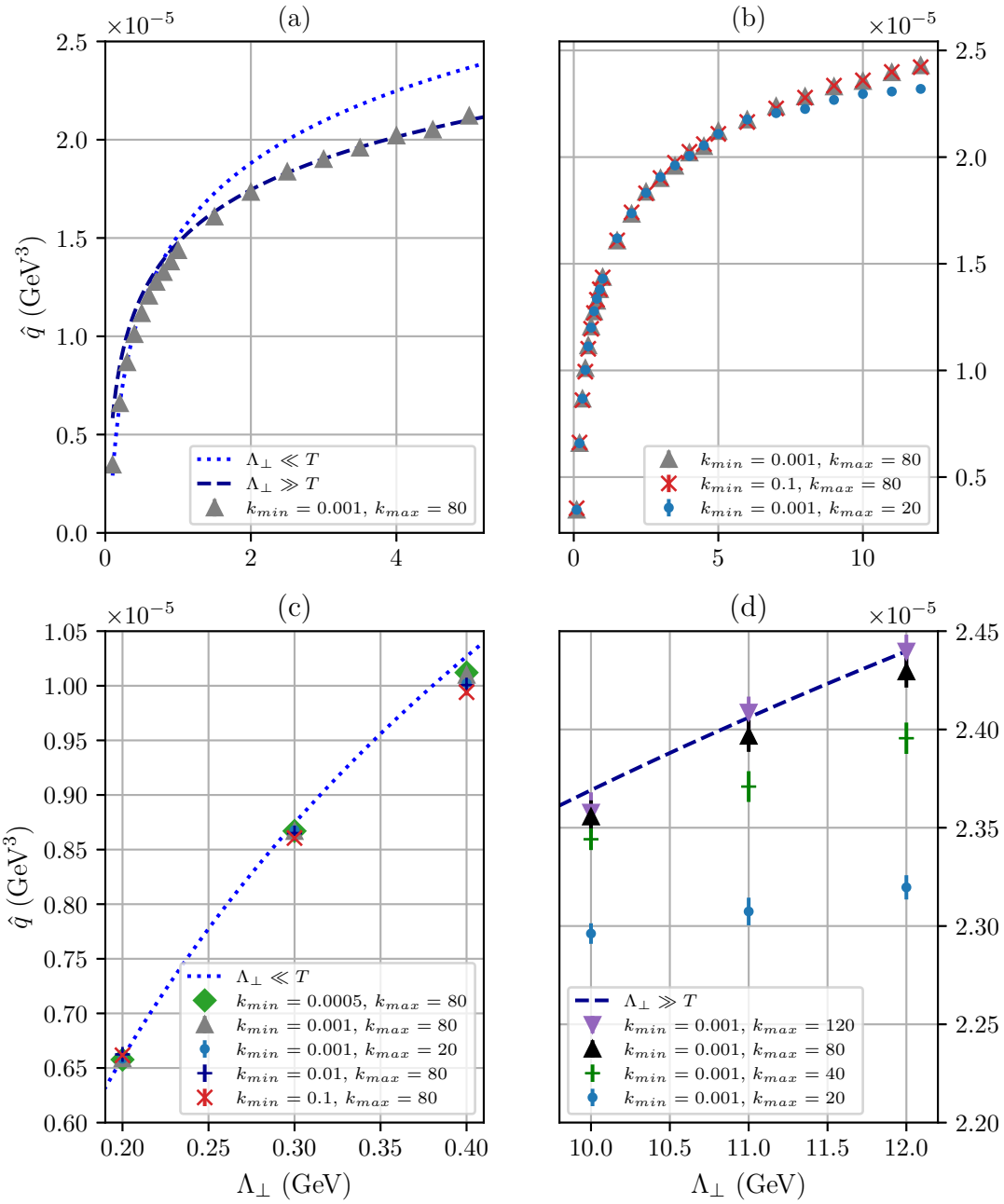

Figure 5.1.: Numerical integration results of $\hat{q}$ for $\lambda = 0.01$, $T = 1\,\text{GeV}$. The numerical values for k_{min} and k_{max} are also given in GeV. In (a) the analytical results for $\Lambda_\perp \ll T$, (5.2); $\Lambda_\perp \gg T$, (5.3); and the result of our numerical integration is shown. The results agree well with (5.2) and (5.3). In (b) different k_{min} and k_{max} are used. As shown in the plot, they agree very well. In (c) we look at different k_{min} and k_{max} in the small $\Lambda_\perp$ region. In this region we see a weak dependence on k_{min}. In (d) we look at different k_{max} in the large $\Lambda_\perp$ region, where we see a weak dependence on k_{max}.

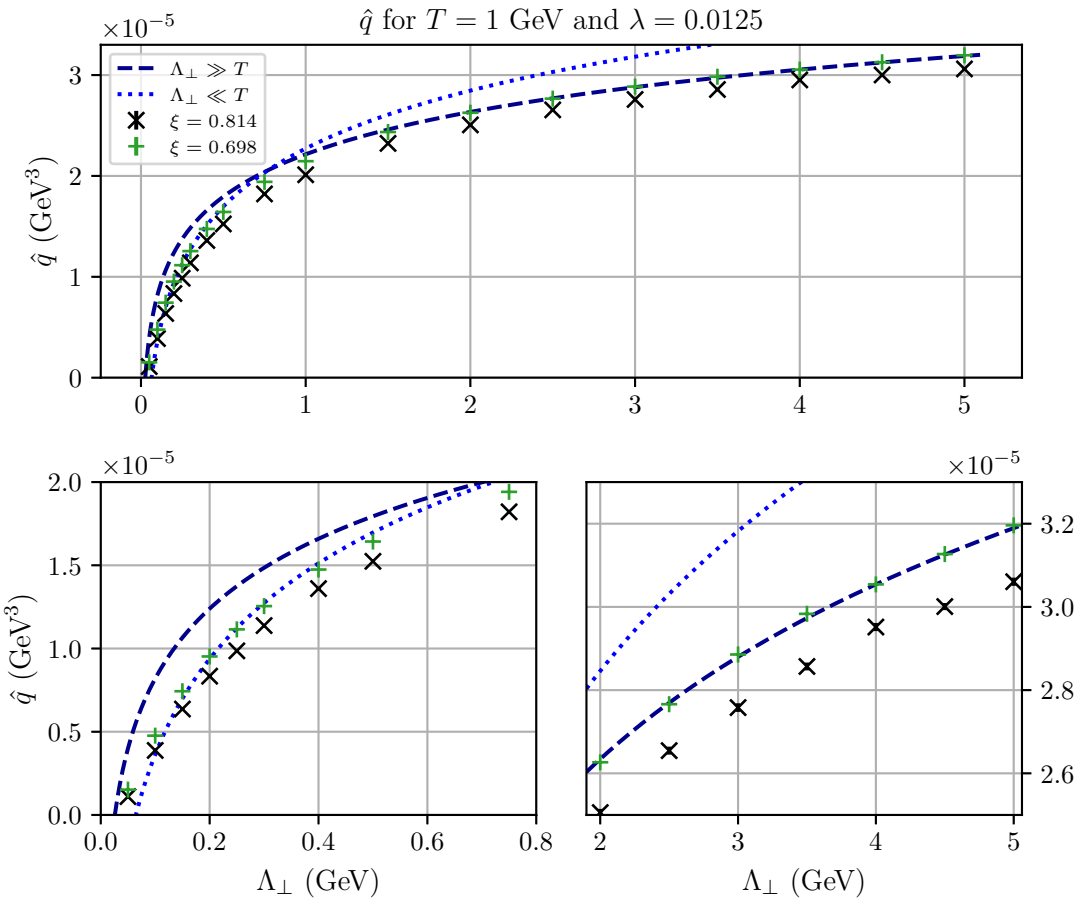

Figure 5.2.: Behavior of $\hat{q}$ for small $\lambda = 0.0125$, $T = 1$ GeV and different $\Lambda_\perp$. Different values for the screening mass have been used. $\xi = 0.814$ is from [12], whereas $\xi = 0.698$ is chosen such that our result matches the soft limit. $\Lambda_\perp \gg T$ denotes (5.3), while $\Lambda_\perp \ll T$ denotes (5.2).

influences especially the low $\Lambda_\perp$ behavior, while changing k_{max} influences the large $\Lambda_\perp$ behavior. In (4.12) we want $\Lambda_\perp$ to dictate the integral boundaries, not k_{max}, thus we see immediately that, if k_{max} is too small, we lose a part of our integration region, which can explain the deviations.

In Figure 5.2 we plot $\hat{q}$ for $\lambda = 0.0125$ for different regularization parameters ξ, which also matches well with (5.2) and (5.3) for $\xi = 0.698$. We obtained this value from matching the soft limit result to analytic calculations, but we see that this value also reproduces (5.3), which is valid for $\Lambda_\perp \gg T$. The parameter $\xi = 0.814$ from [12] also quoted in Section 2.2.3 yields slightly different results.

A comparison of different λ is given in Figure 5.3. For $\lambda = 1$ we have no region in which our results for $\hat{q}$ follow (5.2). This is no surprise, because (5.2) is only valid for $m_D \ll \Lambda_\perp \ll T$. From (2.60) we can calculate the Debye mass, $m_D = \frac{T}{\sqrt{3}} \approx 0.58\,\text{GeV}$. Thus the required condition is not fulfilled.

We find that for different values of λ we need to use different values of $\xi \to \xi(\lambda)$

if we want our result to match with the analytical result (5.3), although the different values of ξ only slightly change the result. As mentioned earlier, the formulae (5.2) and (5.3) were derived under the assumption $m_D \ll T$, which is only satisfied for small λ. Thus we use the constant $\xi_0 = 0.698$, which reproduces the analytic formulae for small couplings λ.

In Figure 5.4 we summarize these behaviors in one plot. We calculate and plot $\hat{q}$ for $\lambda = 10$, where we see that neither of the two screening masses, ξ or ξ_0, agrees with (5.3). The dependence on k_{max} can also clearly be seen. We use $\lambda = 10$ because as we will see later in Section 5.1.3, a comparison with experimental bounds yields approximately $\lambda \approx 10$. This value is also used frequently in the literature [13, 43, 44].

Effect of discretization

We now study the effects resulting from the discretization of our particle distribution function $f(\mathbf{k})$. For the numerical time evolution via the Boltzmann equation we need a discretized version of the particle distribution function. In thermal equilibrium, however, we know and therefore can use its exact form and study the effect of the discretization on $\hat{q}$. We now study this effect at the $q_\perp$ cutoff $\Lambda_\perp = 11\,\text{GeV}$. We use this cutoff because we expect the effects to be largest for larger values of $\Lambda_\perp$ and for $\Lambda_\perp = 11\,\text{GeV}$ our results match the analytic calculation for $k_{max} = 80\,\text{GeV}$. The numerical results for $\hat{q}$ are plotted in Figure 5.5. On the left-hand side, the exact form for f was used, whereas on the right-hand side we used the discretized version of f. We observe that the discretized version behaves differently than the continuous version for different values of the lower momentum cutoff, k_{min}. Whereas for $\lambda = 0.01$ the behavior is qualitatively similar, for $\lambda = 1$ the value for $\hat{q}$ increases with increasing k_{min} in the discretized version, while it decreases in the continuous version. We believe this is a result of the different Debye masses used. For the continuous version we used the exact Debye mass for the screening $m_D = \sqrt{\frac{\lambda}{3}}T$, in the discretized version we calculate the Debye mass from the discretized distribution function $f(\mathbf{k})$ via (2.59). In our case, $f(\mathbf{k})$ is given by the Bose-Einstein distribution, which is sharply peaked for small k. Thus enforcing a non-zero k_{min} changes the outcome of the numerical integral for m_D, which changes the screening mass and therefore changes $\hat{q}$. The error bars in the plot denote the standard error (4.47).

5.1.3. Comparison with RHIC and LHC data

After these simple checks we now compare with constraints for $\hat{q}$ obtained from the measurement of single hadron nuclear modification factors at RHIC and LHC (quark jet energy $E = 10\,\text{GeV}$) [7]:

$$\frac{\hat{q}}{C_R T^3} = \begin{cases} 3.5 \pm 0.9, & T \approx 370\,\text{MeV} \quad \text{(RHIC)} \\ 2.8 \pm 1.1, & T \approx 470\,\text{MeV} \quad \text{(LHC)} \end{cases} \tag{5.12}$$

We now have to establish which cutoff $\Lambda_\perp$ and coupling λ to use. For the cutoff we decide to use values also used in the CUJET model [16]: In CUJET2.0 [17], $\Lambda_\perp = \sqrt{4ET}$ is used, whereas in CUJET3.0 [18], $\Lambda_\perp = \sqrt{6ET}$.

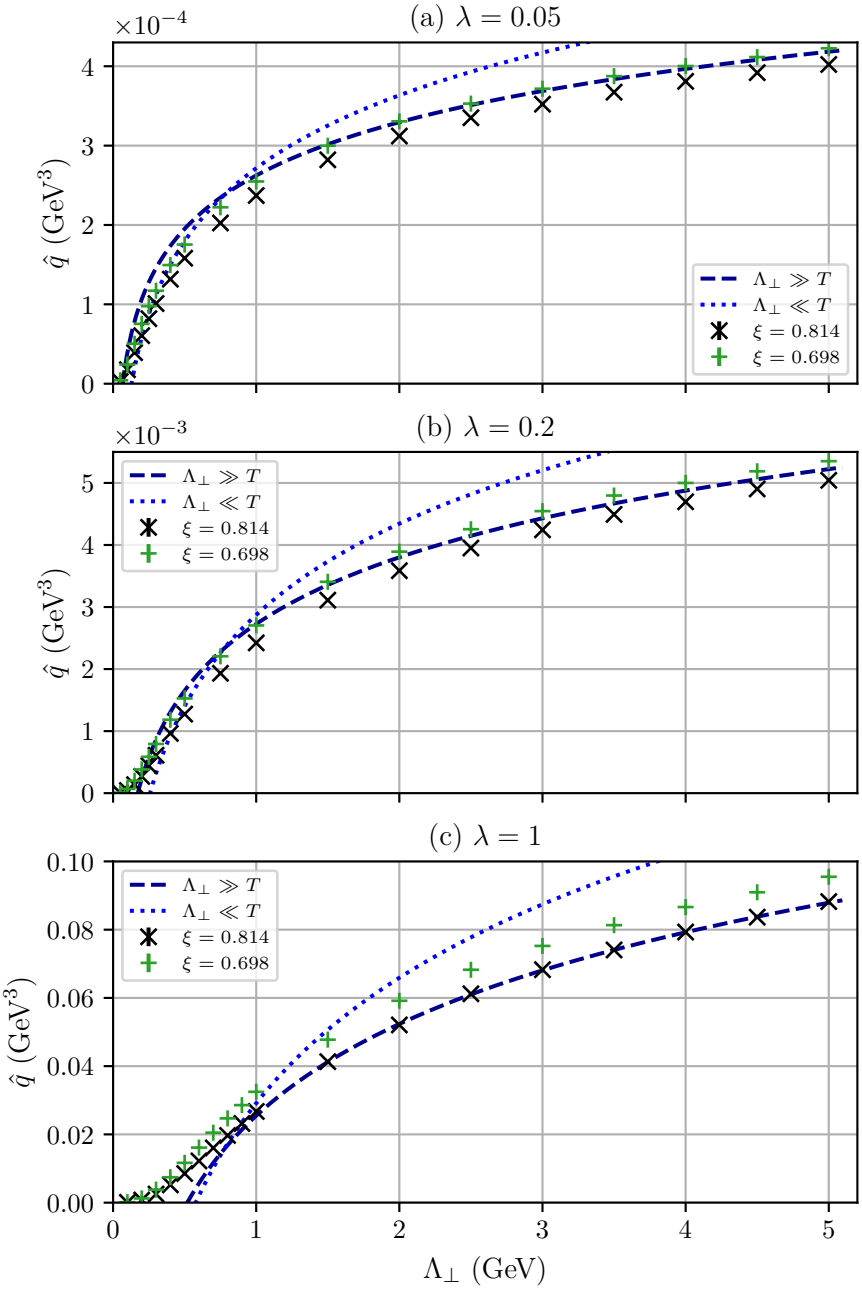

Figure 5.3.: Behavior of $\hat{q}$ for different λ, $T = 1$ GeV and different $\Lambda_\perp$. Different values for the screening mass are used. $\xi = 0.814$ is from [12], whereas $\xi_0 = 0.698$ is the result such that we match the soft result. In (b) both screening masses yield different results than the analytic calculation. $\Lambda_\perp \gg T$ denotes (5.3), while $\Lambda_\perp \ll T$ denotes (5.2).

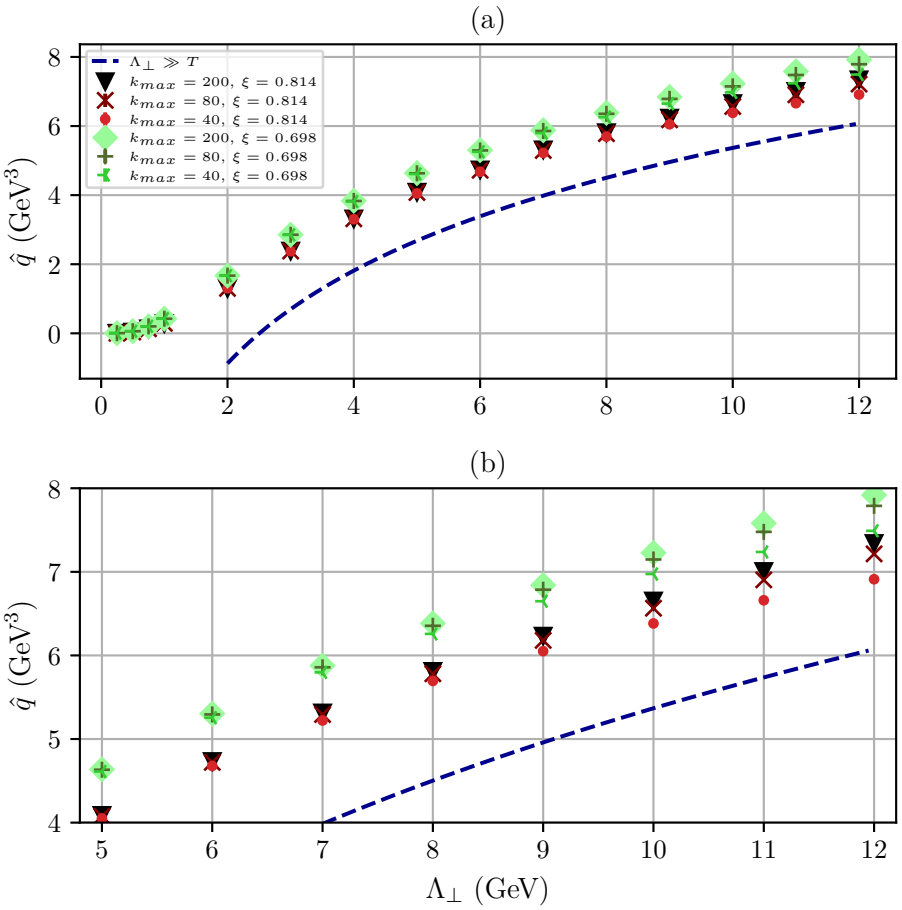

Figure 5.4.: Behavior of $\hat{q}$ for $\lambda = 10$, $T = 1\,\text{GeV}$, $k_{min} = 0.01$ and different k_{max} and screening masses, ξ. The blue dashed curve, labeled $\Lambda_\perp \gg T$ is the analytic result (5.3).

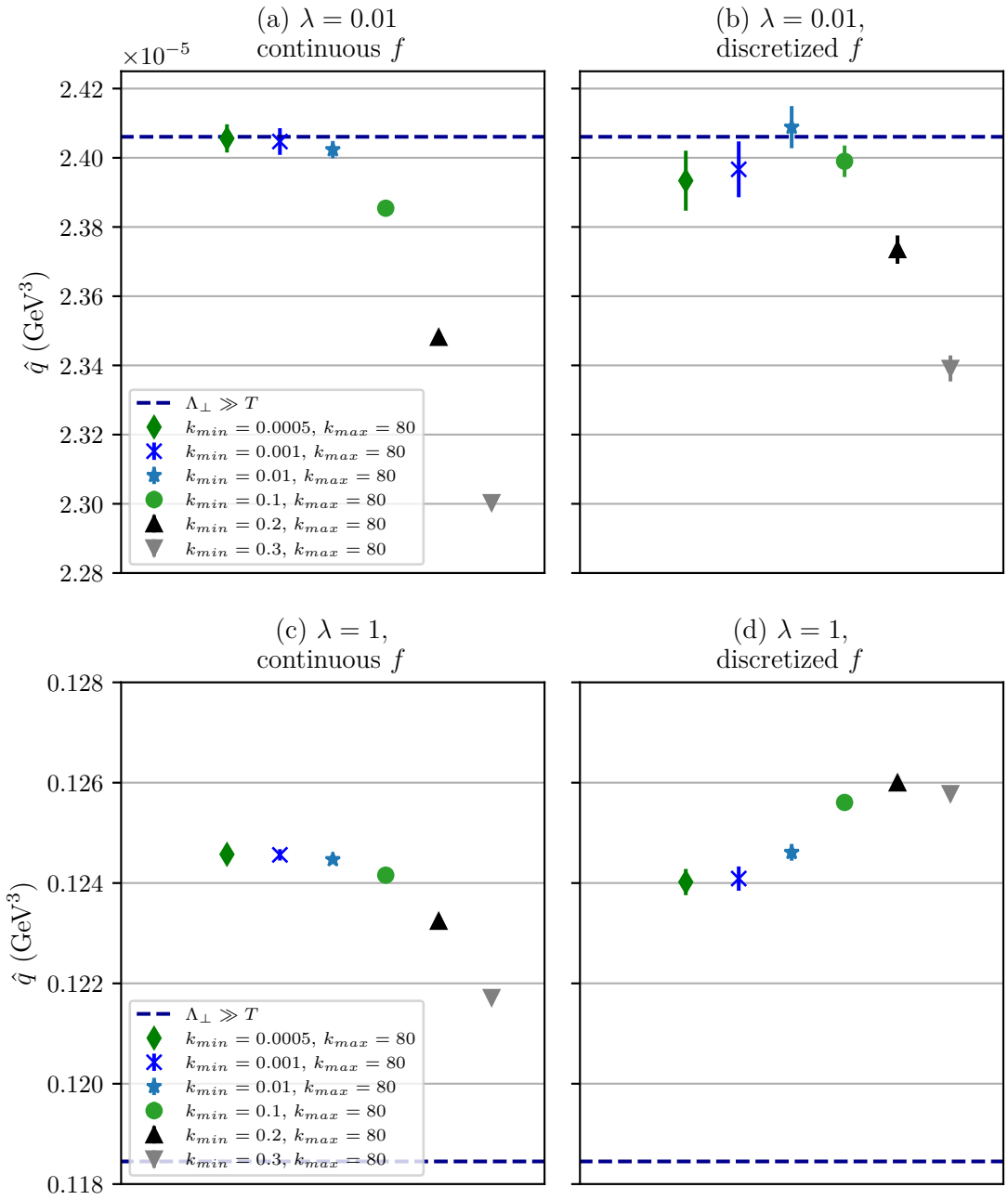

Figure 5.5.: Numerical integration results of $\hat{q}$ for $T = 1\,\text{GeV}$, $\Lambda_\perp = 11\,\text{GeV}$ and different λ. The dependence on k_{min} is shown. (Left) Here we use a continuous form for the distribution function f and the exact value for the Debye mass m_D. We see that for the smallest values, $k_{min} < 0.1$ and $\lambda = 0.01$, the results are compatible with (5.3) (dashed line). (Right) Here we use a discretized form for the distribution function f and the Debye mass is calculated as a numerical integral.

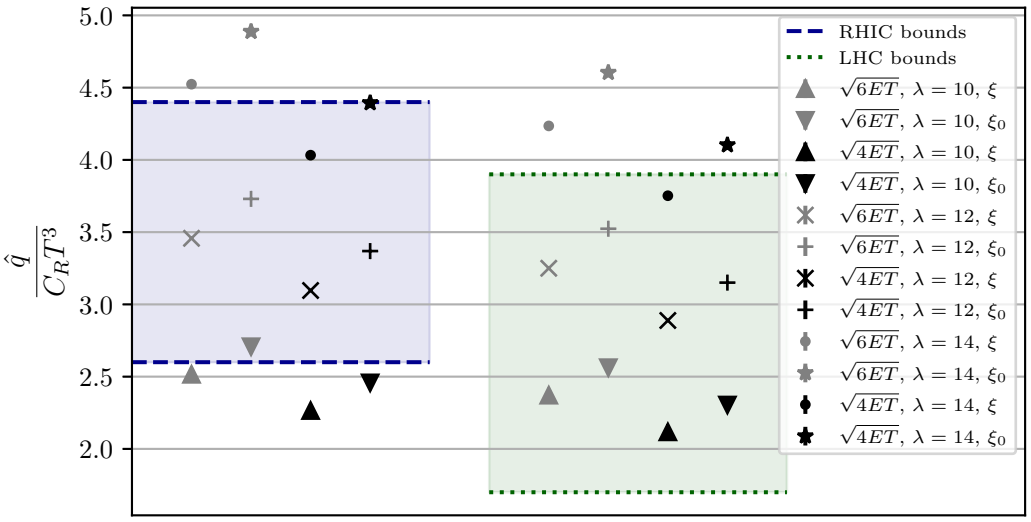

Figure 5.6.: Comparison of $\hat{q}$ with bounds obtained from RHIC and LHC, (5.12). The cutoffs used are given in physical units in (5.13). Different screening masses are used, denoted by $\xi = 0.814$ and $\xi_0 = 0.698$. We used $k_{min} = 0.01$ and $k_{max} = 200$.

Thus we use for $\Lambda_\perp$

$$\Lambda_\perp = \begin{cases} T \approx 370\,\text{MeV} & \begin{cases} \sqrt{6ET} = 4.71\,\text{GeV} \\ \sqrt{4ET} = 3.85\,\text{GeV} \end{cases} \\ T \approx 470\,\text{MeV} & \begin{cases} \sqrt{6ET} = 5.31\,\text{GeV} \\ \sqrt{4ET} = 4.34\,\text{GeV} \end{cases} \end{cases} . \tag{5.13}$$

Because the only scale in our calculation is the temperature T, we can rescale everything with T,

$$\frac{\Lambda_\perp}{T} = \begin{cases} T \approx 370\,\text{MeV} & \begin{cases} 12.73 \\ 10.39 \end{cases} \\ T \approx 470\,\text{MeV} & \begin{cases} 11.30 \\ 9.23 \end{cases} \end{cases} . \tag{5.14}$$

We compare our results for different λ with these bounds in Figure 5.6. We find that $\lambda \sim \mathcal{O}(10)$. A value of $\lambda = 10$ corresponds to $\alpha = 0.27$, see (2.16). The difference between the different regularization masses is about 8 %.

5.2. Scaled thermal distribution

Let us consider a rescaled thermal distribution,

$$f(p; \beta, N_0) = \frac{N_0}{e^{\beta p} - 1} \tag{5.15}$$

and calculate $\hat{q}$ without time evolution, i.e. at initial time t_0.

As independent parameters we have

- the coupling $\lambda = g^2 N_C$,
- Temperature $T = 1/\beta$,
- N_0.

Let's assume that $\beta = 1\,\mathrm{GeV}^{-1}$, i.e. we scale everything with the temperature. Then we have two independent parameters, on which $\hat{q}$ will depend. Every matrix element comes with a factor $g^4 \sim \lambda^2$, which we could factor out. Since the Debye mass scales with $N_0\lambda$, the scaled matrix element then depends only on $N_0\lambda$,

$$\lambda^2 \left|\tilde{M}^{ab}_{cd}(N_0\lambda)\right|^2 = \left|\mathcal{M}^{ab}_{cd}(N_0,\lambda)\right|^2. \tag{5.16}$$

Then $\hat{q}$ becomes

$$\hat{q} = \frac{1}{\nu_a}\frac{1}{2^9\pi^5}\sum_{bcd}\int_0^{2\pi}\mathrm{d}\tilde{\phi}_{pq}\int_0^{2\pi}\mathrm{d}\phi_{kq}\int_0^{\infty}\mathrm{d}k\int_{-\infty}^{k}\mathrm{d}\omega\int_{|\omega|}^{2k-\omega}\mathrm{d}q \\ q^2\sin^2\theta_{pq}\frac{|\tilde{M}^{ab}_{cd}(N_0\lambda)|^2}{p^2}\lambda^2 f_b(k,v_k)\left(1\pm f_d(k-\omega,v_{k'})\right). \tag{5.17}$$

We can now consider the two terms separately and write

$$\hat{q} = \lambda\hat{q}_f(N_0\lambda) \pm \hat{q}_{ff}(N_0\lambda), \tag{5.18}$$

with

$$\lambda\hat{q}_f = \frac{1}{\nu_a}\frac{1}{2^9\pi^5}\sum_{bcd}\int_0^{2\pi}\mathrm{d}\tilde{\phi}_{pq}\int_0^{2\pi}\mathrm{d}\phi_{kq}\int_0^{\infty}\mathrm{d}k\int_{-\infty}^{k}\mathrm{d}\omega\int_{|\omega|}^{2k-\omega}\mathrm{d}q \\ q^2\sin^2\theta_{pq}\frac{|\tilde{M}^{ab}_{cd}(N_0\lambda)|^2}{p^2}\lambda^2 f_b(k,v_k), \tag{5.19}$$

$$\hat{q}_{ff} = \frac{1}{\nu_a}\frac{1}{2^9\pi^5}\sum_{bcd}\int_0^{2\pi}\mathrm{d}\tilde{\phi}_{pq}\int_0^{2\pi}\mathrm{d}\phi_{kq}\int_0^{\infty}\mathrm{d}k\int_{-\infty}^{k}\mathrm{d}\omega\int_{|\omega|}^{2k-\omega}\mathrm{d}q \\ q^2\sin^2\theta_{pq}\frac{|\tilde{M}^{ab}_{cd}(N_0\lambda)|^2}{p^2}\lambda^2 f_b(k,v_k)f_d(k-\omega,v_{k'}). \tag{5.20}$$

Note that f also contains a factor N_0, which, together with λ combines to the $N_0\lambda$ behavior in (5.18). Thus we can simulate $\hat{q}_f$ and $\hat{q}_{ff}$ with one independent parameter, $N_0\lambda$, and then add the second independent parameter later.

The behavior of $\hat{q}$ for different λ and N_0 is plotted in Figure 5.7. We have used different values for λ, N_0 in the code and checked that the result depends only on its product $\lambda \cdot N_0$. We have seen in thermal equilibrium that there are different values for the screening mass constant, ξ. We plot the difference in Figure 5.8. We find that the difference is about 3 %.

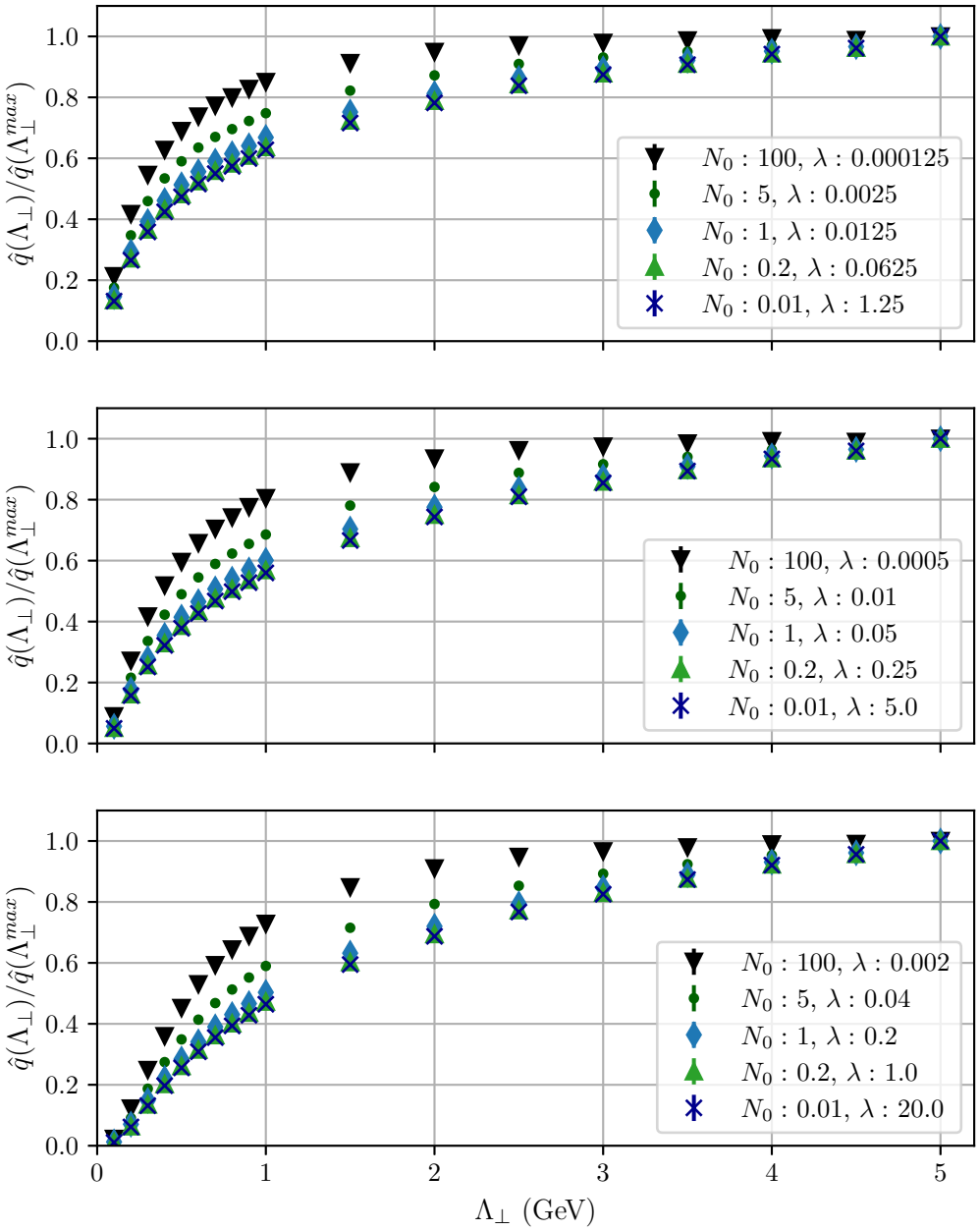

Figure 5.7.: Behavior of $\hat{q}$ for a scaled thermal distribution, (5.15), for different λ, N_0 and different $\Lambda_\perp$ for $T = 1\,\text{GeV}$, $k_{min} = 0.001\,\text{GeV}$, $k_{max} = 80\,\text{GeV}$. The screening mass used is $\xi_0 = 0.698$ obtained previously. The curves have been normalized to its maximum value at $\Lambda_\perp = 5\,\text{GeV}$.

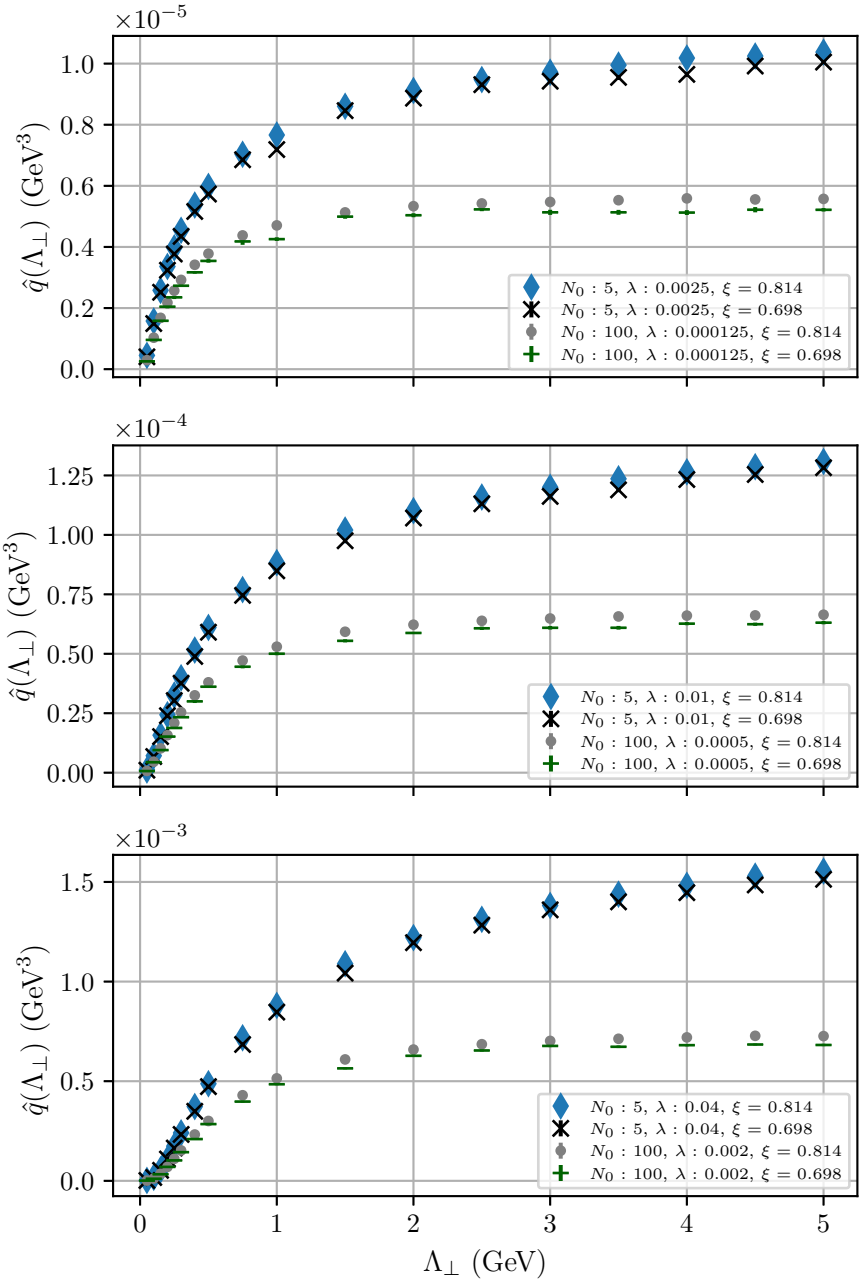

Figure 5.8.: Behavior of $\hat{q}$ for a scaled thermal distribution, (5.15), for different λ, N_0 and ξ as a function of $\Lambda_\perp$ for $T = 1\,\text{GeV}$, $k_{min} = 0.001\,\text{GeV}$, $k_{max} = 80\,\text{GeV}$.

6. Conclusion, summary and outlook

In this thesis I have derived a formula for the jet quenching parameter $\hat{q}$ that describes transverse momentum broadening of jets traversing the Quark-Gluon Plasma, a state of matter that is created in heavy-ion collisions. The formula for $\hat{q}$ is derived from a framework called effective kinetic theory (EKT), of which we presented a short overview. First, we derive the formula for finite jet momentum p and then take the limit $p \to \infty$, where we then need to introduce a cutoff in order to render $\hat{q}$ finite. The formula reproduces correctly the known soft limit in thermal equilibrium, but its scope goes beyond that, as it can be used for different and even anisotropic distribution functions $f(\mathbf{p})$. I have implemented the formula for $\hat{q}$ in a C++ code simulating the evolution of the distribution function f in effective kinetic theory. The formula is implemented for anisotropic distributions. The code reproduces the analytic formulae in thermal equilibrium and the off-diagonal elements $\hat{q}_{xy}$ are zero. By comparison with bounds obtained from RHIC and LHC experiments, we find that the coupling $\lambda \approx 12$. We have then extracted $\hat{q}$ for a scaled thermal distribution.

We have found that the regularization parameter ξ in $\hat{q}$ differs from its counterpart in the matrix elements that describe the evolution in the EKT. This difference originates from a different matching condition, and $\hat{q}$ differs from the value of $\hat{q}$ that employs the usual isotropic screening prescription of the EKT by only a few percent ($\sim 8\,\%$).

The formula I have implemented in the code assumes infinite jet momentum, $p \to \infty$, and needs a momentum cutoff, but we also derived a formula for finite jet momentum p, which in future can be used to compare these two approaches. Additionally, the code can be used to extract $\hat{q}$ in anisotropic systems, for example in systems undergoing Bjorken expansion. However, both in the time evolution and in $\hat{q}$ the assumption of isotropic screening will produce an error which is yet to be quantified. A further possibility is to work on extending the derived $\hat{q}$ formula and the current EKT framework to take anisotropies into account.

A. Mandelstam variables

Here we derive a formula for the Mandelstam variables defined in (2.87),

$$s = -(P+K)^2, \qquad t = -(P'-P)^2, \qquad u = -(K'-P)^2, \tag{A.1}$$

and use (3.58), (3.60), (3.98a) and (3.98b) to express them in terms of p, k, q, ω, ϕ_{kq}. Also, we use that $P^2 = K^2 = P'^2 = K'^2 = 0$.

First we start with t. Recall that we introduced $Q = (\omega, \mathbf{q})$ in (3.19) in such a way that

$$\mathbf{q} = \mathbf{p}' - \mathbf{p}, \qquad \omega - p' - p. \tag{A.2}$$

For t, we then insert

$$t = -(P'-P)^2 = (p'-p)^2 - (\mathbf{p}'-\mathbf{p})^2, \tag{A.3}$$

from which we immediately obtain

$$\boxed{t = \omega^2 - q^2}. \tag{A.4}$$

Next we insert for s,

$$s = -(P+K)^2 = -2P\cdot K = 2pk - 2\mathbf{p}\cdot\mathbf{k}. \tag{A.5}$$

Using (3.58) and (3.60), we obtain

$$s = 2pk - 2pk\left[\sin\theta_{pq}\sin\theta_{kq}\cos\phi_{kq} + \cos\theta_{pq}\cos\theta_{kq}\right], \tag{A.6}$$

in which we can insert (3.98a) and (3.98b),

$$s = 2pk - 2pk\left[\left(1-\left(\frac{\omega}{q}-\frac{q^2-\omega^2}{2pq}\right)\right)^{1/2}\left(1-\left(\frac{\omega}{q}+\frac{q^2-\omega^2}{2kq}\right)^2\right)^{1/2}\cos\phi_{kq} + \left(\frac{\omega}{q}-\frac{q^2-\omega^2}{2pq}\right)\left(\frac{\omega}{q}+\frac{q^2-\omega^2}{2kq}\right)\right] \tag{A.7}$$

$$= 2pk\left[1-\cos\phi_{kq}\left(1-\frac{1}{q^2}\left(\omega^2-\frac{\omega(q^2-\omega^2)}{p}+\frac{(q^2-\omega)^2}{4p^2}\right)\right)^{1/2} \times\left(1-\frac{1}{q^2}\left(\omega^2+\frac{\omega\,(q^2-\omega^2)}{k}+\frac{(q^2-\omega^2)^2}{4k^2}\right)\right)^{1/2} - \frac{\omega^2}{q^2}-\frac{\omega(q^2-\omega^2)}{2pq^2}+\frac{\omega(q^2-\omega^2)}{2kq^2}+\frac{(q^2-\omega^2)^2}{4pq^2}\right] \tag{A.8}$$

$$= 2pq\frac{q^2-\omega^2}{q^2}\left[\frac{q^2-\omega^2}{q^2-\omega^2}-\frac{\omega}{2p}+\frac{\omega}{2k}+\frac{q^2-\omega^2}{4pk} - \cos\phi_{kq}\left(1+\frac{\omega}{p}-\frac{q^2-\omega^2}{4p^2}\right)^{1/2}\left(1-\frac{\omega}{k}-\frac{q^2-\omega^2}{4k^2}\right)^{1/2}\right] \tag{A.9}$$

$$= \frac{2(q^2-\omega^2)}{q^2}\left[pk-\frac{\omega k}{2}+\frac{\omega p}{2}+\frac{1}{4}(q^2-\omega^2) - \cos\phi_{kq}\left(p^2+\omega p+\frac{1}{4}(\omega^2-q^2)\right)^{1/2}\left(k^2-\omega k+\frac{1}{4}(\omega^2-q^2)\right)^{1/2}\right] \tag{A.10}$$

We obtain

$$s = -\frac{t}{2q^2}\left[(2p+\omega)(2k-\omega)+q^2-\cos\phi_{kq}\sqrt{\left[(2p+\omega)^2-q^2\right]\left[(2k-\omega)^2-q^2\right]}\right], \tag{A.11}$$

which can also be rewritten as

$$\boxed{s = -\frac{t}{2q^2}\left[(p+p')(k+k')+q^2-\cos\phi_{kq}\sqrt{[4pp'+t]\,[4kk'+t]}\right]}. \tag{A.12}$$

Using

$$s+t+u=0, \tag{A.13}$$

we find

$$\boxed{u = \frac{t}{2q^2}\left[(p+p')(k+k')-q^2-\cos\phi_{kq}\sqrt{[4pp'+t]\,[4kk'+t]}\right]}. \tag{A.14}$$

Bibliography

[1] K. Adcox et al. "Formation of dense partonic matter in relativistic nucleus–nucleus collisions at RHIC: Experimental evaluation by the PHENIX Collaboration". In: *Nuclear Physics A* 757.1 (2005). First Three Years of Operation of RHIC, pp. 184–283. DOI: https://doi.org/10.1016/j.nuclphysa.2005.03.086. URL: https://www.sciencedirect.com/science/article/pii/S0375947405005300.

[2] Panagiota Foka and Małgorzata Anna Janik. "An overview of experimental results from ultra-relativistic heavy-ion collisions at the CERN LHC: Bulk properties and dynamical evolution". In: *Rev. Phys.* 1 (2016), pp. 154–171. DOI: 10.1016/j.revip.2016.11.002. arXiv: 1702.07233 [hep-ex].

[3] Peter Brockway Arnold, Guy D. Moore, and Laurence G. Yaffe. "Effective kinetic theory for high temperature gauge theories". In: *JHEP* 01 (2003), p. 030. DOI: 10.1088/1126-6708/2003/01/030. arXiv: hep-ph/0209353.

[4] Jürgen Berges, Michal P. Heller, Aleksas Mazeliauskas, and Raju Venugopalan. "QCD thermalization: Ab initio approaches and interdisciplinary connections". In: *Rev. Mod. Phys.* 93.3 (2021), p. 035003. DOI: 10.1103/RevModPhys.93.035003. arXiv: 2005.12299 [hep-th].

[5] Soeren Schlichting and Derek Teaney. "The First fm/c of Heavy-Ion Collisions". In: *Ann. Rev. Nucl. Part. Sci.* 69 (2019), pp. 447–476. DOI: 10.1146/annurev-nucl-101918-023825. arXiv: 1908.02113 [nucl-th].

[6] J. D. Bjorken. "Energy Loss of Energetic Partons in Quark - Gluon Plasma: Possible Extinction of High p(t) Jets in Hadron - Hadron Collisions". In: (Aug. 1982).

[7] Guang-You Qin and Xin-Nian Wang. "Jet quenching in high-energy heavy-ion collisions". In: *Int. J. Mod. Phys. E* 24.11 (2015). Ed. by Xin-Nian Wang, p. 1530014. DOI: 10.1142/S0218301315300143. arXiv: 1511.00790 [hep-ph].

[8] Peter Brockway Arnold and Wei Xiao. "High-energy jet quenching in weakly-coupled quark-gluon plasmas". In: *Phys. Rev. D* 78 (2008), p. 125008. DOI: 10.1103/PhysRevD.78.125008. arXiv: 0810.1026 [hep-ph].

[9] Simon Caron-Huot. "O(g) plasma effects in jet quenching". In: *Phys. Rev. D* 79 (2009), p. 065039. DOI: 10.1103/PhysRevD.79.065039. arXiv: 0811.1603 [hep-ph].

[10] Andreas Ipp, David I. Müller, and Daniel Schuh. "Anisotropic momentum broadening in the 2+1D Glasma: analytic weak field approximation and lattice simulations". In: *Phys. Rev. D* 102.7 (2020), p. 074001. DOI: 10.1103/PhysRevD.102.074001. arXiv: 2001.10001 [hep-ph].

[11] S. Mrowczynski. "Plasma instability at the initial stage of ultrarelativistic heavy ion collisions". In: *Phys. Lett. B* 314 (1993), pp. 118–121. DOI: 10.1016/0370-2693(93)91330-P.

[12] Mark C. Abraao York, Aleksi Kurkela, Egang Lu, and Guy D. Moore. "UV cascade in classical Yang-Mills theory via kinetic theory". In: *Phys. Rev. D* 89.7 (2014), p. 074036. DOI: 10.1103/PhysRevD.89.074036. arXiv: 1401.3751 [hep-ph].

[13] Aleksi Kurkela and Yan Zhu. "Isotropization and hydrodynamization in weakly coupled heavy-ion collisions". In: *Phys. Rev. Lett.* 115.18 (2015), p. 182301. DOI: 10.1103/PhysRevLett.115.182301. arXiv: 1506.06647 [hep-ph].

[14] Sigtryggur Hauksson, Sangyong Jeon, and Charles Gale. "Momentum broadening of energetic partons in an anisotropic plasma". In: *Phys. Rev. C* 105.1 (2022), p. 014914. DOI: 10.1103/PhysRevC.105.014914. arXiv: 2109.04575 [hep-ph].

[15] Jacopo Ghiglieri, Guy D. Moore, and Derek Teaney. "Jet-Medium Interactions at NLO in a Weakly-Coupled Quark-Gluon Plasma". In: *JHEP* 03 (2016), p. 095. DOI: 10.1007/JHEP03(2016)095. arXiv: 1509.07773 [hep-ph].

[16] Alessandro Buzzatti and Miklos Gyulassy. "An overview of the CUJET model: Jet Flavor Tomography applied at RHIC and LHC". In: *Nucl. Phys. A* 910-911 (2013). Ed. by Federico Antinori et al., pp. 490–493. DOI: 10.1016/j.nuclphysa.2012.12.009. arXiv: 1207.6020 [hep-ph].

[17] Jiechen Xu, Alessandro Buzzatti, and Miklos Gyulassy. "Azimuthal jet flavor tomography with CUJET2.0 of nuclear collisions at RHIC and LHC". In: *JHEP* 08 (2014), p. 063. DOI: 10.1007/JHEP08(2014)063. arXiv: 1402.2956 [hep-ph].

[18] Jiechen Xu, Jinfeng Liao, and Miklos Gyulassy. "Consistency of Perfect Fluidity and Jet Quenching in semi-Quark-Gluon Monopole Plasmas". In: *Chin. Phys. Lett.* 32.9 (2015), p. 092501. DOI: 10.1088/0256-307X/32/9/092501. arXiv: 1411.3673 [hep-ph].

[19] Michel Le Bellac. *Thermal Field Theory*. Cambridge Monographs on Mathematical Physics. Cambridge University Press, 1996.

[20] Jacopo Ghiglieri, Aleksi Kurkela, Michael Strickland, and Aleksi Vuorinen. "Perturbative Thermal QCD: Formalism and Applications". In: *Phys. Rept.* 880 (2020), pp. 1–73. DOI: 10.1016/j.physrep.2020.07.004. arXiv: 2002.10188 [hep-ph].

[21] Simon Caron-Huot. "Heavy quark energy losses in the quark-gluon plasma: beyond leading order". MA thesis. McGill U., 2007.

[22] M. Srednicki. *Quantum field theory*. Cambridge University Press, Jan. 2007.

[23] M.E. Peskin and D.V. Schroeder. *An Introduction To Quantum Field Theory*. CRC Press, 1995.

[24] Matthew D. Schwartz. *Quantum Field Theory and the Standard Model*. Cambridge University Press, Mar. 2014.

[25] J. I. Kapusta and Charles Gale. *Finite-temperature field theory: Principles and applications*. Cambridge Monographs on Mathematical Physics. Cambridge University Press, 2006.

[26] John David Jackson. *Classical Electrodynamics*. New York: John Wiley & Sons, 1962.

[27] Brian C. Hall. *Lie Groups, Lie Algebras, and Representations*. Springer International Publishing, 2015. DOI: 10.1007/978-3-319-13467-3. URL: http://dx.doi.org/10.1007/978-3-319-13467-3.

[28] Jean-Paul Blaizot and Edmond Iancu. "The Quark gluon plasma: Collective dynamics and hard thermal loops". In: *Phys. Rept.* 359 (2002), pp. 355–528. DOI: 10.1016/S0370-1573(01)00061-8. arXiv: hep-ph/0101103.

[29] Kuang-chao Chou, Zhao-bin Su, Bai-lin Hao, and Lu Yu. "Equilibrium and nonequilibrium formalisms made unified". In: *Physics Reports* 118.1 (1985), pp. 1–131. DOI: https://doi.org/10.1016/0370-1573(85)90136-X. URL: https://www.sciencedirect.com/science/article/pii/037015738590136X.

[30] Leo P. Kadanoff and Gordon Baym. *Quantum Statistical Mechanics. Green's Function Methods in Equilibrium and Nonequilibrium Problems*. New York: W. A. Benjamin, Inc., 1962.

[31] Juergen Berges. "N-particle irreducible effective action techniques for gauge theories". In: *Phys. Rev. D* 70 (2004), p. 105010. DOI: 10.1103/PhysRevD.70.105010. arXiv: hep-ph/0401172.

[32] Alfred H. Mueller. "The Boltzmann equation for gluons at early times after a heavy ion collision". In: *Phys. Lett. B* 475 (2000), pp. 220–224. DOI: 10.1016/S0370-2693(00)00084-8. arXiv: hep-ph/9909388.

[33] Lev Davidovič Landau and Evgenij M Lifšic. *The classical theory of fields*. eng. 4. rev. engl. ed., reprint. with corr.. Course of theoretical physics. Amsterdam [u.a.]: Elsevier Butterworth-Heinemann, 2005.

[34] William H. Press, Saul A. Teukolsky, William T. Vetterling, and Brian P. Flannery. *Numerical Recipes. The Art of Scientific Computing. Third Edition*. Cambridge University Press, 2007.

[35] Lev P. Pitaevskii and Evgenij M. Lifšic. *Physical Kinetics*. Vol. 10. Pergamon Press, 1981.

[36] Mark Thomson. *Modern particle physics*. New York: Cambridge University Press, 2013.

[37] Peter Brockway Arnold, Guy D Moore, and Laurence G. Yaffe. "Transport coefficients in high temperature gauge theories. 2. Beyond leading log". In: *JHEP* 05 (2003), p. 051. DOI: 10.1088/1126-6708/2003/05/051. arXiv: hep-ph/0302165.

[38] Milton Abramowitz and Irene A. Stegun. *Handbook of Mathematical Functions With Formulas, Graphs, and Mathematical Tables*. National Bureau of Standards, 1964.

[39] Shirley Dowdy, Stanley Weardon, and Daniel Chilko. *Statistics for Research*. John Wiley & Sons, Inc., Jan. 2004. DOI: 10.1002/0471477435. URL: http://dx.doi.org/10.1002/0471477435.

[40] Charles R. Harris et al. "Array programming with NumPy". In: *Nature* 585.7825 (Sept. 2020), pp. 357–362. DOI: 10.1038/s41586-020-2649-2. URL: https://doi.org/10.1038/s41586-020-2649-2.

[41] J. D. Hunter. "Matplotlib: A 2D graphics environment". In: *Computing in Science & Engineering* 9.3 (2007), pp. 90–95. DOI: 10.1109/MCSE.2007.55.

[42] Steven R. Finch. *Mathematical Constants*. Cambridge University Press, 2003.

[43] Liam Keegan, Aleksi Kurkela, Aleksas Mazeliauskas, and Derek Teaney. "Initial conditions for hydrodynamics from weakly coupled pre-equilibrium evolution". In: *JHEP* 08 (2016), p. 171. DOI: 10.1007/JHEP08(2016)171. arXiv: 1605.04287 [hep-ph].

[44] Aleksi Kurkela et al. "Matching the Nonequilibrium Initial Stage of Heavy Ion Collisions to Hydrodynamics with QCD Kinetic Theory". In: *Phys. Rev. Lett.* 122.12 (2019), p. 122302. DOI: 10.1103/PhysRevLett.122.122302. arXiv: 1805.01604 [hep-ph].